Comparative Genomic Analysis, Transcriptome and Hydrocarbon-Degrading Capability of *Vibrio* sp. Strain J502

by

A thesis submitted to the

School of Graduate Studies

in partial fulfillment of the requirements for the degree of

Master of Science

Marine Biology

Department of Ocean Sciences, Faculty of Science

Memorial University of Newfoundland

St. John's, Newfoundland & Labrador, Canada

June 2024

ABSTRACT

Marine oil spills occurring as a result of anthropogenic activity pose a threat to marine birds, mammals, fish, and human health due to the toxicity of the compounds present in crude oil. Petroleum hydrocarbons are one of the most widespread organic contaminants impacting marine ecosystem, and contamination of marine sediments or coastal environments by hydrocarbons presents a major threat and challenge for remediation. Hydrocarbons in the marine environment are degraded abiotically by wave action, wind, and currents, and biotically by marine microorganisms. The bacterial genera *Vibrio, Alteromonas, Bacillus* and *Pseudomonas* are examples of species that have been identified as having hydrocarbon degrading metabolic capabilities.

The genus *Vibrio* is extremely diverse and can be found in a wide variety of environments. Several environmental isolates of *Vibrio* spp. have been identified as hydrocarbon-degraders. Due to their widespread presence and adaptability, it is worthwhile studying the characteristics and metabolic traits of locally isolated *Vibrio* to understand their potential interaction with crude oil that is introduced into the marine environment.

Here, I investigate the genomic, phylogenetic, and biochemical properties of a hydrocarbon-degrading marine bacterium isolated in Logy Bay, Newfoundland. Additionally, I determine the transcriptomic profile of this bacterium in crude oil exposure conditions and conduct an experiment to determine the chemical composition of chemically dispersed crude oil over time when it is incubated with a culture of this bacterium.

ACKNOWLEDGMENTS

I would like to thank my supervisors, Dr. Javier Santander, and Dr. Uta Passow for their guidance, time, and patience in working with me to complete all aspects of this thesis. I would like to thank the Marine Microbial Pathogenesis and Vaccinology Lab and Anthropogenic Effects on the Ocean of Newfoundland Lab members for their support throughout the completion of my research. I would like to thank Dr. Mary Abercrombie for her guidance and advice as a member of my thesis committee. I am grateful for the funding supplied by NSERC Collaborative Research and Training Experience Program: PEOPLE and Multi-Partner Oil Research Initiative (MPRI) and CRC-1 and the Canada First - Ocean Frontier Institute (sub-module J3), and NSERC-Discovery grant (RGPIN-2018-05942). Most of all, I would like to thank my family for all of their support over the years and their unwavering patience and encouragement as I worked to complete this thesis. It would not have been possible without you.

TABLE OF CONTENTS

LIST OF FIGURES

LIST OF TABLES

LIST OF SUPPLEMENTARY FILES

CO-AUTHORSHIP STATEMENT

The research described in this thesis was conducted by Emma Wells with guidance from Dr. Javier Santander and Dr. Uta Passow. Emma Wells was responsible for conducting the experiments, all of the laboratory work, data collection and analysis and thesis writing. Ignacio Vasquez[1], Ph.D. candidate collaborated in the experiments and data analysis of chapter II. All of the chapters were written by Emma Wells, with suggestions, recommendations and edits provided by Dr. Javier Santander, Dr. Uta Passow and Dr. Mary Abercrombie.

[1] Marine Microbial Pathogenesis and Vaccinology Laboratory, Department of Ocean Sciences, Memorial University of Newfoundland, St. John's, NL, Canada.

1. CHAPTER I: General Introduction

1.1 Oil Exploration in the Northeast Atlantic

The expansion of the offshore oil and gas industry in the North Atlantic comes with economic benefits and environmental risks for the region. Drilling and production operations of offshore oil companies in Atlantic Canada are associated with both regulated discharge and accidental spills of oil into the ocean [1]. In Newfoundland and Labrador, the offshore oil and gas industry has been a significant contributor to the local economy since major development and oil exploration began in the 1960s.

The Grand Banks off Newfoundland are home to four of the eleven most significant oil discoveries in North America, estimated to contain >16 million cubic meters of recoverable hydrocarbon reserves [2]. The first exploratory wells located on the Grand Banks off the southeast coast of the island were drilled in 1966-1967 [3]. Hibernia, a concrete gravity-based structure which became operational in 1997, is located 170 nautical miles from St. John's and is the world's heaviest offshore oil platform [4]. The Hibernia platform is predicted to continue operations until 2036 [5].

Increases in oil and gas activity on the Grand Banks have been accompanied by an increase in the amount of oil spilled from offshore oil platforms, with as many as 381 small (<7.95 m^3) oil spills reported by the Husky, Terra Nova, and Hibernia oil platforms between 1997 and 2010, with 126 of these spills identified as crude oil or mixed hydrocarbons and the remainder as diesel or other oil-based products [5]. The risk associated with oil spills is heightened in this region due to the cold and harsh climate conditions, which can impact the effectiveness of prevention, control and cleanup strategies used in the case of a spill [4,6].

1.2 Risks Associated with Offshore Oil and Gas Exploration and Spill Response

Oil spills in the ocean pose a direct threat to marine birds, mammals, and fish due to the toxicity of the oil and the formation of oil slicks. A single ton of spilled oil can form an oil slick covering 5 x 10^6 m^2 of sea surface [7]. The lightest components of the oil slick evaporate into the atmosphere, while the heavier components float on the sea surface where they undergo physical and photochemical weathering or become incorporated into aggregates and sink to the ocean floor [8]. These oil containing aggregates can become adsorbed into sediments and re-deposited into the water column through currents and wave action, creating a slow-release secondary source of pollution [9].

The initial stages of environmental recovery from large-scale marine oil spills in most cases takes between two and ten years, with long-term impacts related to changes in ecosystem structure persisting due to the longevity of some of the affected species [10]. The Deepwater Horizon accident of April 2010 is a prominent and thoroughly studied example of a large-scale oil spill occurring in a biodiversity-rich marine ecosystem. Up to 54% of macrofaunal and 38% of meiofaunal diversity in the benthic environment within close range of the oil spill was lost and estimates for recovery of the ecosystem are of at least several decades [11]. From a local perspective, the Grand Banks are ecologically valuable and support an estimated 40 million seabirds annually [5]. The region was also considered one of the most productive fishing grounds in the world before heavy fishing and environmental shifts caused the collapse of the fish biomass in the early 1990s [12]. Nevertheless, the Grand Banks still represents a critical environmental and economic resource for the province. A large-scale oil spill in the Grand Banks area would have devastating impacts on the marine biota of the region and on the economy of Newfoundland and Labrador.

When an oil spill occurs in the ocean, the initial response is to collect as much of the oil as possible and remove it mechanically using where weather and climate conditions allow [13]. Physical barriers used to control the spread of an oil spill include booms, skimmer and absorbents. Booms are long rolls of adsorbent, buoyant material placed around a spill or the source of a spill that prevent the oil from spreading further or forming a larger slick [14]. Skimmer are used to remove oil from the surface of the water. Skimmers can be categorized into five types: sorbent surface, weir, suction, elevating and submersion [15]. Sorbent skimmers are the most commonly used, and recovery is based on adhesion of the oil to an oleophilic sorbent surface which then passes by a scraper or roller to remove and contain the oil [15]. Once oil has been gathered, another technique, in-situ burning, is sometimes employed. In-situ burning involves burning an oil slick, causing the vaporisation of the oil. The rate at which oil burns is a function of the amount of available oxygen, the type of fuel and the area occupied by the slick [16]. The residue from oil spill burning is largely unburned oil with some lighter and more volatile compounds removed, although burning of heavier oils may produce some oil dense oil residues that may sink in seawater [16].

If appropriate conditions prevail, chemical dispersants may be added to oil slicks to disperse the oil, which is thought to make the hydrocarbons more bioavailable for biodegradation by marine microorganisms [17]. Some of the most used commercially available oil dispersants include Corexit 9500A, Finasol OSR52, Slickgone NS, Slickgone EW and Accell DWD [18]. These dispersants contain ingredients such as monopropylene glycol, sorbitan monooleate, carboxylic acid derivatives, 2-butoxyethanol, surfactants like Span 80, Tween 80, and Tween 85, dearomatized kerosene, and other light petroleum distillates [18].

The amount of chemical dispersant used to treat an oil spill is determined by estimating the optimal dispersant/oil ratio (DOR) suggested by the manufacturer, which is designed to maximize the effectiveness of the dispersant [19]. The main purpose of applying dispersant to a surface oil slick is to break the oil down into smaller droplets. It is argued that the smaller the droplets of oil, the higher the surface area available for microbial colonization, and thus the higher the rate of biodegradation [20]. During the Deepwater Horizon oil spill, 65% of the 4.9 million barrels of oil spilled at a depth of approximately 1500 meters rose to the sea surface [21]. The resultant surface oil slick was treated with 2 million gallons of Corexit EC9500A and EC9527A chemical dispersant, which was sprayed on the slick by a plane flying above it, for a targeted 1:20-1:25 dispersant-to-oil ratio [22]. Additionally, dispersant was introduced near the source of the oil spill on the seafloor. This was the first time that chemical dispersants were used in deep water [23], and the dispersant added at the recommended 1:100 DOR successfully prevented some of the oil from rising to the sea surface by creating small droplets, which remained at depth. Since 2010, research into the effectiveness and environmental impacts of chemical dispersants has continued and there are still many questions left to be answered.

In contrast to the methods previously described where interventions were involved, natural attenuation is an approach to oil spill remediation that involves relying on the metabolic activity of indigenous microorganisms and natural abiotic conditions to degrade oil. Oil is transformed by physical and chemical processes such as evaporation, dissolution, dispersion, photooxidation, and formation of aggregates over the course of days to months in the environment [24]. Microbial degradation can typically remove many low molecular weight compounds within the first few weeks after an oil spill, with higher molecular weight compounds persisting in the environment for a longer time [24]. It is important to develop an understanding

of the efficacy of natural attenuation in specific locations and conditions to determine whether additional methods of control, removal and treatment would be required in the case of an oil spill.

1.3 Crude Oil Composition

The composition of oil varies greatly depending on the source and the level of refining and production which the oil has undergone. Unrefined crude oil is composed primarily of polycyclic aromatic hydrocarbons (PAHs) and alkanes, but also contains sulfides, nitrogen-containing pyrroles and pyridines, oxygen-containing phenols, acids, and furans [25]. Aliphatic compounds are also known as saturates and are single-bond hydrocarbons classified as alkanes or cycloalkanes based on their chemical structure and properties [26]. PAHs are organic pollutants that are composed of two or more benzene rings and are released into the marine environment through incomplete combustion of fossil fuels, petroleum refinery effluents and crude oil spills [27]. Resins and asphaltenes include the non-hydrocarbon polar molecules present in oil and are typically heavier and more recalcitrant compounds [26]. The degradation rate of oil in the marine environment varies widely depending on its specific hydrocarbon composition; however, some hydrocarbons found in crude oil are virtually non-biodegradable. It has been estimated that the biodegradability of crude oils ranges from 70 to 97% [28].

Much of the degradation of oil in the marine environment can be attributed to weathering due to exposure to abiotic conditions. When oil is leaked or spilled into the ocean, it undergoes weathering processes such as evaporation, emulsification, dispersion, dissolution, photo-oxidation, sedimentation, adhesion to minerals and biodegradation [29]. These processes alter the chemical composition of the oil and may even render it more toxic to marine organisms. Generally, the less complex compounds such as *n*-alkanes, isoprenoids, monocyclic

naphthalenes, polycyclic naphthalenes, diasteranes, and aromatic steroids are degraded first [29,30]. Understanding the chemical changes that occur to oil once it is exposed to the elements and weathered in the marine environment is critical to understanding its interactions with the microorganisms present in the ecosystem.

1.4 Interaction of Marine Bacteria and Hydrocarbons in the Marine Environment

It is well established in scientific literature that many species of marine bacteria can degrade a variety of hydrocarbons found in crude oil. Hydrocarbons are ubiquitous in the marine environment, originating from natural oil seeps, natural gas deposits and from anthropogenic sources. Prolonged exposure of marine bacteria to these sources has allowed some species to develop a specialized metabolism to be able to degrade hydrocarbon compounds [31]. Many of these specialized species are always present in seawater in low abundances but increase significantly when a hydrocarbon source is introduced [32].

Crude oil present in the ocean can be in the form of dissolved petroleum hydrocarbons in the aqueous phase, large hydrocarbon droplets, or small pseudosoluble or encapsulated hydrocarbon droplets; all of which interact with marine bacteria [33]. The solubility and droplet size of the oil can greatly impact its rate of biodegradation by microorganisms. Bacteria with higher hydrophobicity experience increased absorption with oil droplets, therefore, the production of surfactants by bacteria is a strategy that is commonly used to improve their hydrophobicity, and thus increase their interaction with oil droplets in the marine environment [33]. Microorganisms may metabolize hydrocarbons aerobically or anaerobically, through oxidation, reduction, hydroxylation, and dehydrogenation reactions [26]. The main enzymes involved in hydrocarbon degradation are oxygenases and dehydrogenases [34].

Lighter more volatile compounds found in crude oil, such as low-molecular weight (LMW) PAHs, undergo adsorption, volatilization, photolysis, and chemical degradation when exposed to the elements [34]. Microbial degradation is also responsible for breaking down PAHs into less complex metabolites, although the extent and rate of biodegradation depends on environmental factors such as pH, temperature, oxygen, microbial population, degree of acclimation, access to nutrients, chemical structure of the compound and chemical partitioning in the growth medium [34]. Aerobic biodegradation of PAHs is made up of upper and lower metabolic pathway components. The upper pathway consists of the activation of the aromatic compounds by mono- or dioxygenases, which transforms them into intermediates such as catechol [32]. In the lower pathway, ring-cleaving dioxygenases produce intermediates, which are incorporated into the tricarboxylic acid cycle for energy production [32].

Hydrocarbon degrading bacteria produce biosurfactants containing extracellular matrix, also known as extracellular polymeric substances (EPS), which may function as natural dispersants and reduce the oil-water interfacial tension [35]. EPS is primarily composed of amino acids, sugars, or fatty acids linked to a functional group such as a carboxylic acid [32]. The EPS forms a barrier at the oil-water interface to stabilize oil droplets, serves as an anchoring material for microbes to attach to, helps regulate the movement of nutrients and waste, provides protection from the environment, and adsorbs metals and organic compounds [35].

1.5 Research Gaps

While there is significant research published on biodegradation of oil in the marine environment by bacterial species, there are fewer studies that examine the specific metabolic capabilities of individual species and strains of bacteria. It is critical to study the interactions between bacteria but is also important to develop a detailed understanding of individual species'

metabolism when it comes to biodegradation of hydrocarbons. In addition, there are a lack of studies focused on species isolated from the Northwest Atlantic Ocean, although there is a lot of offshore oil production and exploration in this region and therefore heightened risk of oil spills. The objective of this thesis is to characterize a hydrocarbon-degrading species isolated in coastal waters in Newfoundland and Labrador, which provides regionally relevant data and helps develop the general understanding of the community of biodegrading microorganisms present in the region.

This thesis combines a wide range of techniques and perspectives to generate a well-rounded understanding of the metabolic capabilities of *Vibrio* sp. strain J502. While most studies focus on either a genomic or chemical perspective on biodegradation of oil in the marine environment, this thesis explores both. The research presented here provides a unique perspective and valuable insight into how the genomic and chemistry components can inform each other and provide a deeper understanding of marine microbial biodegradation of hydrocarbons.

1.6 General Objectives

The general objective for Chapter II was to genomically, phylogenetically and phenotypically characterize *Vibrio* sp. strain J502, as well as to determine the effect of exposure to crude oil on its cellular functions and metabolism. The general objective for Chapter III was to determine the ability of *Vibrio* sp. strain J502 to grow in the presence of chemically enhanced water accommodated fraction (CEWAF) of crude oil, and to determine which type of hydrocarbons (if any) it can biodegrade.

1.7 Specific Objectives

The specific objectives for Chapter II were to: i) compare the genome of *Vibrio* sp. strain J502 to other members of the genus *Vibrio* to determine its phylogenetic position within the genus; ii) to genomically characterize *Vibrio* sp. strain J502 and identify genes related to metabolism of aromatic compounds and hydrocarbons, stress and interactions with environmental conditions; iii) to determine the impact of exposure to crude oil on the gene expression of genes identified in the genomic profile of *Vibrio* sp. strain J502.

In Chapter III, the specific objectives were to: i) determine the growth of *Vibrio* sp. strain J502 when exposed to CEWAF and chemical dispersant compared to an artificial seawater control; ii) to evaluate the ability of *Vibrio* sp. strain J502 to degrade hydrocarbons found in crude oil through incubation with CEWAF and compositional analysis of oil over time.

2. CHAPTER II: Comparative Genomic Analysis and Transcriptome of *Vibrio* sp. strain J502, a Hydrocarbon-Degrading Marine Bacterium

2.1 Abstract

Marine bacteria with the ability to degrade oil in cold environments may have bio-technological applications. *Vibrio* sp. strain J502 is a Gram-negative marine bacterium, isolated from North Atlantic seawater using marine minimal media supplemented with crude oil as the sole carbon source. Here, we describe the phenotypic and genomic characteristics of this isolate from surface seawater in Logy Bay, Newfoundland, Canada. *Vibrio* sp. strain J502 is motile, halophilic, psychrotrophic, and O129 (vibrio-static agent used to identify Vibrios) susceptible, matching with *Vibrio* sp. characteristics. The genome of *Vibrio* sp. strain J502 has two chromosomes [chromosome I – (NZ_CP104554) and chromosome II – (NZ_CP104555)] and one small plasmid [Plasmid pJ502 - NZ_CP104556] for a total size of 4.55 Mb and 44.7% G+C content. Whole genome genomic and phylogenetic analysis showed that *Vibrio* sp. strain J502 is closely related to *V. anguillarum*, with an ANI of 93.27% for chromosome I and 98.87% for chromosome II. The lipid profile and respiratory quinones identified from *Vibrio* sp. strain J502 do not match that of other members of the genus *Vibrio*, suggesting that this may be a novel isolate. Additionally, based on genomic and phylogenetic characteristics, it is proposed that this isolate represents a potential new species, and definitively represents a novel isolate. *Vibrio* sp. strain J502 has genes related to the degradation of aromatic hydrocarbons, which we found were upregulated when the bacteria was exposed to water accommodated fraction of oil (WAF).

2.2 Introduction

Vibrio spp. are ubiquitous, Gram-negative, mesophilic, typically motile rod-shaped bacteria belonging to the *Gammaproteobacteria* [36]. *Vibrio* spp. can be classified as either halophilic or nonhalophilic, depending on their environment and salinity requirements for growth [37]. Many members of the genus have a facultative fermentative metabolism and can grow on marine agar [38]. The genus *Vibrio* contains over 130 confirmed species, which are found primarily in aquatic environments such as estuaries, marine coastal water and sediments, and aquaculture settings globally [36,39]. Various *Vibrio* spp. have also been isolated from marine organisms such as corals, fish, and shrimp [38].

Species within the genus *Vibrio* can cause infections in humans, including *V. cholerae*, *V. parahaemolyticus* and *V. vulnificus* [39]. Other pathogenic *Vibrio* sp. cause infection in marine organisms, such as *V. shilonii* and *V. coralliilyticus* in corals and anemones, *V. ordaii* and *V. logei* in scallops, and *V. anguillarum* and *V. salmonicida* in fish [38,40]. The genus *Vibrio* is extremely diverse, and genomic events such as mutations, chromosomal rearrangements, loss of genes by deletion or decay and gene acquisitions through duplication or horizontal transfer are thought to drive the continuing evolution and speciation within the genus [38]. All previously identified members of the genus *Vibrio* have two chromosomes, with chromosome I usually being larger and encoding proteins for essential functions and chromosome II being smaller and carrying genes related to more environment-specific functions [41]. In addition to the existence of pathogenic strains, environmental isolates of *Vibrio* spp. have been associated with hydrocarbon degradation [38,42].

Naturally occurring marine bacteria play a major role in recycling carbon in the ocean by transforming organic pollutants into a variety of metabolites, many of which are ultimately

recycled into inorganic carbon [43]. Many of these bacteria can utilize specific hydrocarbons as an energy source [44]. The most common marine bacterial genera that include hydrocarbon-degrading bacteria are *Pseudomonas*, *Nocardia, Acinetobacter*, and *Vibrio* [45]. The activity of hydrocarbon-degrading marine bacteria depends on oil type and seawater conditions, including temperature, oxygen, and nutrient availability, creating niches with site-specific microbial communities [46].

Biodegradation of hydrocarbons by marine bacteria is the result of oxidative processes carried out by oxygenases and peroxidases, which convert organic pollutants into intermediates of the tricarboxylic acid cycle [11]. Many *n*-alkanes and PAHs, especially the smaller molecules, have been shown to be degraded effectively by aerobic marine bacteria [12]. For instance, *V. alginolyticus* strain MF15 isolated from diesel-contaminated seawater can degrade up to 26.78% of diesel in 10% dilution in seawater within 14 days [49]. Similarly, *V. cyclotrophicus* strain P-2P44T, isolated from creosote contaminated marine sediments can degrade three and four-ring PAHs [42]. Bioremediation of oil spills via natural attenuation with hydrocarbon-degrading marine bacteria is a well recognized as a cleanup strategy in many areas of the world as it may save between 50 and 70% of the costs of oil spill cleanup compared to physical and chemical methods [7,50]. There are many other additional benefits to bioremediation, including reduced environmental impact, sustainability and its suitability to be used alongside other cleanup methods.

Four of the eleven most significant oil deposits found in North America are in the Newfoundland offshore [2]. There is a heightened risk of oil spills in this coastal region due to the cold and harsh climate, and potential oil spill cleanup measures are challenging to execute in adverse weather conditions [6]. Isolation and characterization of local marine microbes with

hydrocarbon-degrading potential is critical to understanding the impacts of an oil spill in this region, and for developing local oil spill response plans. Although there are many studies on oil-degrading marine bacteria, there is generally a lack of information on species found in the North Atlantic, and there is very little information available on the bacteria found in the ocean around Newfoundland and Labrador. This study focuses on a hydrocarbon-degrading marine bacteria isolated from the coastal surface waters of Newfoundland, which provides new insights into the marine bacterial diversity found in this ecosystem.

In this study, we isolate a marine bacteria strain in marine minimal media using crude oil as the sole source of carbon and describe its complete genome and phenotypic characteristics. We found that the hydrocarbon-degrading marine *Vibrio* sp. strain J502, isolated from surface waters in Logy Bay, Newfoundland, Canada, is a novel isolate. We determined that *Vibrio* sp. strain J502 is a Gram-negative, psychotropic, hydrocarbon degrading marine bacterium. Functional analysis of the genome of *Vibrio* sp. strain J502 determined that this bacterium might possess resistance to some heavy metals and antibiotics and is capable of aerobically metabolizing aromatic compounds. Its ability to grow in the presence of crude oil and chemical dispersant makes this strain a potential tool for ecofriendly bioremediation of oil spills in Atlantic Canada.

2.3 Materials and Methods

2.3.1 *Vibrio sp. strain J502 Isolation*

Vibrio sp. strain J502 was isolated and purified in 2017 from sea water (Logy Bay, NL) using enrichment with crude oil (un-weathered Hibernia crude oil). Sterile flasks of 350 mL containing 100 mL of raw sea water were inoculated with 1 mL of crude oil and incubated at 15°C with aeration (180 rpm) for 60 days (d). After this period marine M9 minimal media agar

(M9 salts [51] without $MgSO_4$ and $CaCl_3$, 1.5% noble agar, 50% filtered sterilized seawater) containing 100 µL of crude oil as the only carbon source was inoculated with bacteria enriched seawater. The plates were incubated at 15°C for up to 2 weeks, until solid bacterial colony growth appeared. A single colony was repurified in Trypticase Soy Agar (TSA, 1.5% agar, Difco, Franklin Lakes, NJ, USA) supplemented with up to 2% NaCl using a streaking technique [52]. *Vibrio* sp. strain J502 was stocked in peptone 1% (Difco) and glycerol 10% (Sigma) at -80°C according to established protocols [53]**.**

2.3.2 Bacterial Culture Conditions

Vibrio sp. strain J502 was grown routinely in 3 mL of Trypticase Soy Broth (TSB, Difco, Franklin Lakes, NJ, USA) supplemented with 2% NaCl at 15°C in a 16 mm-diameter glass tube and placed in a roller drum (TC7, New Brunswick, MA, USA) for 24 h with aeration (180 rpm). When required, the media was supplemented with 1.5% bacto-agar (Difco).

2.3.3 Biochemical, Enzymatic and Physiological Characterization

Vibrio sp. strain J502 growth was evaluated at 4, 15, 28 and 37°C, and 0, 0.5 and 2% NaCl concentrations. The biochemical profile of *Vibrio* sp. strain J502 was characterized using API20E, API20NE, and API ZYM systems (BioMerieux, Marcy-l'Etoile, France) according to the manufacturer's instructions. The strips were incubated at 15°C for 48 h. Vibrio sp. strain J502 antibiogram profile was determined for tetracycline (10 µg), oxytetracycline (30 µg), ampicillin (10 µg), sulfamethoxazole (25 µg), chloramphenicol (30 µg), colistin sulphate (10 µg), oxalinic acid (2 µg) and O-129. Antibiotic sensitivity discs (Difco) were placed onto the surface of TSA 2% NaCl agar plates inoculated evenly with routinely grown bacterial culture following standard methods [54]. Resistance to each antibiotic was determined based on the

diameter of the zone of inhibition [55,56]. Motility, hemolytic activity (Figure S1), and catalase activity were determined using standard methods [55].

2.3.4 DNA Extraction and Sequencing

Vibrio sp. strain J502 was grown as described in 2.2. Bacterial cells were harvested at mid-log phase, at an optic density (OD_{600}≈0.7; 2.5 x 10^8 CFU/mL). Total DNA extraction was conducted using a Wizard Genomic DNA Purification Kit (Promega, Madison, WI, USA) according to the manufacturer's instructions. The DNA integrity and purity were evaluated using gel electrophoresis (agarose gel 0.8%) and spectrophotometry based on the 260/280 and 260/230 ratios value (Genova-Nano Spectrophotometer, Jenway, UK). Libraries and sequencing were conducted at Genome Quebec (Montreal, QC, Canada) using long-read PacBio SMART whole genome sequencing and short-read MiSeq Illumina next-generation sequencing platform.

2.3.5 Genome Assembly and Annotation

PacBio sequences were assembled at Genome Quebec using Celera Assembler (August 2013 Version). Illumina sequences were examined using FastQC version 12 (http://www.bioinformatics.babraham.ac.uk/projects/fastqc/). The MiSeq sequences were trimmed and assembled using the CLC Genomics Workbench (CCGW) version 20.0 (Qiagen) *de novo* tool. The assembled sequences were annotated by the NCBI Prokaryotic Genome Annotation Pipeline (https://www.ncbi.nlm.nih.gov/genome/annotation_prok; last accessed January 20, 2024). Annotation was completed using the Rapid Annotation Subsystem Technology pipeline (RAST) (http://rast.nmpdr.org/ last accessed January 20, 2024).

2.3.6 Whole Genome Comparison and Phylogenetic Analysis

The genomes utilized are listed in Table S1. Whole genomes were aligned to calculate the average nucleotide identity (ANI) using CGWB v22.1 (Qiagen) whole genome analysis tool. A comparative heat map was constructed using the heat map tool with default parameters. Phylogenetic analysis was performed using CGWB and MEGA 11 [57]. Evolutionary history was calculated using the neighbor-joining method and with a bootstrap consensus of 1000 replicates, and evolutionary distance was computed using the Jukes-Cantor method. *Photobacterium damselae* strain AS-16-0555-7 was used as an outgroup (GCF_014775695.1).

2.3.7 Genomic Islands Analysis

Detection of genomic islands (GIs) was carried out using IslandViewer 4 pipeline (https://www.pathogenomics.sfu.ca/islandviewer; last accessed June 10, 2023), which integrates integrate IslandPath-DIMOB, SIGH-HMM, and IslandPick analysis tools into a single analysis [4]. This analysis was performed on both chromosomes and the plasmid.

2.3.8 Identification of Genes Associated with Metabolism, Virulence and Environmental Adaptation in Vibrio sp. strain J502

Analysis of the genome of *Vibrio* sp. strain J502 using the Rapid Annotation Subsystem Technology pipeline (RAST) (http://rast.nmpdr.org/) revealed the distribution of the coding sequences in various subsystem functions. The *Vibrio* sp. strain J502 chromosome was examined for metabolism, virulence, and environmental adaptation-related genes using the analysis from the NCBI Prokaryotic Genome Annotation Pipeline (https://www.ncbi.nlm.nih.gov/genome/annotation_prok).

2.3.9 Plasmid profile

The plasmid profile of *Vibrio* sp. strain J502 was determined by alkaline lysis and gel electrophoresis [59]. Briefly, 1.5 mL of *Vibrio* sp. strain J502 exponential culture was transferred to an Eppendorf tube and centrifuged for 5 minutes at 10,000 rpm at room temperature. The pellet was resuspended in 200 µL of TAE1 buffer (Tris acetate 2M, 20 mL; EDTA 0.5M, 4 mL; ddH_2O, 976 mL), and 400 µL of lysis solution (SDS 20%, 1.5 mL; NaOH 10M, 64 µL; Tris 1M, 0.5 mL; ddH_2O, 7.9 mL) was added and mixed gently. The sample was incubated for 45 min at 37°C. After incubation, 600 µl of acid phenol-chloroform was added, mixed and centrifuged at 6,000 rpm for 15 minutes at 15°C. The supernatant was collected and 50 µL was loaded in a 0.5% agarose gel separated for electrophoresis at 45V for 18 h. The gel was stained in 200 mL of TAE1 buffer with 6 µl of ethidium bromide (0.05%) for 1 h, then washed 3 times for 15 minutes in distilled water prior to visualization in a gel doc unit (iBraght, Thermo fisher) (Figure S2).

2.3.10 Lipid Content and Quinolone Analysis

A 1 L flask containing 500 mL of TSB 2% NaCl was inoculated with *Vibrio* sp. strain J502 and grown at 15°C with aeration (180 rpm) for 24 h. The culture was centrifuged for 10 min at 10,000 rpm. The pellet was washed twice with 10 mL of PBS and then twice with 5 mL of filtered sterilized cryoprotectant Reagent 18 (TSB 7.5 g; BSA [Bovin Serum Albumin] 25 g; sucrose 50 g). The pellet was then resuspended in 15 mL of cryoprotectant Reagent 18, transferred to a 50 mL falcon tube and stored at -80°C. *Vibrio* sp. strain J502 culture was freeze dried (Labonco Freezone 12) overnight and shipped for analysis. Cellular fatty acid content and quinone analysis were carried out at Leibniz-Institut DSMZ (Deutsche Sammlung von Mikroorganismen und Zellkulturen GmbH, Braunschweig, Germany). Cellular fatty acid content was determined by gas chromatography and a flame ionization detector according to established

protocols [60–65]. Respiratory quinones profile was determined by HPLC and according to stablished methods [61,66].

2.3.11 Bacterial Growth and Metabolic Activity in the Presence of Sea Water and Water Accommodated Fraction of Crude Oil Transcriptomic Experiment Setup

Six flasks of 250 mL containing 50 mL of TSB 2% NaCl were inoculated with *Vibrio* sp. strain J502 and incubated at 15°C with aeration (180 rpm) to $OD_{600} \approx 1.0$ ($\approx 5.6 \times 10^{10}$ CFU/mL). The contents of each flask were transferred to 50 mL tubes and centrifuged at 6000 rpm for 10 minutes. The supernatant was removed, and the cells were washed twice by adding 10 mL of filtered sterilized seawater, centrifuging at 6000 rpm for 10 minutes and pouring off the supernatant. The cells were then resuspended in 50 mL of filtered sterilized seawater and transferred into dialysis bags (Molecular weight cut off 3.5 kDa; Spectra/Por, Cole Parmer, Laval, Quebec, Canada). Dialysis bags were checked for leaks at the beginning and end of the experiment. Initial cell counts were determined via flow cytometry using LIVE/DEAD stain (BacLight Bacterial Viability and Counting Kit, Invitrogen, USA) in three randomly selected dialysis bags. Final cell counts were measured for each dialysis bag.

A water accommodated fraction (WAF) was prepared using loading concentration of 1 g/L of Hibernia light crude oil according to the protocol developed by de Jourdan, (pers. Comm. Huntsman Marine Science Centre, St. Andrews, NB, Canada) to simulate local conditions. The Hibernia crude oil used has a density of 0.925 g/cm^3 and a viscosity of 18 centistokes (cSt) (which equals to 0.18 cm^2/s). Briefly, a 2 L baffled flask was filled with room-temperature unfiltered, UV-sterilized seawater, allowing for exactly 20% headspace. A sterile positive-displacement pipette was used to add 1 g/L of Hibernia light crude oil to the central surface of the water. The flask was sealed with Duraseal and allowed to mix on an orbital shaker at 150 rpm for 1 hour. This was followed by a 1 hour settling time. The WAF was harvested through the

spigot at the bottom of the baffled flask, discarding the first and last 100 ml of WAF and collecting the middle portion.

Three dialysis bags of culture were placed into a 2 L beaker containing 1.8 L of filtered seawater to act as the control, and three bags were placed into a 2 L beaker containing 1.8 L of WAF. A magnetic stir bar at 60 rpm was added to each beaker. The beakers were covered with foil and incubated at 15°C for 3 d (Figure 2-1).

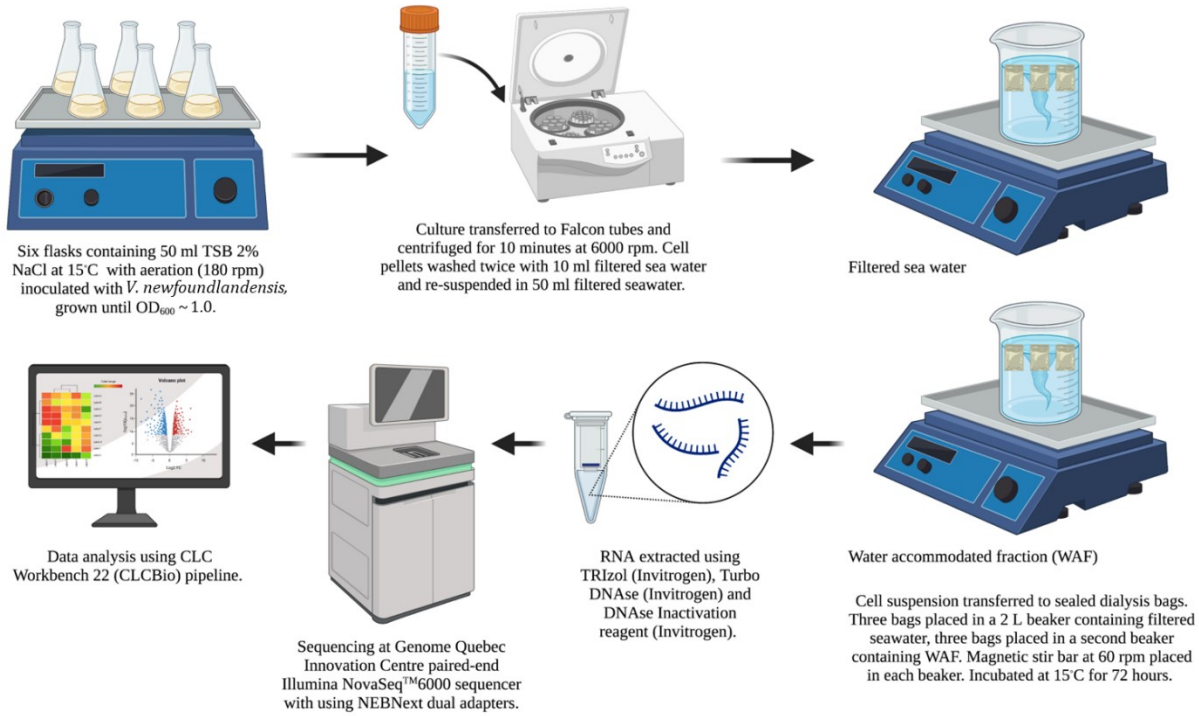

Figure 2-1. Experimental setup for determination of transcriptomic profile of *Vibrio* sp. strain J502 in the presence of a filtered sea water control and water accommodated fraction (WAF) of crude oil.

2.3.12 Bacterial RNA Extraction

Triplicate samples of the control seawater condition and experimental WAF condition were utilized for RNA extraction. The cells were harvested through centrifuging at 6000 rpm for 10 minutes. The supernatant was discarded, and the cell pellet was utilized for total RNA extraction following the manufacturer's instructions (Invitrogen, Waltham, MA, USA). RNA was extracted using TRIzol (Invitrogen) and to remove any DNA, the samples were treated with 2 µL of Turbo DNase (TURBO DNA-freeTM Kit, Invitrogen) and incubated at 37°C for 30 min. Next, 2.5 µL of DNase Inactivation Reagent was added to the samples and they were incubated at room temperature for 5 minutes. The samples were then centrifuged at 10,000 rpm for 1.5 minutes and the supernatant was transferred to a new tube. The RNA samples were quantified, and the quality was evaluated (A260/280 and A260/230 ratios) using the GenovaNano-spectrophotometer (Genway, UK) and RNA integrity was evaluated by agarose gel electrophoresis (Figure S2). The A260/280 and A260/230 ratios of purified RNA samples were 2.097–2.132 and 2.043–2.289, respectively. RNA samples were shipped to Genome Quebec Innovation Centre (Montreal, Canada) for RNA sequencing.

2.3.13 Library Preparation and RNA-Sequencing

For each condition, there were three biological replicates of the control and experimental conditions. Library preparation and sequencing were completed at Genome Quebec. RNA samples were rRNA-depleted, and libraries were prepared using NEBNext dual adapters and paired-end sequenced using Illumina NovaSeq^{TM}6000.

2.3.14 RNA-Seq Data Analysis

For all samples, raw reads were pair-end and filtered to remove low-quality reads using CGWB v 22.0 using default parameters (paired-read information, minimum distance = 1;

maximum distance = 1000). Adapter trimming was conducted by CGWB using the trim reads tool with default parameters (quality trimming, trim using quality scores, limit: 0.05; and trim ambiguous nucleotides, maximum number of ambiguities =2). The nucleotides and number of reads removed are indicated in Table S2. The quality of the reads sequence was evaluated using FastQC (v.0.11.9) before and after trimming [67]. Trimmed reads were then mapped by CGWB against the *Vibrio* sp. strain J502 genome using the RNA-Seq analysis tool. Quantification and normalization of mapped reads were performed using a previously described standardized protocol [52,68,69]. Transcript per million (TPM) values were computed from the counts assigned to each transcript, after normalization by the trimmed mean of M-values (TMM) [70]. A global correlation analysis was performed using $\log_2$-tranformed TPM values (x + 1) of each gene under sea water control and WAF treatment conditions. The global expression plot was generated using Rstudio 2022.07.2 and ggplot2 v3.3.1, and TPMs listed in File S1 and File S2. A standard selection of differential expressed genes (DEGs) was performed by comparing treatment reads to control reads and filtered using cut-off values of Log2 fold-change (FC) ≥ 1, and false discovery rate (FDR), $p \leq 0.05$. Gene ontology (GO) analyses of DEGs were conducted to determine the most significant DEGs. These DEGs were used for Gene Ontology (GO) and KEGG enrichment analysis performed using Cytoscape v3.9.0 and ClueGO plug-in v2.5.8 + CluePedia v1.5.8.

2.4 Results

2.4.1 Biochemical and Enzymatic and Physiological Characteristics of Vibrio sp. strain J502

Phenotypic, biochemical, and enzymatic characteristics of *Vibrio* sp. strain J502 are summarized in Table 1 (Figure S1), along with data for *V. anguillarum* J360 and *V. anguillarum* J382 for comparison. *Vibrio* sp. strain J502 is a Gram-negative, motile, rod-shaped bacterium

capable of growth in TSB 2% NaCl up to 28°C. *Vibrio* sp. strain J502 did not grow well in the absence of NaCl and grows best in TSB 2% NaCl at 15°C. The antibiogram analysis showed that *Vibrio* sp. strain J502 is resistant to ampicillin, and susceptible to tetracycline, oxytetracycline, oxalinic acid, trimethoprim, colistin and O-129. The biochemical and enzymatic profiles indicate that *Vibrio* sp. strain J502 produces urease, β-galactosidase, indole, alkaline phosphatase, arginine dihydrolase, and can hydrolyze esculin and gelatin. *Vibrio* sp. strain J502 can utilize glucose, arabinose, mannose, mannitol, N-acetyl-glucosamine, and maltose. It can synthesize esterase (C-4), esterase lipase (C-8), lipase (C-14), leucine, valine and cystine arylamidase, and acid phosphatase. *Vibrio* sp. strain J502 is catalase-positive and was determined to be a facultative anaerobe. Hemolytic activity was evaluated on blood agar plates at 15°C and 28°C, and *Vibrio* sp. strain J502 hemolytic activity was observed at both temperatures. The APIE identification code was 727700456 and the API20NE was 7777745.

Table 2-1. Phenotypic characteristics and API profiles of *Vibrio* sp. strain J502.

Phenotypic Characteristics	***Vibrio* sp. strain J502**	***V. anguillarum* J360** [71]	***V. anguillarum* J382** [72]	***V. anguillarum DSM 21597***
Growth at:				
4°C	+	+	+	+
15°C	+	+	+	+
28°C	+	+	+	+
37°C	-	-	-	+
LB NaCl 0%	-	-	-	+
LB NaCl 0.5%	+	+	+	+
TSB NaCl 2%	+	+	+	+
Gram Stain	-	-	-	-
Cell Shape	Rod	Rod	Rod	Rod
Motility	+	+	+	+
Pigmentation	Orange pigmented	-	-	-
Capsule stain	+			
Oxygen requirements	Facultative anaerobe			Facultative anaerobe
Catalase	+	+	+	
Hemolysis activity	+ (β-hemolysis)	+	+	
API 20NE				
Reduction of nitrates	+	+	+	
Indole production	+	+	+	
Glucose fermentation	+	+	+	
Arginine dihydrolase	+	+	+	
Urease	+	+	-	
Esculin hydrolysis (β-glucosidase)	+	+	+	
β-galactosidase	+	+	+	
Gelatin hydrolysis (protease)	+	+	+	
Assimilation of:				
D-Glucose	+	+	+	
L-Arabinose	+	+	+	
D-Mannose	+	+	+	
D-Mannitol	+	+	+	
N-Acetyl-Glucosamine	+	+	+	
D-Maltose	+	+	-	
Potassium gluconate	+	+	+	
Capric acid	-	-	-	
Adipic acid	-	-	-	
Malic acid	+	+	+	

Table 2-1. Continued.

Trisodium citrate	+	+	-	
Phenylacetic acid	-	-	-	
API 20E				
β-Galactosidase	+	+	+	
Indole production	+	-	+	
Acetoin production	+	+	+	+
Citrate utilization	+	+	+	
Production of H_2S	-	-	-	-
Urease	+	+	-	-
Hydrolysis of:				
L-Arginine	+	+	+	
L-Lysine	+	+	-	-
L-Orthinine	-	-	-	-
L-Tryptophane	+	-	-	-
Gelatinase	+	+	+	+
Assimilation of:				
D-Glucose	+	+	+	
D-Mannitol	-	-	+	
Inositol	-	-	-	-
D-Sorbitol	-	-	+	
L-Rhamnose	-	-	-	-
D-Saccharose	-	-	+	
D-Melibiose	-	-	-	-
D-Amygdaline	-	-	+	
L-Arabinose	-	-	+	-
API ZYM				
Alkaline phosphatase	+	+	+	+
Esterase (C-4)	+	+	+	+
Esterase lipase (C-8)	+	+	+	+
Lipase (C-14)	+	+	+	+
Leucine arylamidase	+	+	+	+
Valine arylamidase	+	+	+	+
Cystine arylamidase	+	+	+	-
Trypsin	-	-	-	-
α-chymotrypsin	-	-	-	-
Acid phosphatase	+	+	+	+
Naphthol-AS-BI-phosphohydrolase	-	-	+	+
α-galactosidase	+	-	-	-

Table 2-1. Continued.

β-glucuronidase	-	-	-	-
α-glucosidase	+	-	+	+
β-glucosidase	+	-	-	-
N-acetyl- β-glucosaminidase	+	-	+	+
α-mannosidase	-	-	-	-
α-fucosidase	-	-	-	-
Antibiogram				
Oxytetracycline (30 mg)	48 mm (Susceptible)	34 mm (Susceptible)	40 mm (Susceptible)	
Tetracycline (30 mg)	48 mm (Susceptible)	31 mm (Susceptible)	39 mm (Susceptible)	
Oxalinic acid (2 mg)	55 mm (Susceptible)	39 mm (Susceptible)	38 mm (Susceptible)	
Trimethoprim/ sulphamethoxate (25 mg)	31 mm (Susceptible)	33 mm (Susceptible)	25 mm (Susceptible)	
Ampicillin (10 mg)	0 mm (Resistant)	0 mm (Resistant)	0 mm (Resistant)	
Colistin (10mg)	16 mm (Susceptible)	15 mm (Susceptible)	0 mm (Resistant)	
O-129	25 mm (Susceptible)	39 mm (Susceptible)	22 mm (Susceptible)	

2.4.2 Vibrio sp. strain J502 Genome sequencing and Annotation

Vibrio sp. strain J502 genomic DNA sequenced using PacBio II and MiSeq (Illumina) platforms and assembled. The genome of *Vibrio* sp. strain J502 has been deposited to NCBI under the accession number (NZ_CP104554), BioProject (PRJNA880584) and BioSample (SAMN30853963) (Table 2-2). The genome of *Vibrio* sp. strain J502 is made up of two chromosomes [chromosome I – (NZ_CP104554) and chromosome II – (NZ_CP104555)] and one small plasmid [Plasmid pJ502 - NZ_CP104556] and has a total length of 4.55 Mb and a GC content of 44.7% (Table 2-3, Figure 2-2). NCBI analysis pipeline predicted a total of 4238 genes, including 4085 genes with CDSs, 14 (5S), 11 (16S) and 11 (23S) rRNAs, 113 tRNAs, 4 non-coding RNAs (ncRNAs), and 251 pseudogenes for the whole genome (Table 2-2).

Table 2-2. *Vibrio* sp. strain J502 genomic data summary.

Attribute	Data Provided
Annotation pipeline	NCBI
Accession number	NZ_CP104554 (Chromosome I), NZ_CP104555 (Chromosome 2), NZ_CP104556 (Plasmid)
Bio project	PRJNA880584
Bio sample	SAMN30853963
Genome size (bp)	4,540,400
G+C content (%)	44.692
Genome type	Circular
Genes (total)	4238
Genes (coding)	4085
tRNAs	113
rRNAs	14, 11, 11 (5S, 16S, 23S)
ncRNAs	4
Pseudogenes (total)	251
Pseudogenes (ambiguous)	0 of 251
Pseudogenes (frameshifted)	120 of 251
Pseudogenes (incomplete)	136 of 251
Pseudogenes (internal stop)	54 of 251
Pseudogenes (multiple problems)	55 of 251

Table 2-3. *Vibrio* sp. strain J502 genome summary.

Labels	Size (Mb)	Topology	RefSeq ID	INSDC Identifier
Chromosome I	3.37	Circular	NZ_CP104554	CP104554
Chromosome II	1.16	Circular	NZ_CP104555	CP104555
Plasmid pJ502	0.02	Circular	NZ_CP104556	CP104556

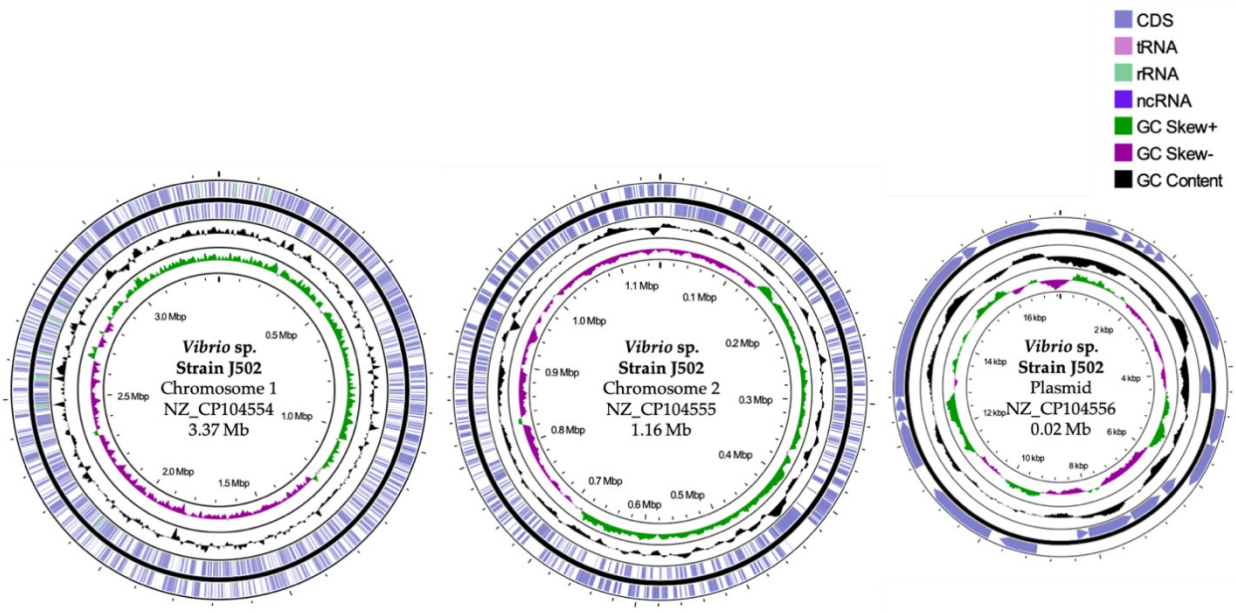

Figure 2-2. Genomic map of *Vibrio* sp. strain J502. The genome map was generated using CGViewer. Different elements and features of the chromosomes and plasmid are illustrated by colours described in the legend.

2.4.3 Whole Genome Alignment and Phylogenetic Analysis

Twenty whole genomes of selected *Vibrios* were aligned with the genome of *Vibrio* sp. strain J502 (Table S1). The ANI analysis was conducted on this whole genome alignment using CLC Genomic Workbench v20 (CLC Bio). Phylogenetic analysis of the whole genomes showed that *Vibrio* sp. strain J502 clustered more closely with *V. anguillarum* VIB43 and *V. anguillarum* J360 than any of the other species when comparing the sequences of each of the chromosomes. *Vibrio* sp. strain J502 shares the highest percent identity (100.00%) with *Vibrio anguillarum* J360 for both chromosome I and II, while the percent similarity between the two species is 93.27% (chromosome I) and 98.87% (chromosome II) (Figure S4). The heat map showed that there is a high identity between *Vibrio* sp. strain J502 and *Vibrio anguillarum* J360 alignments of chromosome I and II (Figure 2-3).

A BLAST analysis was conducted to identify nucleotide sequences similar to that of the plasmid of *Vibrio* sp. strain J502 (https://blast.ncbi.nlm.nih.gov/Blast.cgi). The plasmid pVaJ360 (CP034674.1) belonging to *V. anguillarum* was the closest match with a 99.95% identity.

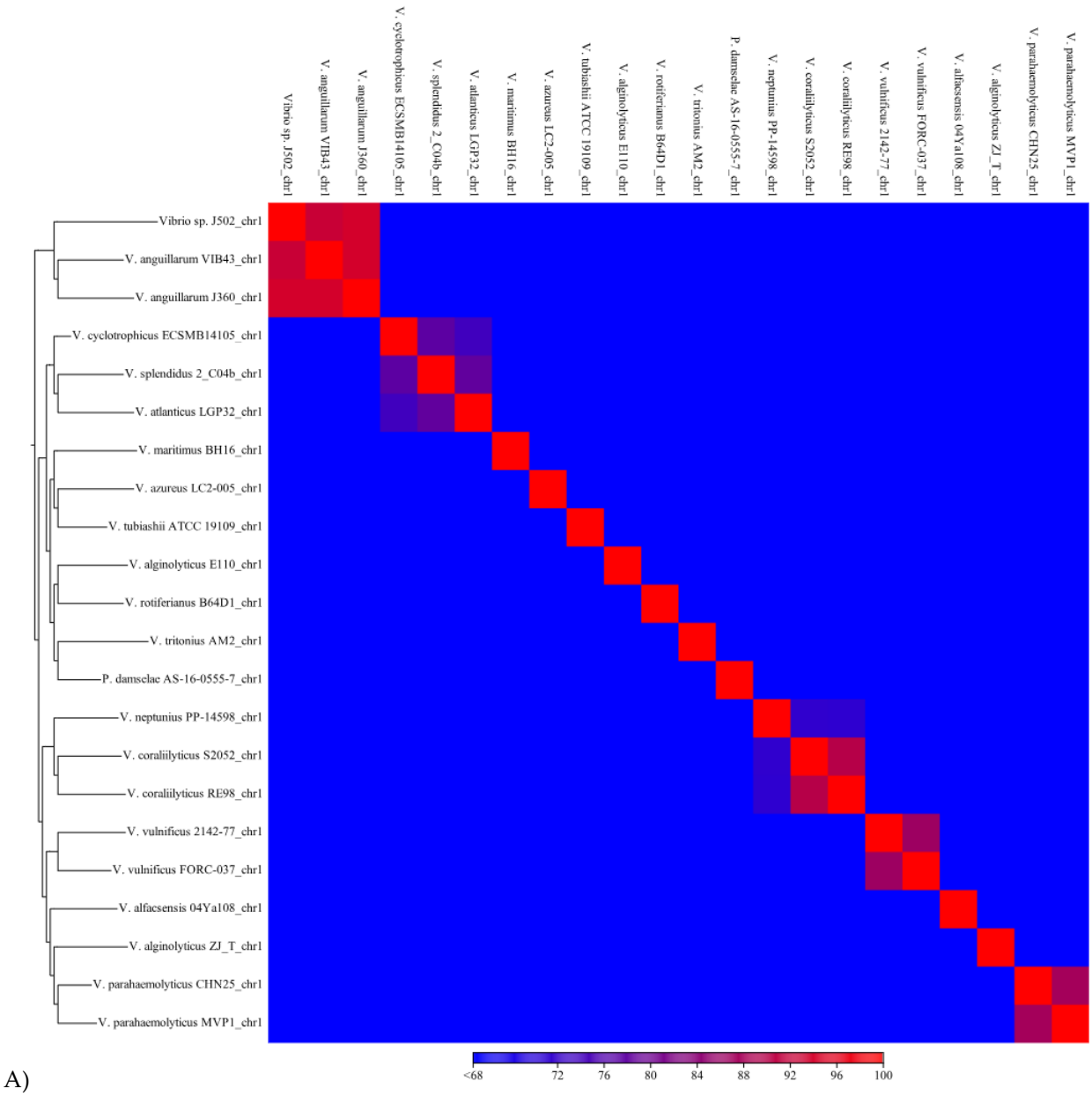
Vibrio sp. J502_chr1
V. anguillarum VIB43_chr1
V. anguillarum J360_chr1
V. cyclotrophicus ECSMB14105_chr1
V. splendidus 2_C04b_chr1
V. atlanticus LGP32_chr1
V. maritimus BH16_chr1
V. azureus LC2-005_chr1
V. tubiashii ATCC 19109_chr1
V. alginolyticus E110_chr1
V. rotiferianus B64D1_chr1
V. tritonius AM2_chr1
P. damselae AS-16-0555-7_chr1
V. neptunius PP-14598_chr1
V. coralilyticus S2052_chr1
V. coralilyticus RE98_chr1
V. vulnificus 2142-77_chr1
V. vulnificus FORC-037_chr1
V. alfacsensis 04Ya108_chr1
V. alginolyticus ZJ_T_chr1
V. parahaemolyticus CHN25_chr1
V. parahaemolyticus MVP1_chr1
<68
72
76
80
84
88
92
96
100

A)

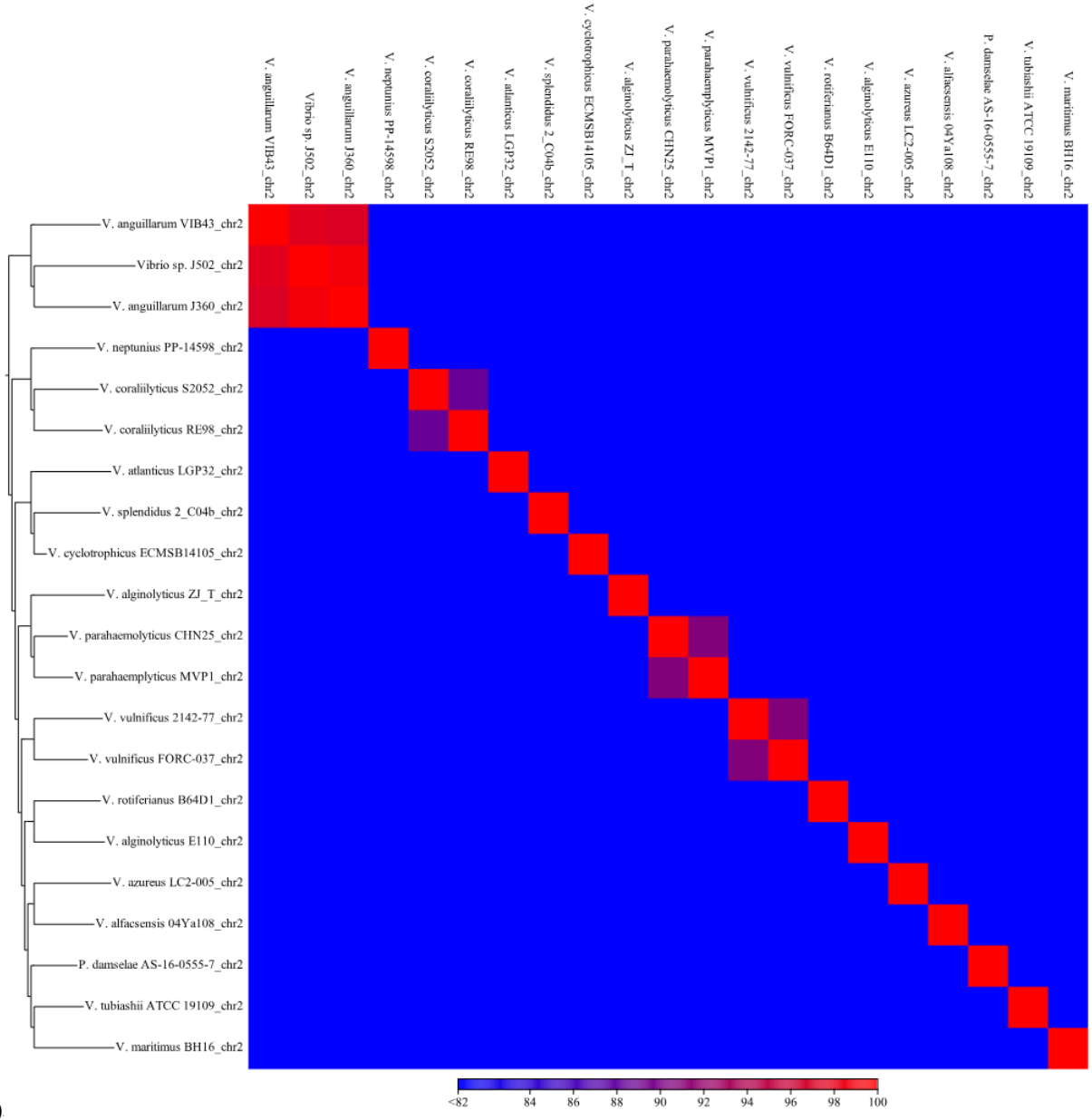
V. anguillarum VIB43_chr2
Vibrio sp. J502_chr2
V. anguillarum J360_chr2
V. neptunius PP-14598_chr2
V. coraliilyticus S2052_chr2
V. coraliilyticus RE98_chr2
V. atlanticus LGP32_chr2
V. splendidus 2_C04b_chr2
V. cyclotrophicus ECMSB14105_chr2
V. alginolyticus ZJ_T_chr2
V. parahaemolyticus CHN25_chr2
V. parahaemplyticus MVP1_chr2
V. vulnificus 2142-77_chr2
V. vulnificus FORC-037_chr2
V. rotiferianus B64D1_chr2
V. alginolyticus E110_chr2
V. azureus LC2-005_chr2
V. alfacsensis 04Ya108_chr2
P. damselae AS-16-0555-7_chr2
V. tubiashii ATCC 19109_chr2
V. maritimus BH16_chr2
<82
84
86
88
90
92
94
96
98
100

B)

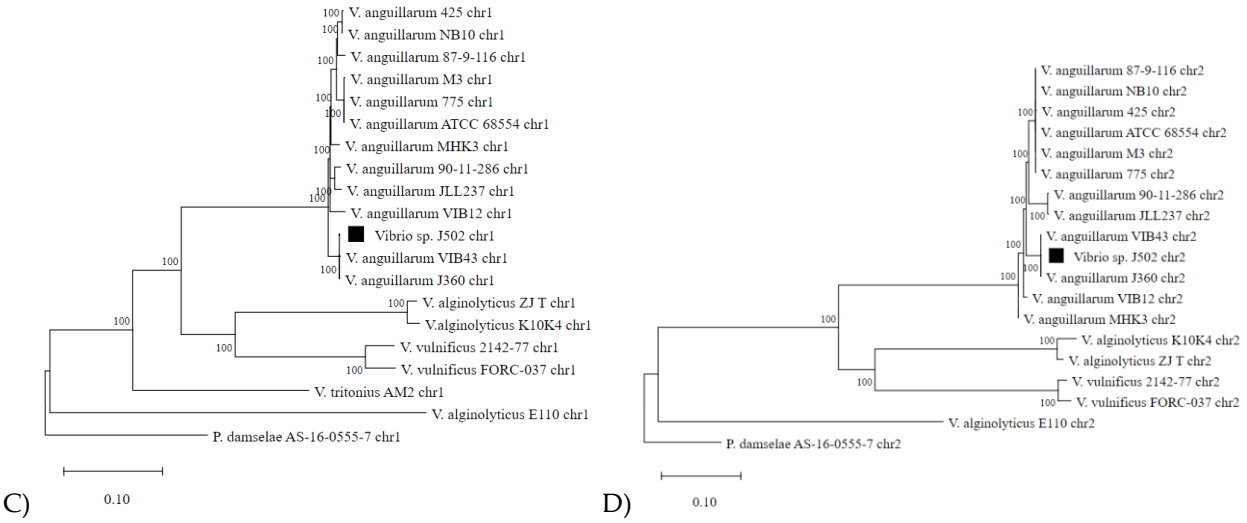

Figure 2-3. Phylogenetic and comparative genomic analysis of *Vibrio* sp. strain J502. Heat map visualization of aligned sequence identity for *Vibrio* sp. strain J502 (**A**) chromosome I and (**B**) chromosome II. Phylogenetic tree visualization or aligned sequence identity for *Vibrio* sp. strain J502 (**C**) chromosome I and (**D**) chromosome II. Table S1 contains supplementary data related to this analysis.

2.4.4 Lipid Content and Quinone Analysis

Respiratory quinone analysis of *Vibrio* sp. strain J502 indicated that quinones were 100% type Q8. Respiratory quinone Q8 is a ubiquinone, which is a redox-active lipid consisting of a conserved aromatic ring and a polyprenyl hydrophobic tail [73]. The quinone Q8 has eight isoprenyl units in the hydrophobic tail and is found in the bacterial plasma membrane where it is involved in aerobic respiration, gene regulation, and oxidative stress adaptation [73].

Genomic analysis identified several genes on chromosome I related to the biosynthesis of Q8, including *ubiA* (WP_012126569.1), *ubiB* (WP_013855638.1), *ubiD* (WP_029388360.1), *ubiE* (WP_010319838.1), *ubiG* (WP_017044298.1), *ubiH* (WP_017066017.1, and *ubiX* family flavin prenyltransferase (WP_019282527.1, WP_017049791.1, WP_017049791.1). Additional genes such as *CvpA* family protein (WP_019282275.1), NAD(P)H-flavin reductase (WP_017044373.1), and *purF* (WP_013857289.1) were also located on chromosome I and have been linked to the *ubi* genes [73].

Fatty acid analysis was able to identify 97.07% of the fatty acids associated with *Vibrio* sp. strain J502. In term of saturated fatty acids, *Vibrio* sp. strain J502 is made up of 3.22% $C_{12:0}$, 5.41% $C_{14:0}$, 22.16% $C_{16:0}$, and 1.41% $C_{18:0}$. Unsaturated fatty acids present include 0.42% $C_{16:1}\omega5c$, 2.26% $C_{16:1}\omega9c$, 10.93% $C_{18:1}\omega7c$, 1.27% $C_{18:1}\omega9c$, and 0.84% $C_{18:2}\omega6,9c$. A single methylated fatty acid, $C_{18:12}\omega7c$ 11-CH_3 was detected at 0.47%. Three hydroxy fatty acids were also detected, including $C_{12:0}$2-OH at 0.22%, $C_{12:0}$3-OH at 2.07%, and $C_{14:0}$2-OH at 1.70% (Table 2-4). Fatty acid analysis identified *Vibrio* sp. strain J502 as closely related to *Vibrio fischeri* with a Sim index of 0.713.

The lipidomic profile of *Vibrio* sp. strain J502 is shown in Figure 2-4.

Table 2-4. Cellular fatty acids (%) for *Vibrio* sp. strain J502 and its relatives in the genus *Vibrio* [41].

Fatty acid	***Vibrio* sp. strain J502**	***V. anguillarum 9063-79^T***	***V. parahaemolyticus* 9062-79^T**	***V. alginolyticus 9065-79^T***	***V. vulnificus 9107-79^T***	***V. anguillarum DSM 21597*** [74]
Saturated						
$C_{12:0}$	3.22	4	2	2	ND	2.5
$C_{14:0}$	5.41	6	4	4	2	5
$C_{16:0}$	22.16	21	12	13	18	26
$C_{18:0}$	1.41	1	1	Trace*	1	1
Unsaturated						
$C_{16:1}\omega5c$	0.42	ND	ND	ND	ND	
$C_{16:1}\ \omega9c$	2.26	43	25	31	17	0.6
$C_{18:1}\ \omega7c$	10.93					
$C_{18:1}\ \omega9c$	1.27	ND	ND	ND	ND	0.4
$C_{18:2}\ \omega6,9c$	0.84					1
Methylated						
$C_{18:1}\ \omega7c$ 11-CH_3	0.47					13.7
Hydroxy						
$C_{12:0}$ 2-OH	0.22	ND	ND	ND	Trace*	
$C_{12:0}$ 3-OH	2.07	2	2	3	4	1.3
$C_{14:0}$ 3-OH	1.70	1	2	2	4	1.3
Summed feature 2* **	2.16					
Summed feature 3** **	47.17					

* Trace amount = <1%

** ND = not detected.

*** Summed feature 2 contains 12:0 Aldehyde.

**** Summed feature 3 contains $C_{16:1}\omega6c$ /$C_{16:1}\omega7c$.

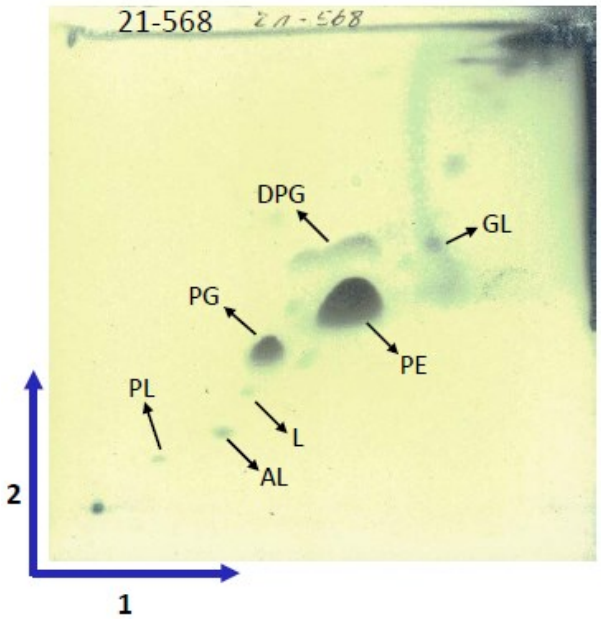

Figure 2-4. Lipid chromatogram profile of *Vibrio* sp. strain J502 (DPG = diphosphatidylglycerol, PE = phosphatidylethanolamine, PG = phosphatidylglycerol, AL = aminolipid, PL = phospholipid, GL = glycolipid, L = lipid).

2.4.5 Distribution of Genes Associated with Degradation of Aromatic Compounds, Virulence and Environmental Adaptation in Vibrio sp. strain J502

Gene distribution within the chromosomes of *Vibrio* sp. strain J502 was examined for metabolism of aromatic compounds, environmental adaptation, stress response, and pathogenesis related genes (Table S3). Genes related to cell wall and capsule synthesis were located on chromosome I, including *amiB* (WP_013857934.1), *dacB* (WP_017049781.1), *murA* (WP_020329542.1) and phosphoglucosamine mutase (WP_013857621.1). Chemotaxis genes such as *cheA* (WP_013856368.1), *cheV* (WP_011078343.1), *cheW* (WP_010318881.1), *cheY* (WP_006879571.1), and motility genes such as *flgA* (WP_010319387.1), *flgB* (WP_001007975.1), *flgO* (WP_014204584.1), *flgP* (WP_014231085.1) and *flgT* (WP_010319392.1) were also located on chromosome I. The genes *hipA* (WP_019282267.1) and *rmf* (WP_017074275.1) were found on chromosome I and are related to dormancy and formation of persister cells.

Genes related to membrane transport and the protein secretion system type IV were located on chromosome I, including *pilP* (WP_000792034.1) and *pilQ* (WP_002044686.1). Three hemolysin-encoding genes were located on chromosome I, including a thermostable hemolysin (WP_000803565.1). Genes for antibiotic resistance were found on both chromosome I and II, including *bcr/cflA* (WP_017044312.1, WP_017686533.1), which encodes a family drug resistance efflux transporter, and another gene encoding a MATE family efflux transporter (WP_011082191.1, WP_017045090.1). Type II toxin-antitoxin system genes were located on chromosome II, including the *relE/parE* family toxin (WP_017052837.1), *parD* family antitoxin (WP_004748747.1), *txe/yoeB* family addiction module toxin (WP_008951908.1), and *phd/yefM* family antitoxin (WP_017046216.1).

Fermentation genes were located on both chromosome I and II. On chromosome I, four genes were associated with the synthesis of acetolactate were located (WP_001887412.1, WP_004728751.1, WP_019283327.1, WP_001961753.1). On chromosome II, FMN-dependent L-lactate dehydrogenase (WP_010320215.1), *alsS* (WP_017050276.1) and acetolactate decarboxylase (WP_013868129.1) were found.

Carbon starvation protein A (WP_017017697.1) was found on chromosome I, as well as *csrA*, which is related to carbon storage regulation (WP_009847619.1). Sequences related to stress response and stress-regulator glutathione were located on both chromosome I and II, including glutathione S-transferase family protein (WP_010319731.1, WP_013867810.1). A gene related to detoxification, *dedA* (WP_017042402.1), was found on chromosome II; while several genes related to metal transport and homeostasis were found on chromosome I (WP_001001301.1, WP_010320570.1, WP_017038025.1).

Genes related to the metabolism of aromatic compounds were located on both chromosomes. Genes found on chromosome I included fumarylacetoacetate hydrolase family protein (WP_017047616.1), homogentisate 1,2-dioxygenase (WP_009701555.1), maleylacetoacetate isomerase (WP_010319351.1), and *ubiG* (WP_011080845.1), while a copy of a fifth gene, fumarylacetoacetate hydrolase family protein, was located on both chromosomes (WP_017047616.1, WP_013868096.1).

2.4.6 Genomic Islands (GIs)

Twenty-five GIs were identified within the genome of *Vibrio* sp. strain J502. Seventeen of these are located on chromosome I, and eight are located on chromosome II (Figure 2-5, Table S5). The GI range in size from 4.9 to 110.9 kb, with a total of 665 genes (predicted by at least

one of three software used, see Methods section). The largest genomic island was located on chromosome I and consisted of 113 genes.

Genes encoding for integrases, transposases, transcriptional regulators, and genes related to virulence, disease and defence were found on the GIs. Genes such as *hipA* domain-containing protein, associated with persistence and multidrug tolerance [75] elongation factor Tu, which is related to pathogenesis [76], DNA-directed RNA polymerase, integron integrase, and translation initiation factor IF-3 were identified on these GIs.

The smallest genomic island was also located on chromosome I and consisted of 5 genes, which encode for acyltransferase, oligosaccharide flipase family protein, asparagine synthase, formyltransferase family protein, and GNAT family N-acetyltransferase (Table S5).

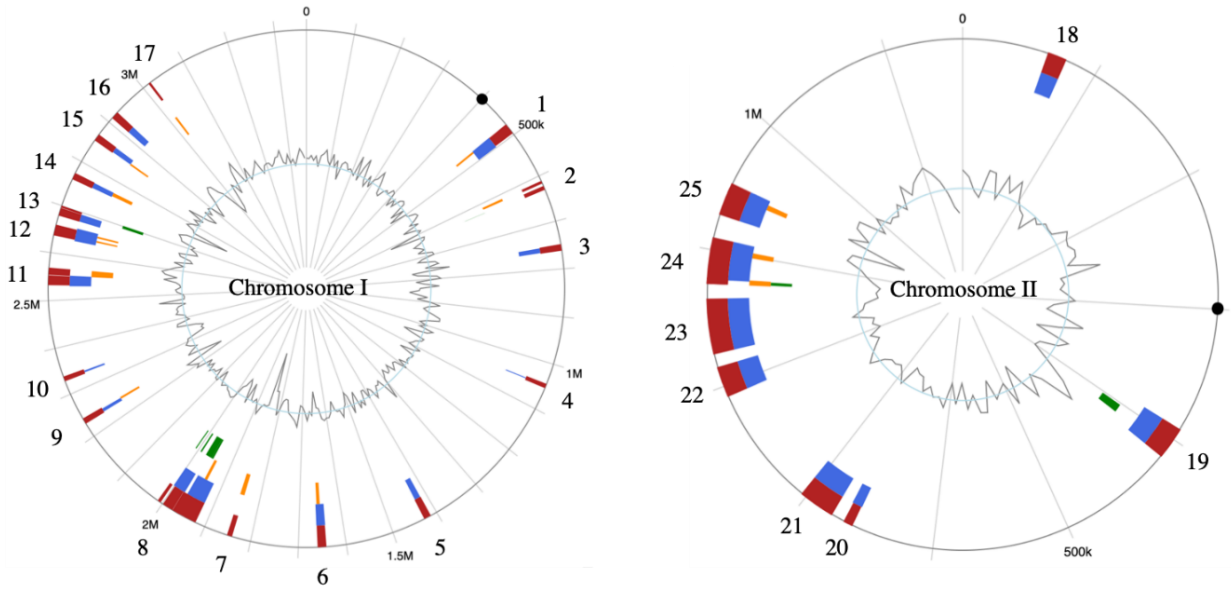

Figure 2-5. Genomic map of *Vibrio* sp. strain J502. The genome map was generated using CGViewer (IslandViewer 4). Red represents genomic islands identified by multiple methods, blue represents those only identified by IslandPath-DIMOB, orange represents those only identified by SIGI-HMM and green represents those only identified by IslandPick.

2.4.7 Transcriptomic profile of Vibrio sp. strain J502 in the Presence of Sea Water and Water Accommodated Fraction (WAF) of Crude Oil

It was hypothesized that *Vibrio* sp. strain J502 may have genes related to the metabolism of hydrocarbons found in crude oil, as it has been confirmed that *Vibrio* sp. strain J502 is capable of growth and survival in the presence of crude oil. To study the physiological and environmental adaptation mechanisms of *Vibrio* sp. strain J502 in the presence of crude oil, RNA-Seq was used to determine the global gene expression profile in the presence of filtered sea water (control) and water accommodated fraction of crude oil (WAF).

Figure S2 and Table S2 (in the supplementary data) provide information regarding the sequencing statistics and data quality. A global expression correlation analysis showed a high degree of expression correlation ($r^2 = 0.96$; $p < 2.2 \times 10^{-16}$) between seawater vs. WAF samples (Figure 2-6). The PCA plot and heat map results show a clear separation between samples based on exposure conditions (Figure 2-6). PC1 and PC2 explained 74.8% of the total variation in expression data (Figure 2-6). The $\log_2$ fold-change (FC) $\geq |1|$ and false discovery rate (FDR) p-value of ≤ 0.05 were selected as the cut-off values for significant differential expression. We found 469 differentially expressed genes (DEGs) for exposure to WAF compared to sea water. These DEGs included 238 upregulated and 231 downregulated genes.

Flow cytometry using LIVE/DEAD staining was used to determine the initial and final concentration of *Vibrio* sp. strain J502 in the dialysis bags. The average initial concentration for the control and treatment was 1.07×10^9 cells/mL ($\pm 3.68 \times 10^8$ cells/mL). The average final concentration in the control was 4.14×10^8 cells/mL ($\pm 1.19 \times 10^8$ cells/mL) and in the treatment

was 5.85 x 10^8 cells/mL (± 6.19 x 10^7 cells/mL). The final concentration in the control was not significantly different than in the treatment (unpaired t-test; t -stat = -2.21, df = 3, p = 3.18).

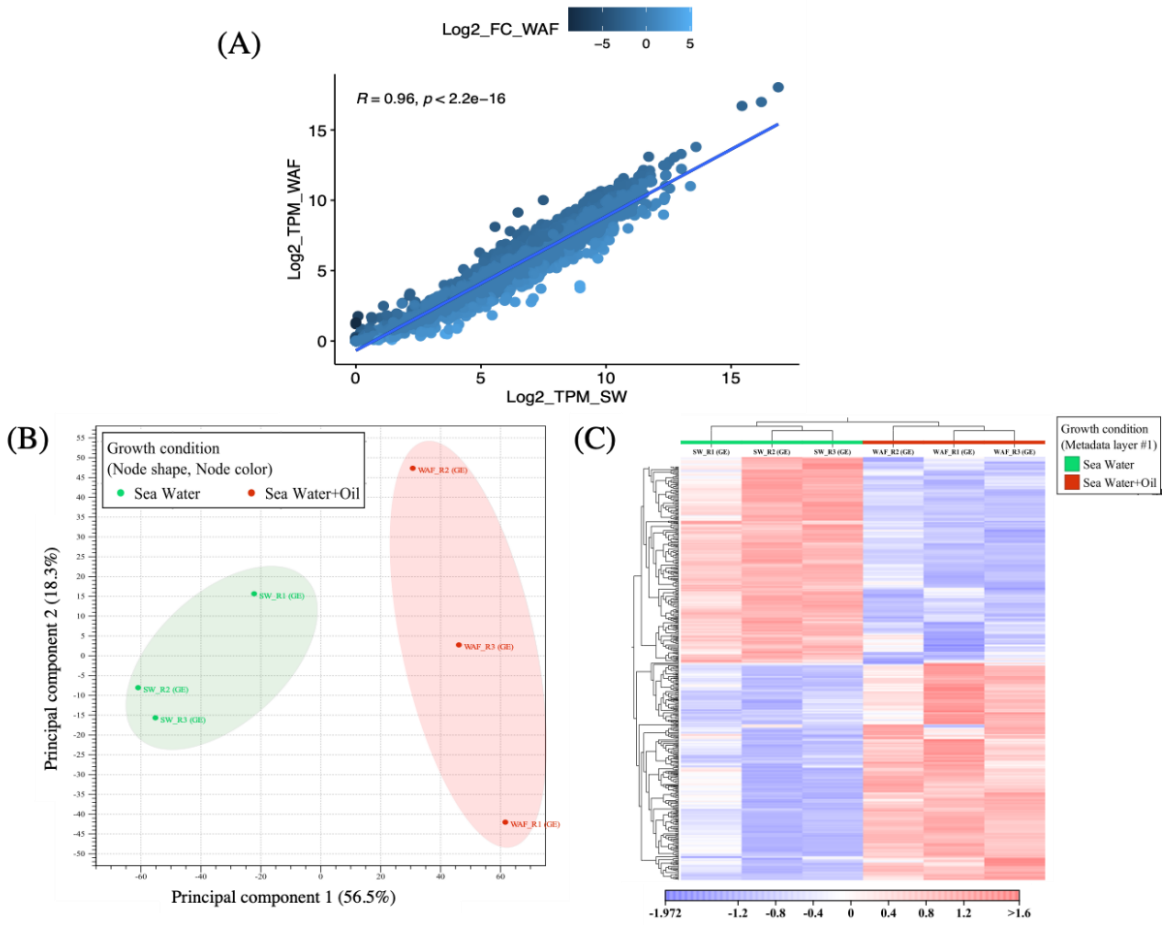

Figure 2-6. Global transcriptomic profiling of *Vibrio* sp. strain J502 by RNA-Seq. A total of six RNA libraries comprising three biological replicates for two different (sea water and WAF) conditions were included in the RNA-Seq experiment. (**A**) Scatter plot of RNA-Seq expression under sea water and sea water + oil (WAF) conditions. Each dot represents a gene, where blue and black represent up-, downregulated and non-differentially expressed genes. (**B**) Principal component analysis (PCA) of bacterial samples from sea water and sea water + oil (WAF) conditions based on the expression of all datasets. (**C**) Heat map clustering of differentially expressed genes (DEGs), color bars below the horizontal cluster indicate control (sea water, green) and experimental (sea water + oil (WAF), red) samples.

2.5 Discussion

2.5.1 Characterization of Biochemical and Enzymatic and Physiological Features

Vibrios are ubiquitous in the marine environment, including estuaries, marine coastal waters, sediments, and aquaculture settings [77]. Some *Vibrio* sp can degrade toxic PAHs within the marine ecosystem [77,78]. *Vibrio* sp. strain J502 was isolated from seawater in Logy Bay, Newfoundland, and grown in marine minimal media with un-weathered crude oil as the sole carbon source present. This isolation method suggests that *Vibrio* sp. strain J502 can utilize the hydrocarbons found in crude oil as a carbon source, thus degrading some components of the oil.

Vibrio sp. strain J502 is halophilic and mesophilic, suggesting that it is adapted to marine environment surface waters. Vibrios generally grow well at temperatures between 15 – 30°C [77], and *Vibrio* sp. strain J502 has optimal growth at 15°C but can tolerate and grow in temperatures between 4 – 28°C. All *Vibrio* species are gram-negative, and many are motile rods, with a facultative fermentative metabolism. *Vibrio* sp. strain J502 matches this general description, and in addition produces a cellular capsule and forms orange pigmented colonies.

The biochemical profile obtained using API 20NE, API 20E and API ZYM showed that *Vibrio* sp. strain J502 was able to reduce nitrates and sugars, and produce indole, urease, and protease. The biochemical profile of *Vibrio* sp. strain J502 closely resembles that of *Vibrio anguillarum* J360, except that *Vibrio* sp. strain J502 tested positive for α-galactosidase, α-glucosidase, β-glucosidase, and N-acetyl- β-glucosaminidase. However, the use of phenotypic characteristics for identification of genera and species of *Vibrionaceae* is complex due to the great variability of phenotypic features in the genus [77]. The APIE identification code was 727700456, and the API20NE was 7777745, suggesting a possibility of *V. fluvialis* for both tests.

Vibrio sp. strain J502 showed hemolytic activity on blood agar plates at both 15°C and 28°C, which suggests that this species may be pathogenic and capable of hemolysis at a range of

temperatures. Further investigation will be required to determine if *Vibrio* sp. strain J502 has pathogenic properties.

Generally, *Vibrio* sp. is susceptible to the O-129 agent and β-lactam antibiotics [79]. The antibiogram analysis of *Vibrio* sp. strain J502 indicated that it is susceptible to all antibiotics tested except for ampicillin. The class C beta lactamase (N5E84_RS20505) gene located in the genome of *Vibrio* sp. strain J502 is involved in the process of breaking the β-lactam ring of β-lactam antibiotics, such as ampicillin, and providing the bacteria with resistance [80]. *Vibrio* sp. strain J502 was susceptible to the vibriostatic agent O-129, further supporting the evidence that it is a member of the genus *Vibrio* [81,82].

2.5.2 Characterization of Genomic Features, Alignment and Phylogenetic Analysis

The *Vibrio* sp. strain J502 genome is composed of two chromosomes, 3.37 and 1.16 Mb, respectively, and one small plasmid of 0.02 Mb. A total of 4238 genes and 4085 coding sequences were detected. There were 381 (8.99%) hypothetical genes with no identified function. The size and GC content of *Vibrio* sp. strain J502 was comparable to other closely related members of the genus *Vibrio* (Table S1).

Phylogenetic analysis based on whole-genome alignment analysis of chromosome I and II showed that *Vibrio* sp. strain J502 is closely related to *V. anguillarum* J360 and *V. anguillarum* VIB43 (Figure 3). While *Vibrio* sp. strain J502 was isolated from coastal sea water and incubated with crude oil, both *V. anguillarum* J360 and VIB43 were isolated as pathogens from infected host species. *V. anguillarum* J360 was isolated from lumpfish (*Cyclopterus lumpus*) in Newfoundland, Canada [71], while *V. anguillarum* VIB43 was isolated from sea bass (*Dicentrarchus labrax*) in Scotland [83]. The ANI analysis between *Vibrio* sp. strain J502 and *V.*

anguillarum J360 determined a 93.27% similarity for chromosome I, and a 98.87% similarity for chromosome II, indicating a close phylogenetic relationship.

ANI is broadly used and has been proposed as reliable method for the determination of boundaries between species and confirming species identification [84]. A 95-96% ANI with 90% genome coverage has been recommended as the cutoff criterion for the boundary between different species [84–86]. In the case of *Vibrio* sp. strain J502, there is a <95% ANI for chromosome I with its closest identified relative, and a >95% ANI for chromosome II, with 100% genome coverage for both genomes used in the analysis. This suggests that chromosome I is unique, while chromosome II shares a high nucleotide identity with *V. anguillarum* J360. These results contradict the suggested theory that chromosome I of *Vibrio* sp. is shared by a common ancestor and has been largely conserved between species, while chromosome II exhibits a greater diversity between species and represents a collection of accessory elements that differ depending on the niche of the particular species [87,88]. It has also been suggested that chromosome II originated as a megaplasmid has been shaped by horizontal gene transfer, explaining why it shows a greater diversity between members of the same genus [41]. The results presented here suggest that it may be chromosome I of *Vibrio* sp. strain J502 might have modifications that are not shared with *Vibrio* ancestors, supporting our conclusion that *Vibrio* sp. strain J502 is a novel isolate.

2.5.3 Lipid Content and Quinone Analysis in Relation to Identity

Vibrio sp. strain J502 has 100% type Q8 quinones, which is a very common quinone among Proteobacteria [89]. Other *Vibrio* species have been shown to have a variety of respiratory quinones, such as *Vibrio alginolyticus* which has menaquinone 8 (MK-8) as its

primary quinone type [90], and *Vibrio zhugei*, a novel species which has both Q7 and Q8 quinones [91].

Comparison between the fatty acid content profile of *Vibrio* sp. strain J502 and other *Vibrio* species (*V. anguillarum, V. parahaemolyticus, V. alginolyticus* and *V.vulnificus*) shows that there are several differences between them. Based on this comparison, the most closely related to *Vibrio* sp. strain J502 is *V. anguillarum*. The most significant differences between *Vibrio* sp. strain J502 and *V. anguillarum* are the percentages of $C_{16:1}$ ω9c and $C_{18:1}$ ω7c present in the bacterial membranes. *Vibrio* sp. strain J502 has 2.26% $C_{16:1}$ ω9c, while *V. anguillarum* has 43% $C_{16:1}$ ω9c. In addition, *Vibrio* sp. strain J502 has 1.27% $C_{18:1}$ ω9c, while this fatty acid was undetected in all other strains that were compared. These differences suggest that the lipid profile of *Vibrio* sp. strain J502 is unique.

2.5.4 Genes Associated with Virulence, Environmental Adaptation and Degradation of Aromatic Hydrocarbons

Pathogenesis-related genes were located on both chromosome I and II, with all the hemolysin-related genes being found on chromosome I. Hemolysins are exotoxins, which lyse erythrocyte membranes and lead to the release of the iron-binding protein, hemoglobin [92]. Hemolysins are among the most common toxins found in pathogenic *Vibrio* sp. and are categorized into four families including thermostable, E1 Tor, thermolabile and thermostable hemolysins [92]. *Vibrio* sp. strain J502 chromosome I have genes encoding for a hemolysin (N5E84_RS040200), hemolysin III family protein (N5E84_RS12835) and thermostable hemolysin (N5E84_RS03585). The presence of these genes supports the positive result obtained from the β-hemolysis phenotypic test.

Genes related to the type VI secretion system were located on chromosome I and II. The type VI secretion system was first identified in *V. cholerae* and is involved in the pathogenic

mechanism of many Gram-negative Proteobacteria [93]. Two copies of Hcp, hemolysin-coregulated protein, were in the genome of *Vibrio* sp. strain J502, one on each of the chromosomes (N5E84_RS04855, N5E84_RS19720). Two copies of ImpA family N-terminal domain-containing protein, which is associated with the structural components of the type VI secretion system [94], were located on chromosome II (N5E84_RS16045, N5E84_RS04850). In addition, six genes related to the type IV secretion system were located on chromosome I. Type IV secretion systems are protein complexes that are found in the cell envelope of bacteria and contain a channel through which proteins and DNA can be translocated [95]. The system's functions range from transferring DNA from one cell to another via conjugation, to DNA uptake from the extracellular environment to host-pathogen interactions in pathogenic species through the transfer of proteins [95]. The specific functions of the *pilO, pilM, pilP, pilQ, pilT* and *pilW* genes located on chromosome I of *Vibrio* sp. strain J502 are unknown but could be related to virulence and pathogenesis given the strain's close phylogenetic relationship to several pathogenic Vibrios.

Vibrio sp. strain J502 possesses several genes associated with motility, including the operons *fliIJK* (N5E84_RS02650, N5E84_RS02655, N5E84_RS02660) and *flgABCFGHIKMNOPT* (N5E84_RS02090, N5E84_RS02105, N5E84_RS02110, N5E84_RS02125, N5E84_RS02130, N5E84_RS02135, N5E84_RS02140, N5E84_RS02150, N5E84_RS02085, N5E84_RS02080, N5E84_RS02070, N5E84_RS02075, N5E84_RS02065) located on chromosome I, which is consistent with the mot+ phenotypic test (Table 1).

Seven genes related to fermentation were located on *Vibrio* sp. strain J502 chromosome I and II (N5E84_RS16985, N5E84_RS13315, N5E84_RS13310, N5E84_RS00845, N5E84_RS16980, N5E84_RS00850, N5E84_RS16955), which is consistent with the phenotypic

test result that determined that this species is a facultative anaerobe. Many *Vibrio* species are facultative anaerobes, capable of both a fermentative and respiratory metabolism [96].

Several genes of interest encoding proteins related to antibiotic resistance were located within the genome of *Vibrio* sp. strain J502. Two of these genes, *hipA* and *rmf*, are related to persistence and multidrug tolerance functions. The *hipA* gene encodes a serine-threonine kinase that has been linked to inhibiting cell growth and inducing persistence in *Escherichia coli* [97], while *rmf* encodes a ribosomal modulation factor that has been linked to cellular resistance to heat stress, acid stress and osmotic stress in *E. coli* [98]. The *hipA* gene was located on a GI within the genome of *Vibrio* sp. strain J502. Multi-drug efflux transporters (N5E84_RS12980, N5E84_RS01650, N5E84_RS20655, N5E84_RS01500, N5E84_RS20655) were found of *Vibrio* sp. strain J502 chromosome I and II. These efflux pumps are ubiquitous transmembrane transporters found within both Gram-positive and Gram-negative bacteria and facilitate the extrusion of a variety of toxic compounds, including antibiotics [15]. Despite the presence of these genes, *Vibrio* sp. strain J502 was susceptible to all the antibiotics tested in the antibiogram except for ampicillin (Table 1), suggesting that perhaps these efflux transporters are involved in the extrusion of other compounds such as bacterial metabolites or virulence factors [100].

Environmental stress response genes were in the genome of *Vibrio* sp. strain J502. The universal stress genes, *uspB* and *uspE* were found on chromosome I. In *E. coli*, the Usp protein family has been found to be stimulated by conditions including stationary phase, carbon, nitrogen, phosphate, sulphate or amino acid starvation, heat exposure, oxidants, metals, and antibiotics [101]. The envelope stress response genes, *pspB* and *pspC*, were also located on chromosome I. Envelope stress proteins are found in Gram-negative bacteria and are integral to the cell's response to changing environmental conditions and restoring envelope homeostasis

[102]. These proteins have been shown to respond to changing environmental temperature and pH, osmolarity, unfavourable redox conditions, and the presence of toxins and antimicrobials [102]. In addition, carbon starvation protein A, CsrA and DNA starvation/stationary phase protection protein were located on chromosome I. Carbon starvation protein A, CstA, is an inner membrane protein that is highly conserved across multiple species and is involved in biofilm formation and motility [103]. Carbon starvation protein A has been shown to be negatively regulated at the translational level by the carbon storage regulator CsrA, which regulates glycogen synthesis, glycolysis, motility, and biofilm production [103,104]. The DNA starvation/stationary phase protection protein functions in protecting bacterial cells against stressors including starvation, oxidative stress, metal toxicity and thermal stress [105].

Four genes associated with glutathione stress response, including two copies of glutathione S-transferase, glutathione-disulfide reductase and glutathione binding-like protein were found in the *Vibrio* sp. strain J502 genome. The glutathione S-transferase family of enzymes are involved in the inactivation, degradation, and excretion of a variety of toxic compounds [106,107]. In addition, these genes have been found in bacterial operons and gene clusters related to growth on recalcitrant compounds and degradation of aromatic compounds [106].

Vibrio sp. strain J502 possesses several genes related to the degradation of aromatic hydrocarbons including homogentisate 1,2-dioxygenase, maleylacetoacetate isomerase and two copies of fumarylacetoacetate hydrolase. These genes are related to the metabolism of naphthalene to central carbon metabolites via the gentisate pathway. Based on genetic and metabolic studies, the naphthalene degradation pathway has been organized into the “upper” carbaryl to salicylate pathway, “middle” salicylate to gentisate pathway, and “lower” gentisate to

central carbon intermediates pathway [108]. The LysR- and TetR-type transcriptional regulators have been identified in the lower naphthalene degradation pathway [108]. Homogentisate 1,2-dioxygenase converts gentisate to maleylpyruvate, maleylacetoacetate isomerase converts maleylpyruvate to fumarylpyruvate, and fumarylacetoacetate hydrolase converts fumarylpyruvate to fumarate and pyruvate [109]. The presence of homogentisate 1,2-dioxygenase is used as an indicator of an organism's ability to degrade PAHs [110]. *Vibrio* sp. strain J502's ability to utilize gentisate as a carbon explains how it can grow in the presence of crude oil as a sole source of carbon.

2.5.5 Transcriptomic profile of Vibrio sp. strain J502 in the Presence of Sea Water and Water Accommodated Fraction (WAF) of Crude Oil

2.5.5.1 Genes Related to Stress Response

Genes related to stress response, such as *uspB*, *pspC*, *pspB*, DNA starvation/stationary phase protection protein, and carbon starvation protein were upregulated in the presence of crude oil. The *uspB* gene is a member of the Usp family of proteins and is known to be stimulated in conditions including carbon, nitrogen, and phosphate starvation [101]. *Vibrio* sp. strain J502 was incubated in UV-sterilized natural seawater without additional nutrients, therefore, it is likely that the levels of nitrogen and phosphate were below ideal conditions for bacterial growth. While it is not possible to determine the exact cause of the stress response, it was likely related to multiple environmental factors.

The envelope stress response genes *pspB* and *pspC* are involved in responding to changing environmental conditions and restoring envelope homeostasis [102]. In this experiment, the bacteria was grown in TSB 2% NaCl media, then transferred to water accommodated fraction of oil (WAF). This environmental change triggered the upregulation of

genes responsible for regulating the internal cell conditions such as the envelope stress response genes.

Carbon starvation protein A is involved in biofilm formation and motility and is regulated at the translational level by carbon storage regulator, CsrA [111]. CsrA is known to activate processes that support exponential growth, while it represses stationary phase and stress responses such as biofilm formation [111]. Its primary role is as a repressor and its overall effect on gene expression is negative. As carbon starvation protein A was upregulated in oil exposure conditions, it is likely that CrsA regulator was downregulated to some extent, and therefore genes related to stress responses were more highly expressed in the absence of the expression of the repressor. The DNA starvation/stationary phase protection protein is involved in protecting the bacterial cell from stressors and was upregulated in oil exposure conditions. These results suggest that *Vibrio* sp. strain J502 is in a state of stress when exposed to crude oil versus the control seawater conditions, at least during the short-term timeframe examined during this experiment.

Three genes related to glutathione stress response, including glutathione-disulfide reductase, glutathione S-transferase and glutathione S-transferase family protein were upregulated in the presence of crude oil. The glutathione S-transferase family of proteins are known to be involved in the inactivation and degradation of a variety of compounds and growth on recalcitrant compounds. The upregulation of this family of genes indicates that *Vibrio* sp. strain J502 was likely reacting to the presence of hydrocarbons in the treatment.

2.5.5.2 Genes Related to Bacterial Environmental Physiology Response

There was decreased transcription of genes encoding elements of protein secretion systems in oil exposure conditions. The type VI secretion system tube protein Hcp, pilW type IV

pilus biogenesis/stability protein, and pilO type 4a pilus biogenesis protein were downregulated in the presence of oil. As these genes related to bacterial fitness (e.g., communication, anti-bacterial activity, and ion uptake) [93,95,112] were downregulated and stress response related genes were upregulated, confirming that oil at least initially triggers a stress response in *Vibrio* sp. strain J502.

Hemolysins were not significantly up or downregulated in the presence of crude oil, indicating that oil exposure had no significant impact on the hemolysin activity of *Vibrio* sp. strain J502.

The class C β-lactamase gene, which provides the bacteria with antibiotic resistance to β-lactam antibiotics [80], was downregulated in the presence of crude oil. Meanwhile, a multidrug efflux transporter involved in the extrusion of toxic compounds such as antibiotics was upregulated. Therefore, it seems that the need to extrude toxic compounds increases in crude oil exposure conditions, and *Vibrio* sp. strain J502 may become susceptible to β-lactam antibiotics.

The type II toxin-antitoxin system *relE*/*parE* family toxin (N5E84_RS19830), and Type II toxin-antitoxin system *ParD* family antitoxin were both upregulated in the oil treatment. The toxin-antitoxin system comprises a stable toxin and unstable antitoxin that can neutralize the toxin. The type II toxin antitoxin system is widely distributed among bacteria, and are involved in many functions including persistence, stress response and biofilm formation [28]. It is not known what the exact function of these toxin-antitoxin systems is in *Vibrio* sp. strain J502. However, it is interesting to note that they have been associated with stress and persistence, and that many of the other genes associated with these functions were also upregulated in the presence of crude oil (Table S4).

2.5.5.3 Genes Related to Degradation of Aromatic Hydrocarbons

WAF was chosen as a means of exposing *Vibrio* sp. strain J502 to light crude oil, as the production of WAF emulates the natural process of seawater mixing with crude oil in the ocean and is an established method for performing aquatic toxicity tests [113]. WAF contains the soluble and mechanically dispersed droplets with non-soluble compounds. Therefore, the compounds present in WAF at the highest concentrations are typically naphthalenes and methylated naphthalenes, and intermediate PAHs such as fluorene, pyrene, phenanthrene and fluoranthene [114]. The dialysis bag membrane used for the transcriptomic experiment had a pore size of 3.5 kDa, which would allow for these small soluble molecules such as naphthalene (0.128 kDa [115]), fluorene (0.166 kDa [116]), pyrene (0.202 kDa [117]) and phenanthrene (0.178 kDa [117]) to pass through and interact with the bacteria.

The genes encoding for homogentisate 1,2-dioxygenase, fumarylacetoacetate hydrolase and MaiA maleylacetoacetate isomerase were found to be significantly upregulated in the presence of crude oil (Figure 2-7). These genes are part of the metabolism of naphthalene to central carbon metabolites via the gentisate pathway [107,109,110]. The fact that these genes are upregulated in crude oil exposure condition after the timepoint of three days indicates that there was sufficient gentisate present in the crude oil for active degradation by *Vibrio* sp. strain J502 to occur. As we only know the transcriptomic profile for one timepoint, it is not possible to determine when optimal degradation occurred or when the gentisate present was completely degraded. In general, the significant upregulation of these genes in oil exposure conditions supports the hypothesis that *Vibrio* sp. strain J502 is capable of degrading select aromatic hydrocarbons found in crude oil.

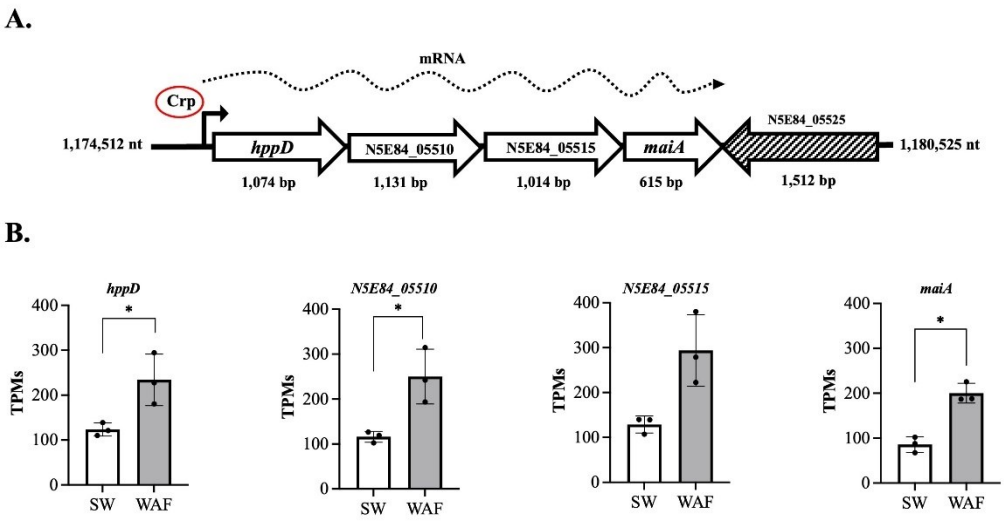

Figure 2-7. Operon containing *hppD* (4-hydroxyphenylpyruvate dioxygenase), N5E84_05510 (homogentisate 1,2-dioxygenase), N5E84_05515 (fumarylacetoacetate hydrolase family protein), and *maiA* (maleylacetoacetate isomerase) upregulated genes.

2.6 Conclusion

In this study, a marine bacterium capable of utilizing compounds found in crude oil as a source of carbon was isolated and identified as a member of the genus *Vibrio*. *Vibrio* sp. strain J502 appears to be a bacterium with a diverse metabolism and variety of mechanisms for surviving in stressful environmental conditions. In oil exposure conditions, genes related to environmental stress management and degradation of aromatic hydrocarbons were upregulated, while genes related to pathogenesis were downregulated. Genomic results showing that chromosome I of *Vibrio* sp. strain J502 shares a 93.25% ANI with its closest phylogenetic relative combined with its unique fatty acid and respiratory quinone profile further support our conclusion that *Vibrio* sp. strain J502 represents a novel isolate.

3. CHAPTER III: The hydrocarbon-degrading potential of a novel isolate, *Vibrio* sp. strain J502

3.1 Abstract

Marine oil spills and seeps may occur naturally or due to anthropogenic activity such as marine shipping or oil and gas exploration and drilling offshore. Oil spills represent a direct threat to marine organisms such as fish, marine mammals, and birds due to the toxicity of chemicals found within crude oil. Crude oils are primarily composed of hydrocarbons, which include aliphatic and aromatic compounds, asphaltenes, resins and many other uncharacterized molecules. Naturally occurring marine bacteria play a vital role in the degradation of hydrocarbons in the marine environment by breaking them down into simpler compounds that can be reintegrated into the marine biogeochemical cycle. Here, I evaluate the hydrocarbon-degrading metabolic capabilities of *Vibrio* sp. strain J502, as well as its ability to survive in the presence of chemically dispersed crude oil. I found that *Vibrio* sp. strain J502 is capable of survival in the presence of crude oil and chemical dispersant, and that it is able to biodegrade LMW PAHs such as naphthalene and its variants. The *n*-C_{17}: Pristane ratio, an established indicator of oil biodegradation, was measured throughout the incubation experiment and the resulting trend indicated that biodegradation of oil did take place in the biotic treatment compared to the abiotic control. However, the results of the incubation experiment were unable to conclusively determine if this bacterium is capable of degrading higher weight PAHs or heavy aliphatic and aromatic compounds. These results suggest that *Vibrio* sp. strain J502 has the metabolic capability of degrading low weight aromatic hydrocarbons found in crude oil, which supports the conclusions drawn based on the genomic and transcriptomic data presented in chapter II.

3.2 Introduction

Over 35 million barrels of oil are transported by sea across the world's oceans every year, putting the marine environment at risk for pollution from oil spills [45]. In addition to increased marine transport tanker traffic, there has also been a dramatic increase in petroleum spills from oil wells, pipelines and drilling rigs as the global oil industry continues to grow [7].

An oil spill can be defined as a release of liquid petroleum hydrocarbons into the environment caused by anthropogenic activity [6]. Oil spills in the ocean pose a direct threat to marine birds, mammals, and fish due to the toxicity of the oil and the formation of oil slicks. Environmental recovery from large-scale marine oil spills in most cases takes between two and ten years, with long-term impacts related to changes in ecosystem structure persisting due to the longevity of some of the affected species [10].

Naturally occurring marine bacteria play a major role in the recycling of carbon in the ocean by transforming some of the hydrocarbons into substances which can be integrated back into biogeochemical cycles [43]. Many of these bacterial species can utilize hydrocarbons as an energy source [118].

Vibrio sp. strain J502, which was isolated from Newfoundland waters, grows at temperatures between 4 and 37°C, but grows optimally at 15°C. *Vibrio* sp. strain J502 is a Gram-negative, rod shaped, motile, capsule-producing bacterium and produces colonies that are orange pigmented and smooth. The whole genome sequencing of *Vibrio* sp. strain J502 identified two chromosomes and one plasmid with a total genome size of 4,540,400 bp and a G+C content of 44.692% (Wells *et al*., 2024, *in preparation*). The genome of *Vibrio* sp. strain J502 has been deposited to NCBI (accession number NZ_CP104554, BioProject PRJNA880584 and BioSample SAMN30853963). Phylogenetic analysis identified *Vibrio* sp. strain J502 as a member of the

genus *Vibrio* but was unable to identify a close enough match to determine the species. Therefore, this strain was named *Vibrio* sp. strain J502 and has been identified as a novel strain (Wells *et al*., 2024, *in preparation*).

In this study we used a heavy crude oil to explore the metabolic capabilities of *Vibrio* sp. strain J502. Crude oils are composed of many different hydrocarbons, which can be characterized broadly as aliphatics and aromatics, as well as resins, asphaltenes, and many uncharacterized molecules. The specific composition of each oil determines its properties and behaviour. Commonly, oil is described by grouping its aliphatic and aromatic compounds separately and by their carbon content, and additionally determining concentrations of specific aromatics, such as BTEX (Benzene, Toluene, Ethylbenzene, Xylenes), and PAHs (polycyclic aromatic hydrocarbons) [119].

Aliphatic compounds are a group of organic compounds characterized by an open-chain structure with a variable number of single, double, and triple bonds [120]. Aliphatic compounds, including straight-chained alkanes are more easily biodegraded than aromatic compounds due to their more simplistic structure [121] .

Aromatic hydrocarbons are cyclic, planar compounds and include the polycyclic aromatic hydrocarbons (PAHs). The heterocyclic aromatic ring structure, hydrophobicity and thermostability of aromatic hydrocarbons make them recalcitrant and more likely to persist in the environment than aliphatic hydrocarbon compounds [122]. The high molecular weight (HMW) PAHs are made up of four or more aromatic rings, while LMW PAHs are made up of 3 or less aromatic rings [123].

Chemical dispersants are used to emulsify oil found in an oil slick or oil spill, and through interaction with wave activity, oil is broken down into many small droplets. This increases the surface area of the oil and allows it to be colonized by marine bacteria, including those that are capable of degrading compounds found in the oil. Therefore, the addition of dispersants to oil makes it more bioavailable and may increase the rate of biodegradation by marine microbes. In this study, chemical dispersants are utilized to increase the bioavailability of the oil and increase the rate of biodegradation potentially occurring during the experiment. This is important because the experiment has a fixed length and sampling points, so the increased bioavailability of the oil increases the chances that biodegradation trends will be detectable during the timeline of the experiment. In addition, the use of chemical dispersant keep the oil more uniformly distributed in the media and decreases the amount of aggregation and clumping that would occur without the addition of the dispersant. This decreases variability between replicates for oil concentration and increases the quality of data produced throughout the experiment.

Here we present data collected during two experiments exploring the oil degrading ability of a novel bacterial strain isolated in Newfoundland Canada, *Vibrio* sp. strain J502. The objective of the first experiment was to determine the bacterium's survival rate when exposed to crude oil, while the objective of the second experiment was to determine what types of compounds, if any, the bacterium was capable of degrading. This study examines the interaction of the isolated bacterium with a large variety of hydrocarbon compounds, which provides significant information on its metabolic capacity and potential role in biodegradation. While many studies focus on degradation of individual classes of compounds or on degradation by a consortium of

species, this study's scope provides a higher level of detail on *Vibrio* sp. strain J502's ability to degrade hydrocarbons found in crude oil.

3.3 Materials and Methods

The hydrocarbon-degrading potential of *Vibrio* sp. strain J502, was investigated through two experiments; the first of which involved incubating the bacterial culture in chemically dispersed crude oil for a period of six weeks to monitor the ability of the bacterium to survive and adapt its metabolism in these conditions (experiment 1). In a second experiment conducted under identical conditions, the bacterium was incubated for four weeks in chemically dispersed crude oil to monitor for changes in oil composition (experiment 2). Dispersed oil was prepared as a chemically enhanced water accommodated fraction (CEWAF) of conventional crude oil. The incubations were carried out in 250 ml flasks placed on an orbital shaking table at 150 rpm at 15°C. In both experiment 1 and 2, triplicate samples were collected at each sampling points, and concentrations of live bacteria were determined via the Colony Forming Units (CFU) approach (experiment 1), or bulk oil concentration was measured spectrophotometrically as estimated oil equivalent (EOC), and concentrations of specific oil compounds analysed (experiment 2).

3.3.1 Preparation of artificial seawater and incubation media

To prepare 1 L of artificial seawater (ASW), the following were added to 600 ml of milliQ water and stirred using a magnetic stirrer: 23.9 g NaCl (39.8 g/L); 4.0 g Na2SO4 (6.7 g/L); 0.7 g KCl (1.2 g/L); 0.1 g KBr (0.17 g/L) and 0.03 g H3BO3 (0.05 g/L). Additionally, the following were added to 300 ml of milliQ water and stirred using a magnetic stirrer: 10.8 g MgCl2•6H2O (56.0 g/L); 1.5 g CaCl2•2H2O (5.0 g/L); 0.02 g SrCl2•6H2O (0.07 g/L). Both solutions were autoclaved separately and allowed to cool before being mixed under a clean bench. An additional 93.7 ml of milliQ water and 0.172 g of NaHCO3 was added [124]. This

artificial seawater was the base for the media used during incubations, as it mimics natural seawater but is sterile and its composition is known. To prepare media, 0.83 ml of phosphate, nitrate and trace metals solutions and 0.5 ml of vitamin solution were added per 1 L of ASW. Phosphate solution was prepared by mixing 0.5 g of sodium phosphate monobasic with 100 ml of MilliQ water (5.0 g/L), nitrate solution was prepared by mixing 7.5 g of sodium nitrate with 100 ml of MilliQ water (75.0 g/L). Five trace metal stock solutions were prepared by mixing 0.98 g of cupric sulfate (9.8 g/L), 2.2 g of zinc sulfate (22.0 g/L), 1.0 g of cobaltous chloride hexahydrate (10.0 g/L), 18 g of manganese (II) chloride tetrahydrate (180.0 g/L), 0.63 g of sodium molybdate (6.3 g/L) each with 100 ml of MilliQ water. Trace metal stock solution was prepared by adding 1 ml of each of these five trace metal solutions and 5.0 g of ethylenediaminetetraacetic acid iron (III) sodium salt (0.005 g/L) to 1 L of MilliQ water. The vitamin solution was prepared by mixing 1 ml of 0.1 mg/ml biotin stock solution, 0.1 ml of 1.0 mg/ml B12 stock solution, 1 ml of 0.2 mg/ml thiamine HCl stock solution in a volumetric flask and filling to 100 ml of MilliQ water [125]. Artificial seawater and media were autoclaved and mixed under a clean bench to maintain a sterile environment and ensure bacterial activity present throughout the experiment could only be attributed to the presence of *Vibrio* sp. strain J502.

3.3.2 Weathering oil

For this experiment, an unnamed conventional (heavy) crude oil (density 0.925 g cm^{-3}; APIo = 21.3) provided by the MRPI (Multi-Partner Research Initiative – Fisheries and Oceans Canada) was used. The oil was weathered to a 10% weight loss by sparging with clean air. The weathered oil was stored in sealed, dark glass scintillation vials at 4ºC until use.

3.3.3 Preparation of CEWAF (chemically enhanced water accommodated fraction)

A 2 L baffled flask was filled with room-temperature sterile autoclaved ASW allowing for exactly 20% headspace. A sterile positive-displacement pipette was used to add 1 g/L of weathered conventional crude oil to the central surface of the water. A sterile positive-displacement pipette was used to add the dispersant Corexit 9500 to the oil slick at a ratio of 1:20 (dispersant to oil). The flask was sealed with Duraseal and allowed to mix on an orbital shaker at 150 rpm for 1 hour. This was followed by a 1 hour settling time. The CEWAF was harvested through the spigot at the bottom of the baffled flask, discarding the first and last 100 ml of CEWAF and collecting the middle portion. This protocol was developed by de Jourdan [126] to simulate local conditions. ASW was autoclaved and oil and dispersant were added under a clean bench to ensure the media remained sterile.

3.3.4 Bacterial growth media and cultivation conditions

Vibrio sp. strain J502 was isolated and purified in 2017 from seawater (Logy Bay, NL) (47°37'32.6"N 52°39'48.1"W) in marine M9 minimal media containing crude oil (Wells *et al*., 2024 *in preparation*). *Vibrio* sp. strain J502 was routinely grown in Trypticase Soy Broth (TSB, Difco, Franklin Lakes, NJ) supplemented with 2% NaCl at 15°C in a 16 mm diameter glass tube with aeration (roller at 180 rpm) overnight (Wells *et al*., 2024 *in preparation*). When required, the media was supplemented with 1.5% bacto-agar (Difco). *Vibrio* sp. strain J502 was stocked in peptone 1% (Difco) and glycerol 10% (Sigma) at -80°C according to established protocols [53]. For the CFU technique, *Vibrio* sp. strain J502 was plated on Trypticase Soy Agar (TSA, 1.5% agar, Difco, Franklin Lakes, NJ, USA) supplemented with up to 2% NaCl using a streaking technique [52]. It was previously determined that *Vibrio* sp. strain J502 grew well on agar plates.

3.3.5 Inoculation with Vibrio sp. strain J502

In preparation for the experiments, *Vibrio* sp. strain J502 was grown overnight in TSB 2% NaCl at 15°C in a 16 mm diameter glass tube with aeration (roller at 180 rpm). Then, 50 ml of TSB 2% NaCl was inoculated with 500 µl of fresh culture and grown at 15°C with aeration (150 rpm) until reaching an optical density (OD_{600}) of about 1.0 (≈ 5.6 x 10^{10} CFU/ml). The culture was then transferred to two 50 ml falcon tubes and centrifuged at 6000 rpm for 10 minutes. The supernatant was discarded, and cell pellets were resuspended in 10 ml of sterile (autoclaved) phosphate-buffered saline (PBS) and centrifuged at 6000 rpm for 10 minutes. Supernatant was again discarded, and cell pellets were transferred to an Eppendorf tube. The tube was topped up to 500 µl with PBS. This washed and concentrated cell suspension was used to inoculate each incubation flask to a final concentration of ~10^8 cells/ml.

3.3.6 Experimental setup

The first experiment (experiment 1) was focused on determining the growth of *Vibrio* sp. strain J502 in the presence and absence of chemically dispersed oil and Corexit 9500 (three treatments with three replicates each). Three 250 ml flasks containing 150 ml of sterile ASW media were inoculated with bacteria to a concentration of ~10^8 cells/ml to act as a control. Three 250 ml flasks containing 150 ml of sterile ASW media and 8.1 µl of Corexit 9500 (same volume as would be used to prepare CEWAF), and three 250 ml flasks containing 150 ml of CEWAF were inoculated with bacteria to the same concentration. Bacterial concentration was monitored by subsampling from each flask after 0, 7, 14 and 28 days (Supplementary Table S1). A t=0 sample was taken from the control replicates and assumed to be the same for the other two treatments.

The second experiment (experiment 2) was focused on the changes in the chemical composition of the oil to determine if specific oil compounds were degraded in the presence of *Vibrio* sp. strain J502. For each of four time points, six 250 ml flasks were prepared with 150 ml of sterile CEWAF. Half of these flasks (12 replicates) were inoculated with bacteria at a concentration of ~10^8 cells/ml (CEWAF treatment), the second half served as a control treatment. Triplicate flasks of control and treatment were destructively harvested after 0, 7, 14 and 28 days. At each sampling point 3 mL of sample was collected for bulk EOC determination. Three 40 ml samples were collected from each flask at each timepoint and sealed in amber glass vials with Teflon lined caps leaving no headspace for compositional oil analysis. A preservative tablet (sodium-bisulfate) in each 40 mL vial prevented any bacterial activity from continuing. These samples will be referred to as the "aqueous" samples. Additionally, the oil stuck to the walls of each flask was separately sampled by carefully rinsing the walls of each flask with 2 ml of dichloromethane (DCM). The DCM extract from each container was sealed in a small vial with a Teflon cap to prevent evaporation. These samples will be referred to as the "wall" samples. Only aqueous samples were collected at timepoint 0 days because there was no oil stuck to the flask walls initially. All samples (aqueous and wall samples) were shipped directly to RPC (RPC in New Brunswick, Canada) for analysis of *n*-alkanes C_6-C_{32}, and PAHs (Supplementary Table S2 and S3).

3.3.7 Determination of cell growth

The growth of *Vibrio* sp. strain J502 was measured using the dilution plating technique to measure concentration in CFU/ml in triplicate at each timepoint. Several additional methods were initially tested for determining bacterial concentration, including cell staining and flow cytometry [127], as well as DAPI staining and microscopy [128], but were determined not to be

feasible as the oil present in the samples interfered with the ability to accurately count the bacterial cells. In contrast to these other methods, the plating technique measures only actively growing bacteria [129]. Under sterile conditions, 100 µl of sample was added to an Eppendorf tube containing 900 µl of PBS to produce a 1:10 dilution termed a -1 dilution. The sample was vortexed, and a volume of 100 µl of sample was transferred to an Eppendorf tube containing 900 µl of PBS to produce a -2 dilution (1:100). This process was continued until all dilutions up to -8 had been prepared. All dilutions were again vortexed, and 100 µl of each dilution plated on a Trypticase soy agar (TSA) 2% NaCl plate and incubated at 15°C. After four days, colonies were enumerated and CFUs/ml were calculated, based on the dilution(s) that generated between 30 and 300 colonies.

3.3.8 Oil Compound Analysis

All samples for oil composition analysis were stored at 4°C for less than two weeks before analysis at RPC (/www.rpc.ca/english/as-organicchemistry.html). All samples were analysed for PAH and total petroleum hydrocarbons (TPH) (Atlantic MUST), where extractable hydrocarbon compounds (EPH) were fractionated into aliphatic and aromatic compounds. The DCM extracted samples (wall samples) underwent a solvent exchange to hexane before analysis and aqueous samples were extracted with hexane. Volatile hydrocarbons were extracted from the samples by purging with helium. Volatile components were then trapped on an adsorbent and thermally desorbed onto the GC column. Analysis was conducted using mass spectrometry (purge and trap GC/MS). Fractionation of the VPH extract was achieved by quantifying characteristic masses of aromatic compounds within a specific carbon range. The aromatic concentration was then subtracted from the total concentration within the same range to yield the aliphatic concentration. Extractable hydrocarbons were extracted from aqueous samples by

mixing with hexane. The extract was recovered, concentrated, and analyzed via GC-FID. Fractionation of the hexane extract into aliphatic and aromatic fractions was performed on a silica gel column for subsequent GC-FID analysis. Aliphatic compounds, C_6-C_{32} for aqueous and C_{10}-C_{32} for wall samples were measured, as well as aromatic compounds C_8-C_{32} in aqueous samples and C_{10}-C_{32} for wall samples. PAHs were measured for all aqueous and wall samples using mass spectrophotometer gas chromatography (GC-MS). BTEX compounds (benzene, toluene, ethylbenzene, and xylene) were measured in aqueous samples only. The biomarker $n$$C_{17}$: Pristane was measured in both aqueous and wall samples. The reporting limit for fractionated aliphatics and aromatics in aqueous samples ranged between 1.0 and 80.0 µg/L, and between 1000 and 5000 µg/L for wall samples. The reporting limit for PAHs in aqueous samples ranged between 0.01 and 0.05 µg/L and the reporting limit for wall samples was 200 µg/L (Supplementary Tables S2 and S3).

3.3.9 Estimated Oil Concentration (EOC)

EOC was measured in the water phase of all CEWAF samples by collecting a 2 to 5 mL sample from each flask and transferring it to a glass scintillation vial. Between 1 mL and 3 mL of DCM was used to extract the oil, depending on the concentration. The sample volume and DCM volume were adjusted to keep measurement concentrations in the linear range of the calibration curve, which was generated from a serial dilution of the oil that was used to make the CEWAF. One ml of the DCM phase of the sample was transferred to a quartz cuvette, and the absorbance measured spectrophotometrically (GENESYS 150 UV-Vis spectrophotometer) at wavelengths of 340 nm, 370 nm, and 400 nm [130]. These values were then used to calculate the area using the formula below (Supplementary Table S4). A calibration curve prepared with the same oil used to make CEWAF relates the area to oil concentration:

$$\text{Area} = \frac{(A_{340} + A_{370}) \times 30}{2} + \frac{(A_{370} + A_{400}) \times 30}{2}$$

3.3.10 Statistical Analysis

For experiment 1, three replicates of each treatment were prepared: ASW, ASW and Corexit, and CEWAF, all inoculated with the same concentration of *Vibrio* sp. strain J502. Bacterial concentrations were monitored via subsampling from each of the replicate flasks at each timepoint. For timepoint 0, one plate count was prepared for each of the three replicate flasks of the CEWAF treatment and these triplicate samples were assumed to be representative of the concentration in all the flasks at timepoint day 0. For all subsequent timepoints, one plate count was prepared per flask and therefore three concentration values were obtained in CFU/ml of bacteria per treatment. The average and standard deviation of these three concentrations per treatment were calculated using MS Excel. The average concentration of *Vibrio* sp. strain J502 in each treatment in CFU/ml was used to create a graph to visualize the bacterial population over time. Error bars on the graph represent standard deviation between replicates.

For experiment 2, three CEWAF control and three CEWAF with bacterial treatment (CEWAF-BAC) treatment flasks were prepared for each timepoint. At each timepoint, control and treatment flasks were destructively harvested in triplicate. For bulk oil measurement using the EOC method, three samples were collected per flask (9 samples for each the control and the treatment). The average concentration of all nine subsamples was calculated using MS Excel and used to create a graph with error bars representing the standard deviation. To keep headspace minimal the 120 mL of subsamples needed for oil composition analysis of each aqueous sample was shipped in three 40 mL containers and combined for measurement at the RPC lab. The average concentration of each compound or group of compounds for all three replicate flasks

(control and treatment) was calculated from the raw data using MS Excel and a line graph was created with error bars representing the standard deviation of oil concentration in each condition at each timepoint. For the flask wall samples, one sample was extracted in 2 mL of DCM from each flask. The concentration of compounds in each sample was measured at the RPC lab. The average concentration of compounds for all three replicate flasks (control and treatment) and standard deviation between replicates was calculated as described for the aqueous samples. Graphs showing these values were also produced using MS Excel. Error bars are not visible on some data points as the error is very low and the error bars are hidden behind the data point. Unpaired t-tests were completed using GraphPad Prism (version 10.2.2) to compare the concentrations of compounds from the control and treatment. A p-value of <0.05 was considered to be significant.

3.4 Results

3.4.1 Experiment 1: Bacterial Growth in the Presence of Dispersed Crude Oil and Corexit

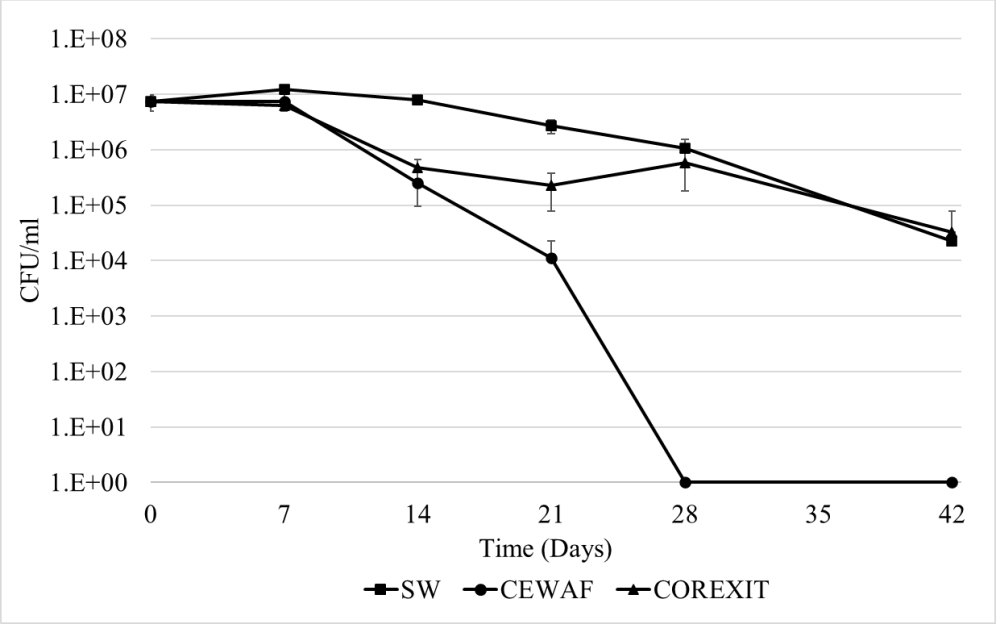

Figure 3-1. Growth of *Vibrio* sp. strain J502 in the presence of the artificial sea water control (SW), CEWAF, and Corexit.

The concentration of *Vibrio* sp. strain J502 decreased in all three treatments, the seawater control (SW), the CEWAF (CEWAF) and the Corexit-only treatment (COREXIT), during the incubation (Figure 3-1). The concentration of *Vibrio* sp. strain J502 decreased most significantly in the CEWAF treatment, dropping from the initial population of 7.36×10^6 CFUs/ml to 0 CFUs/ml by day 28. Meanwhile, the *Vibrio* sp. strain J502 concentration in the Corexit treatment experienced an initial decrease from 7.36×10^6 CFUs/ml to 2.25×10^5 CFUs/ml between day 0 and day 21, before increasing slightly to 5.83×10^5 CFUs/ml at day 28 and decreasing again to a population of 3.23×10^4 CFUs/ml at day 42. The SW control treatment showed a slow decline in bacterial population over the course of the incubation period, decreasing from 7.36×10^6 CFUs/ml at day 0 to 2.22×10^4 CFUs/ml at day 42.

3.4.2 Experiment 2: Bulk Oil Degradation as Measured by EOC

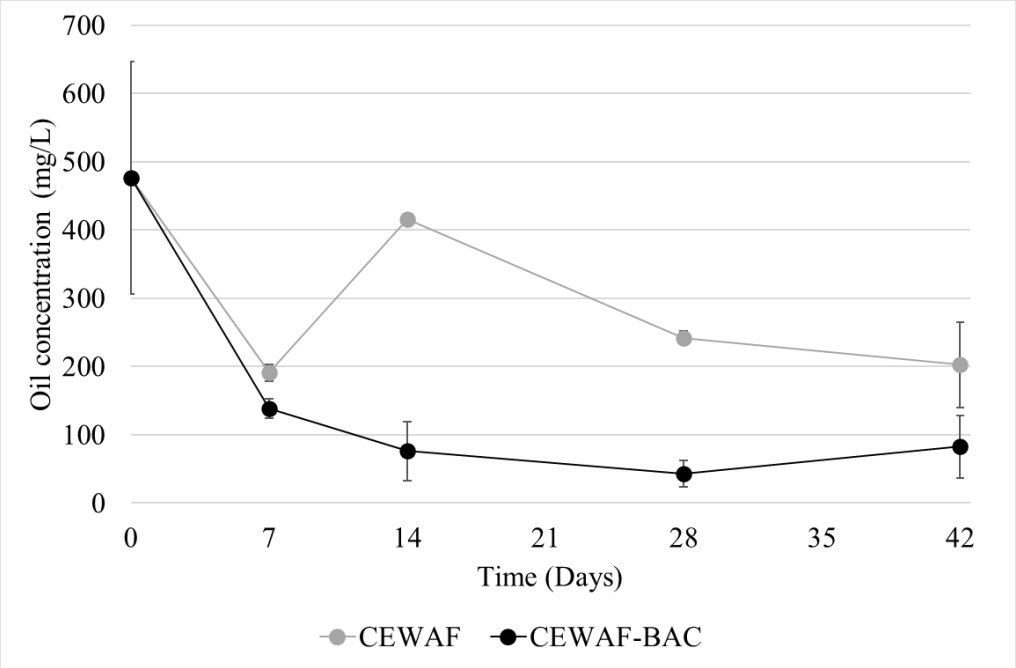

Figure 3-2. Estimated bulk oil concentration in the abiotic control (CEWAF) and the CEWAF and bacteria treatments (CEWAF-BAC) during the 42-day incubation period.

Both the abiotic CEWAF control and the CEWAF-BAC experienced an initial sharp decrease in bulk oil concentration measured as EOC between day 0 and day 7. Thereafter, between days 7 and 28 oil concentration in the control remained above a concentration of ~200 mg/L. In contrast, the oil concentration in the bacteria treatment continued to decrease before plateauing at a concentration of below 100 mg/L. Overall, the CEWAF control experienced a bulk oil concentration decrease of 57%, while the CEWAF-BAC treatment experienced a decrease of 83 % (Figure 3-2).

Between day 7 and 14, there was a sharp increase in the oil concentration in the control. It is likely that this was related to the heterogeneity of the oil-water mixture at this time. At timepoint day 7, it was observed that oil had begun to stick to the walls of the flask and that the aqueous fraction appeared to be transparent and free of large clumps of oil. It was observed that clumps of oil had appeared in the aqueous fraction by day 14, and the oil was visibly no longer homogenously dispersed as it had been at the initial timepoint day 0. At the same time oil concentrations on flask walls decreased appreciably between day 7 and day 14 (see Figure 3-3 below), suggesting that compounds originally attached to flask walls had detached from the wall and entered back into the water phase. This complicated obtaining a representative aqueous bulk concentration sample at the day 7 timepoint and beyond. Nevertheless, the greater decrease in bulk oil concentration in the aqueous phase is clearly visible.

3.4.3 Experiment 2: Degradation of Low-Weight Polycyclic Aromatic Hydrocarbon (PAH)

A)

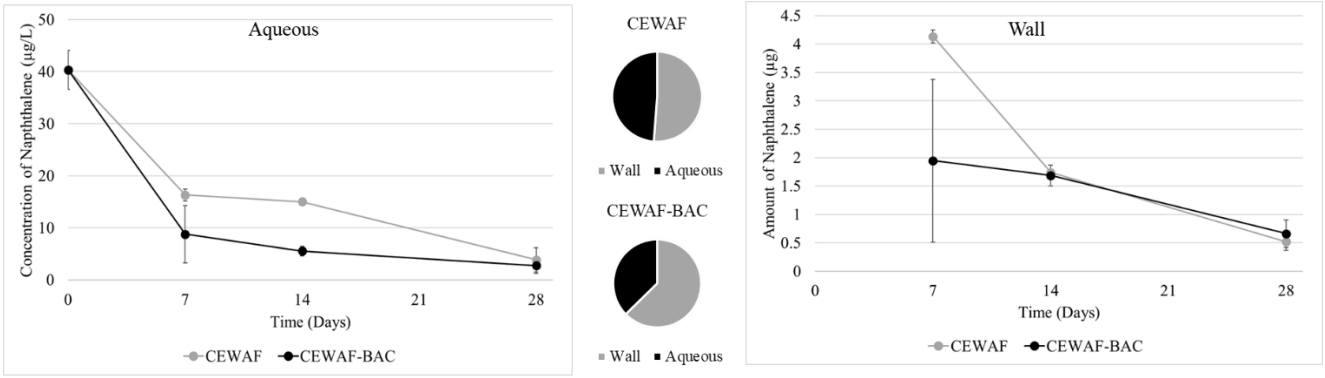

B)

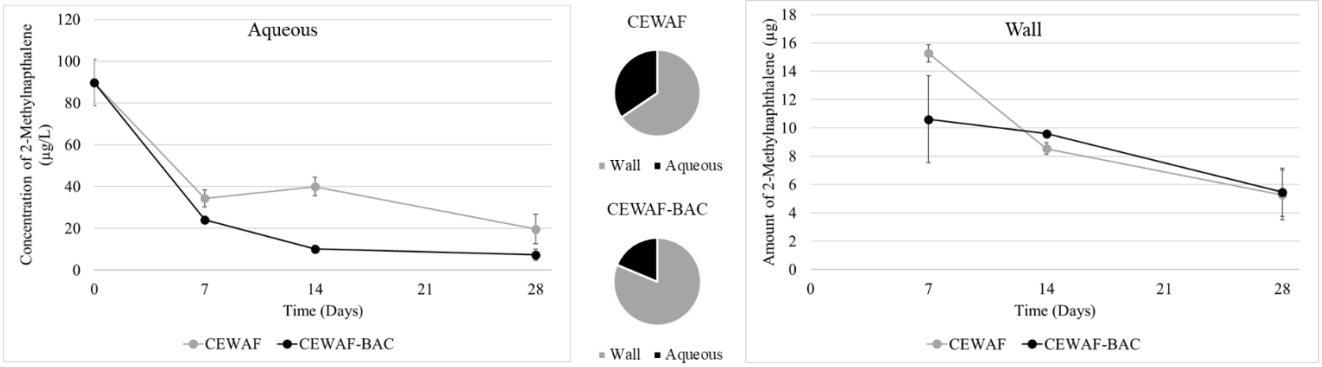

C)

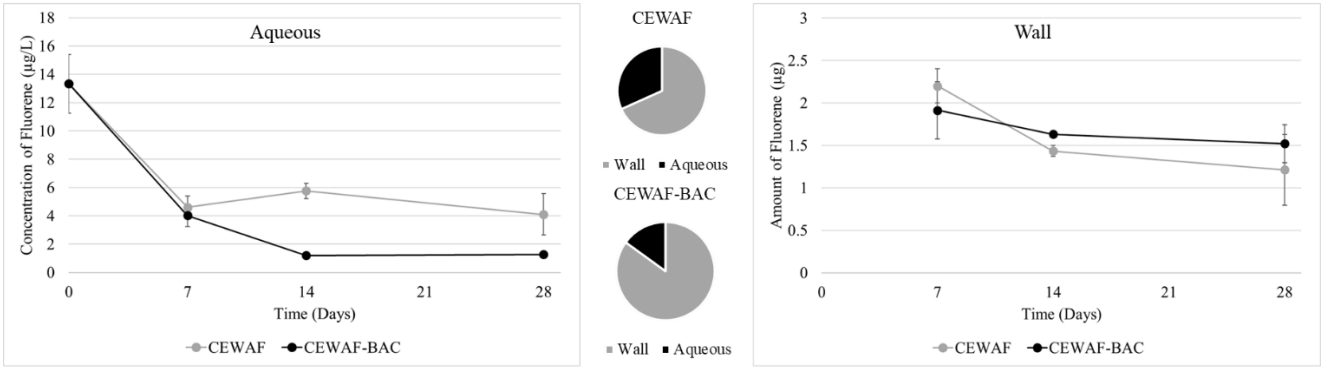

Figure 3-3. Change in concentrations of low weight Polycyclic Aromatic Hydrocarbons (PAHs); A) Naphthalene. B) 2-Methylnaphthalene. C) Fluorene, from the aqueous (left) and wall (right)

fractions, respectively, over time. The central panel depicts the total average oil contribution of each fraction in each treatment (CEWAF, CEWAF-BAC).

Concentrations of naphthalene, 2-methylnaphthalene and fluorene decreased during the incubation in both the CEWAF control and the CEWAF-BAC treatment in both phases, the aqueous phase and on the walls.

In the aqueous phase of the control, concentrations of naphthalene, 2-methylnaphthalene and fluorene decreased by 60%, 62% and 66% respectively during the initial 7 days and continued to decrease thereafter until the final timepoint at day 28. In the bacteria treatment, the initial decreases in the aqueous phase were larger at 78%, 73% and 70% for naphthalene, 2-methylnaphthalene, and fluorene, respectively. After 14 days, concentrations in the aqueous phase of naphthalene, 2-methylnaphthalene and fluorene were always higher in the control compared to the bacterial treatments. By day 28, the concentration of naphthalene in the aqueous phase of the control and the treatment was nearly the same, while the concentrations of 2-methylnaphthalene and fluorene were significantly higher in the control than in the treatment after 28 days ($p = 0.0466$ and $p = 0.0291$, respectively).

The amount of naphthalene, 2-methylnaphthalene, and fluorene on the walls, in contrast showed very little difference between the abiotic control and the bacterial treatment. However, in the control there was a distinct decrease, especially for naphthalene between days 7 and 14, possibly oil compounds previously attached to the flask walls re-entering the aqueous phase and leading to the observed “lumpiness” in the aqueous phase on day 14. At the 14 days timepoint, there was not a large difference in the amount of naphthalene between the control and treatment, however, there was a higher amount of 2-methylnaphthalene and fluorene in the control versus

the treatment. There was no statistically significant difference between the control and treatment at the final timepoint for naphthalene, 2-methylnaphthalene, or fluorene ($p = 0.499$, $p = 0.870$ and $p = 0.32$, respectively).

In the control, approximately 51% of the total naphthalene, 66% of the total 2-methylnaphthalene and 68% of the total fluorene measured in the samples was found stuck to the walls, with the remainder found in the aqueous phase. In the bacteria treatments, approximately 63% of the total naphthalene, 81% of the total 2-methylnaphthalene and 85% of the total fluorene measured in the samples was found in the fraction of oil stuck to the walls, with the remainder found in the aqueous phase.

Additional low-weight PAHs measured included 1-methylnaphthalene, acenaphthene, acenaphthylene, phenanthrene and anthracene. A similar trend to naphthalene, 2-methylnaphthalene and fluorene was also observed for 1-methylnaphthalene and phenanthrene (Supplementary Figure S6). Acenaphthylene, acenaphthene and anthracene were below the detection limit in both aqueous and wall samples.

3.4.4 Trends in Higher-Weight Polycyclic Aromatic Hydrocarbon (PAH) degradation

A)

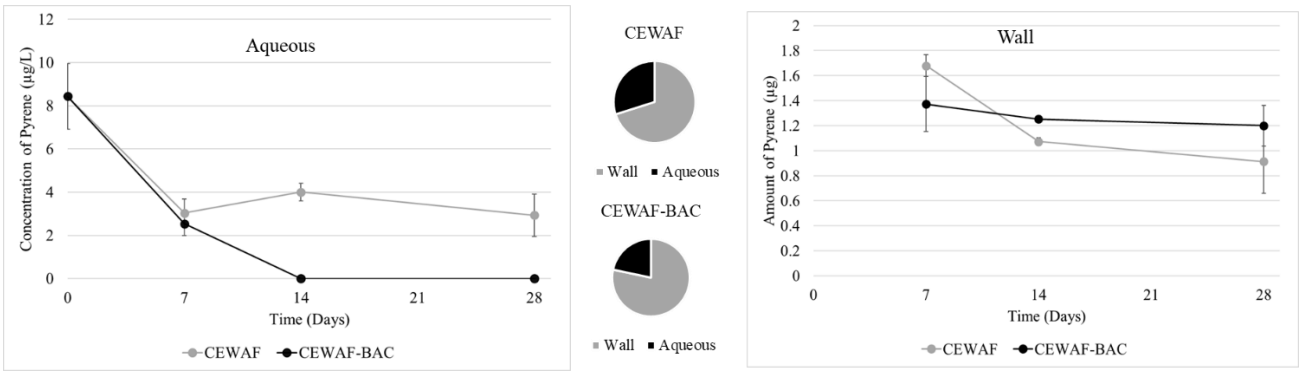

B)

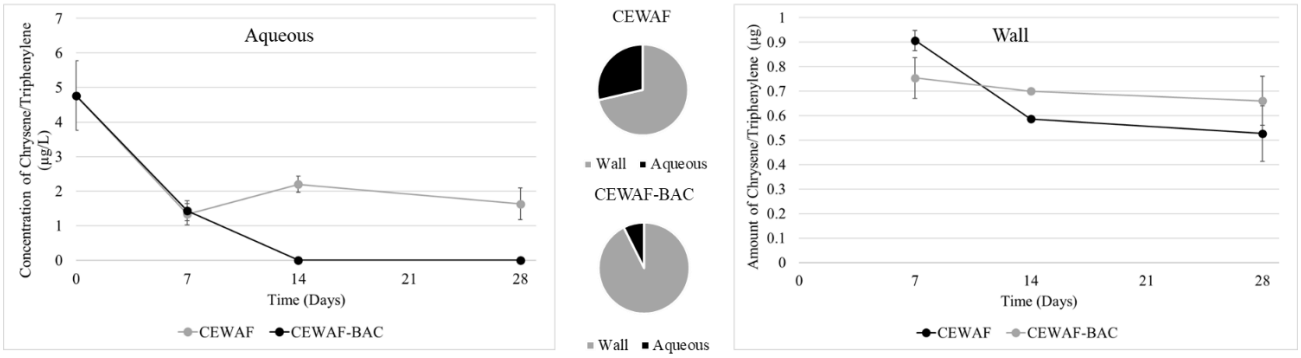

Figure 3-4. Changes in concentrations of high weight polycyclic aromatic hydrocarbons (PAHs); A) Pyrene. B) Chrysene/Triphenylene, from the aqueous (left) and wall (right) fractions, respectively, over time. The central panel depicts the total average oil contribution of each fraction in each treatment (CEWAF, CEWAF-BAC).

Concentrations of pyrene and chrysene-triphenylene decreased during the incubation in both the control and the bacteria treatment in both phases, the aqueous phase and on the walls, but a more pronounced decrease was obvious in the aqueous phase after day 7.

In the aqueous phase of the control, concentrations of pyrene and chrysene/triphenylene decreased by 64% and 72% respectively during the initial 7 days and continued to decrease thereafter reaching concentrations of 2.9 µg/L and 1.6 µg/L by day 28. In the CEWAF-BAC treatment, the initial decrease in concentration in the aqueous phase was 70% for both pyrene and chrysene/triphenylene. After 14 days, concentrations in the aqueous phase of pyrene and chrysene/triphenylene were always higher in the control compared to the bacterial treatments. By day 28, the concentration of pyrene and chrysene/triphenylene was much higher in the control than in the treatment.

The amount of pyrene and chrysene/triphenylene on the walls, in contrast showed very little difference between the abiotic control and the bacterial treatment. At 14 days, the amount of pyrene and chrysene/triphenylene were higher in the treatment than the control but there was no statistically significant difference between the control and treatment at the final timepoint for either compound ($p = 0.176$ and $p = 0.202$, respectively).

In the control, approximately 70% of the total pyrene and the total chrysene/triphenylene measured in the samples was found in the fraction of oil stuck to the walls, with the remainder in the aqueous phase. In the CEWAF-BAC treatment, approximately 78% of the total pyrene and 96% of the total chrysene/triphenylene measured in the samples was found in the fraction of oil stuck to the walls, with the remainder in the aqueous phase.

Additional high-weight PAHs measured included fluoranthene, benz(a)anthracene, benzo(b+j)fluoranthene, benzo(k)fluoranthene, benzo(e)pyrene, benzo(a)pyrene, indeno(1,2,3-c,d)pyrene, benzo(g,h,i)perylene and dibenz(a,h)anthracene. A similar trend to pyrene and chrysene/triphenylene was observed for fluoranthene, benzo(b+j)fluoranthene, benzo(e)pyrene, benzo(a)pyrene and benzo(g,h,i)perylene (Supplementary Figures S7). Concentrations of Benz(a)anthracene, benzo(k)fluoranthene, indeno(1,2,3-c,d)pyrene and dibenz(a,h)anthracene were below the detection limit in both aqueous and wall samples.

3.4.5 Trends in Degradation of Aliphatic Compounds

A)

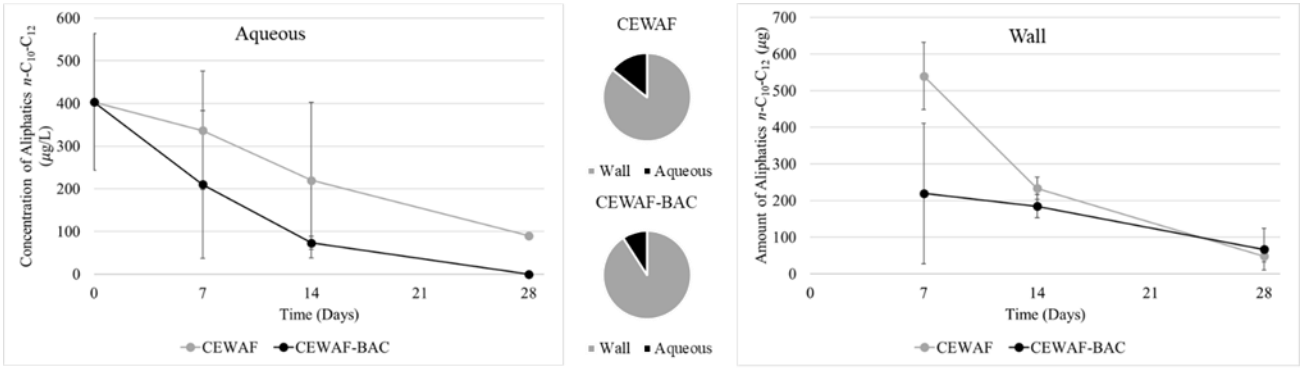

B)

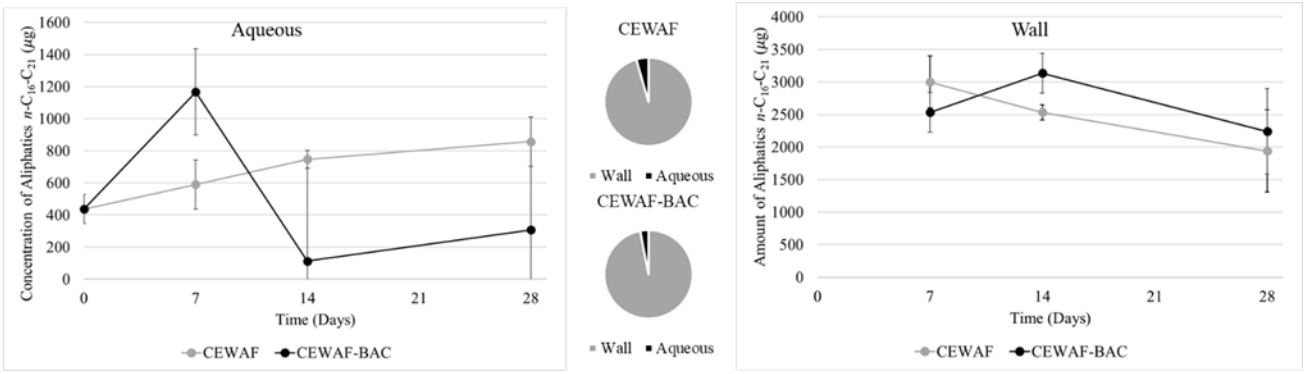

Figure 3-5. Change in concentrations of fractionated aliphatic compounds; A) *n*-C10-C12 B) *n*-C16-C21, from the aqueous (left) and wall (right) fractions, respectively, over time. The central panel depicts the total average oil contribution of each fraction in each treatment (CEWAF, CEWAF-BAC).

Variability between replicates were very high for the concentrations of the volatile *n*-C_{10}-C_{12} aliphatic compounds. Concentrations decreased during the incubation in both the control and the bacteria treatment in both the aqueous phase and on the walls. Average concentrations were always higher in the control compared to the bacteria treatment. Meanwhile, concentrations of *n*-C_{16}-C_{21} aliphatic compounds fluctuated without clear trends in both the control and the CEWAF-BAC treatment in the aqueous phase and on the walls.

In the aqueous phase of the control, concentrations of *n*-C_{10}-C_{12} aliphatic compounds decreased by 17% during the initial 7 days and continued to decrease thereafter reaching a concentration of 90 µg/L by day 28. However, the concentration of *n*-C_{16}-C_{21} control increased by 35% during the first 7 days and then fluctuated up and down throughout the rest of the incubation with high variability and no clear temporal trends (Figure 3-6A). In the aqueous phase of the CEWAF-BAC treatment, the initial decrease after 7 days was 48% for *n*-C_{10}-C_{12} aliphatics, while *n*-C_{16}-C_{21} compounds increased in concentration by 167%. After 14 days, concentrations in the aqueous phase of *n*-C_{10}-C_{12} and *n*-C_{16}-C_{21} aliphatic compounds were always higher in the control compared to the bacterial treatments, but it is important to note that there was a high variability between replicates at this timepoint. The final concentration of *n*-C_{10}-C_{12} aliphatic compounds after 28 days was 0 µg/L, and for *n*-C_{16}-C_{21} aliphatic compounds the final concentration was 307 µg/L. At the final timepoint, there was a higher concentration of *n*-C_{10}-C_{12} in the control than in the treatment, but there was no statistically significant difference in concentration between the control and treatment for *n*-C_{16}-C_{21} ($p = 0.177$).

The amount of *n*-C_{10}-C_{12} and *n*-C_{16}-C_{21} aliphatics on the walls showed very little difference between the abiotic control and the bacterial treatment. There was not a large difference between the control and treatment for *n*-C_{10}-C_{12} aliphatic compounds at day 14,

although there was a difference in concentration for *n*-C_{16}-C_{21} compounds at this timepoint. There was not a statistically significant difference between the control and treatment at the final timepoint for both *n*-C_{10}-C_{12} and *n*-C_{16}-C_{21} aliphatic compounds ($p = 0.612$ and $p = 0.598$, respectively).

In the control, approximately 86% of the total *n*-C_{10}-C_{12} aliphatics and 96% of the total *n*-C_{16}-C_{21} measured in the samples was found in the fraction of oil stuck to the walls, with the remainder in the aqueous phase. In the CEWAF-BAC treatments, approximately 91% of the total *n*-C_{10}-C_{12} and 97% of the total *n*-C_{16}-C_{21} aliphatic compounds measured in the samples was found in the fraction of oil stuck to the walls, with the remainder in the aqueous phase.

Additional fractionated aliphatic compounds measured included *n*- C_6-C_8, C_8-C_{10}, C_{12}-C_{16} and C_{21}-C_{32}. A trend like that of *n*-C_{10}-C_{12}, indicating increased loss of these compounds in the presence of bacteria compared to the control was observed for *n*-C_6-C_8 and *n*-C_8-C_{10}, while a trend like that of *n*-C_{16}-C_{21}, where losses in both the control and the bacteria treatment were similar, was observed for *n*-C_{12}-C_{16} and *n*-C_{21}-C_{32} (Supplementary Figures S8).

3.4.6 Trends in Degradation of Fractionated Aromatic Compounds

A)

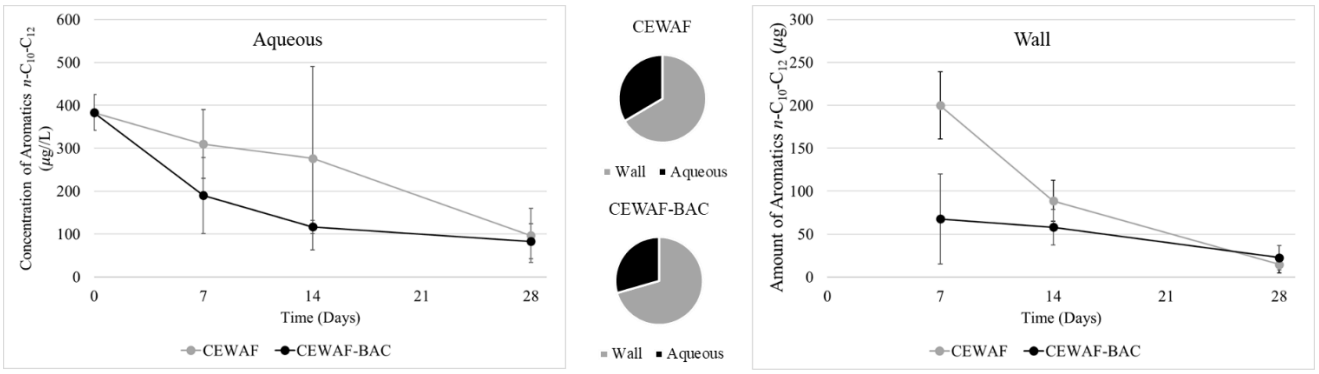

B)

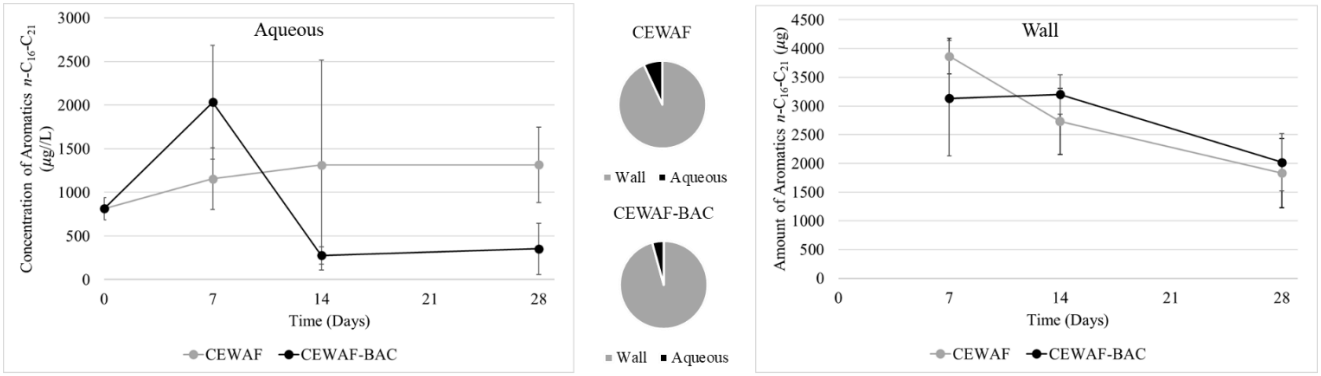

Figure 3-6. Change in concentrations of fractionated aromatic compounds; A) *n*-C10-C12 B) *n*-C16-C21, from the aqueous (left) and wall (right) fractions, respectively, over time. The central panel depicts the total average oil contribution of each fraction in each treatment (CEWAF, CEWAF-BAC).

Concentrations of *n*-C_{10}-C_{12} aromatic compounds decreased during the incubation in the bacteria treatment in both phases, the aqueous phase and on the walls. Meanwhile, concentrations of *n*-C_{16}-C_{21} aromatic compounds fluctuated throughout the incubation in the control and the bacteria treatment in both the aqueous and wall phases.

In the aqueous phase of both the control and treatment for *n*-C_{10}-C_{12} aromatic compounds, the concentration decreased over the incubation period. Although the decrease in concentration was slightly steeper and more rapid in the treatment, there was very high variability between replicates in the aqueous samples of the control and treatment suggesting that this trend may not be significant. The high variability between replicates in the control and treatment is likely because the fraction of oil in the aqueous phase was very low in both, and the compounds found in the aqueous phase are the volatile fraction of aromatic compounds that are more susceptible to evaporation or volatilization during sampling.

The concentration over time of the *n*-C_{16}-C_{21} aromatic compounds in the aqueous phase of the control and treatment displayed no clear trends and no clear differences in trends between the treatment and control. The high variability in concentrations for both the control and treatment are likely related to the fraction of oil in the aqueous phase being very small, and therefore any change in the oil on the flask walls, such as droplets re-entering the aqueous phase, would have a large impact on concentration measurements. There was an overall decrease over time in concentration of *n*-C_{16}-C_{21} aromatic compounds in both the treatment and control, but no clear trends to indicate bacterial degradation.

The amount of *n*-C_{10}-C_{12} and *n*-C_{16}-C_{21} aromatic compounds on the walls showed very little difference between the abiotic control and the bacterial treatment. There was no statistically

significant difference between the control and treatment at day 28 for *n*-C_{10}-C_{12} and *n*-C_{16}-C_{21} aromatic compounds ($p = 0.461$ and $p = 0.700$, respectively).

In the control, approximately 67% of the total *n*-C_{10}-C_{12} and 93% of the total *n*-C_{16}-C_{21} measured in the samples was found in the fraction of oil stuck to the walls, with the remainder in the aqueous phase. In the bacteria treatments, approximately 71% of the total *n*-C_{10}-C_{12} and 96% of the total *n*-C_{16}-C_{21} measured in the samples was found in the fraction of oil stuck to the walls, with the remainder in the aqueous phase.

Additional fractionated aromatic compounds measured included *n*-C_{12}-C_{16} and *n*-C_{21}-C_{32}. A trend like that of *n*-C_{16}-C_{21} was observed for both, *n*-C_{12}-C_{16} and *n*-C_{21}-C_{32}. Like for *n*-C_{16}-C_{21}, there was no clear difference in concentration between the control and treatment present for the *n*-C_{12}-C_{16} and *n*-C_{21}-C_{32} fractions. More than 93% of *n*-C_{12}-C_{16} compounds and 96% of *n*-C_{21}-C_{32} was associated with the flask wall sample, which helps explain the high variability between the replicates of samples measured for these compounds as well (Supplementary Figure S9).

3.4.7 n-C_{17}: Pristane Ratio

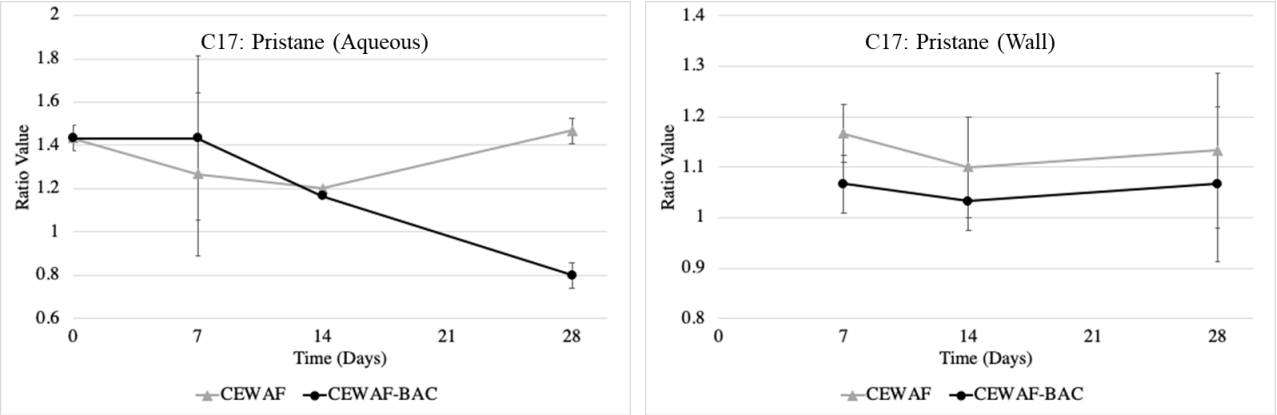

Figure 3-7. Temporal trend of the biomarker ratio *n*-C17: Pristane in the aqueous and wall phase. Error bars denote standard deviation.

The *n*-C_{17}: Pristane ratio measured in the aqueous phase of the CEWAF control fluctuated throughout the incubation period around 1.4 with no clear trend (1.34 ± 0.12) (Figure 3-7). In contrast, the *n*-C_{17}: Pristane ratio measured from the aqueous phase of the CEWAF-BAC treatment decreased from 1.4 on day 0 to 0.8 on day 28. The *n*-C_{17}: Pristane ratio in the treatment is significantly lower than in the control at the final day 28 timepoint ($p = 0.005$).

The *n*-C_{17}: Pristane ratios from the wall samples of both the CEWAF control and CEWAF-BAC treatment did not change significantly over time and fluctuated around 1.1 ± one standard deviation (~ ± 0.09), respectively ($p = 0.621$).

3.5 Discussion

3.5.1 Impact of Chemically Dispersed Crude Oil and Corexit on the Growth of Vibrio sp. strain J502

The more rapid decrease in culturable bacteria in the CEWAF treatment compared to the Corexit and seawater treatments appears contradictory to the expected results since the oil composition data clearly indicated bacterial degradation of several compounds. The decrease in culturable bacteria in the seawater treatment, which contained negligible organic substrate can be explained by the lack of any organic substrates required by the bacteria for growth. The similar decrease of culturable bacteria in the Corexit treatment, suggests that the Corexit was not a usable substrate for this species, although some microorganisms have been shown to use dispersants as growth substrates [131]. Various bacteria including *Colwellia* sp. str. RC25 and *Alcanivorax* sp. str. 31 have been found to be able to degrade various components of Corexit 9500A, such as DOSS and dipropylene glycol n butyl ether [131]. The more extreme drop of culturable bacteria in the treatment with dispersed oil, however, must have a different explanation. The plate counting technique is commonly avoided for marine planktonic bacteria

because many marine bacteria do not grow well when plated. Previous work had indicated that when grown in broth media, the growth of this bacteria could easily be enumerated using the plating technique. So, when grown in TSB 2% NaCl (Trypticase Soy Broth), *Vibrio sp. strain J502* successfully grew when plated on TSB 2% NaCl agar plates. However, when grown in ASW media exposed to oil, the bacteria did not successfully grow on the agar plates, giving the impression that it did not survive the oil exposure.

We suggest that in contrast, the presence of oil led to a shift in gene expression that altered the bacteria's metabolic capacity, with the result that it could no longer grow on these agar plates. The decrease in culturable bacteria would, we hypothesize, represent the change in metabolic capacity rather than a lack of surviving *Vibrio* sp. strain J502. This differs from the traditional view of cells entering the VBNC (viable but non culturable) state [132] which is considered a dormancy state. In our experiment cells must have been actively growing on the oil as shown by the oil compound analysis. Likely these cells were not truly unculturable, but would have needed a different substrate, mimicking their growth conditions to thrive. Alternatively, microscopy or flow cytometry could be utilized to measure bacterial concentrations as they do not require the bacterium to grow in media in order to measure the concentration of cells.

3.5.2 Bulk Oil Degradation measured as EOC

Bulk oil degradation was measured via EOC (estimated oil concentration), a method that employs spectrophotometry to estimate the oil concentration of samples based on an absorbance curve created using known concentrations of the same oil. Although this method is relatively new, it has been used in several studies and been shown to align with results obtained from established methods of determining total petroleum hydrocarbons (TPH) [133–136].

An overall decrease in oil concentration was observed in both the CEWAF control and CEWAF-BAC treatment throughout the incubation period. In both the control and experimental treatment there was a sharp decrease in oil concentration between the initial timepoint and day 7, which we hypothesize represents the loss of simpler, lighter hydrocarbons with short half-lives by photooxidation and evaporation, as well as oil compounds attaching to the flask wall. This abiotic loss of compounds would be roughly similar in both the control and treatment as they were incubated in the same conditions.

The significantly larger decrease of oil concentration in the presence of bacteria (CEWAF-BAC) compared to the control (CEWAF) implies that microbial degradation did take place, especially after the 7-day timepoint (Figure 2). The delay in bacterial degradation between day 0 and 7 would be consistent with the hypothesized period of metabolic adaptation required by the bacteria to degrade hydrocarbons found in the experimental media instead of sugars found in the original growth media. Biodegradation after day 7 was also observed for specific oil compounds and visible in the C_{17}: Pristane ratio.

3.5.3 n-C_{17}: Pristane as an Indicator of Biodegradation

The *n*-C_{17}: Pristane ratio is an established indicators of oil biodegradation [137]. Pristane is an *n*-C19 branched isoprenoid hydrocarbon that is more resistant to biodegradation than the *n*-C_{17} n-alkane, but both have similar volatility [138]. A decrease in their ratio is thus a good indicator for microbial degradation [138]. The initially observed *n*-C_{17}: Pristane value of 1.4 in both control and bacterial treatment is within the expected range for undegraded, slightly weathered crude oils [138]. The lack of a decrease in the ratio for the control, and the clear decrease in the ratio of the bacterial treatment to 0.8 clearly indicates that biodegradation was occurring in the presence of the bacteria [137].

The *n*-C_{17}: pristane ratio for the fractions of the CEWAF-BAC and CEWAF treatments extracted from the cell wall did not increase, indicating that no biodegradation of the oil stuck to the walls took place either with or without bacteria present. One might ask why biodegradation was only significant in aqueous fraction and not for oil on the walls.

The aqueous fraction of the CEWAF mixture contains hydrocarbons both in the dissolved and the droplet form [137,139]. The hydrocarbons attached to the wall as a film had a lower surface area to volume ratio compared to hydrocarbons in the aqueous phase, which existed as small droplets. A larger surface area for the attachment of bacteria likely made the dispersed hydrocarbons more bioavailable. Furthermore, oil compounds attached to the wall were relatively enriched in HMW compounds, which are less likely to be degraded or volatilized compared to their LMW counterparts. Additionally, other studies have demonstrated that the bulk of organic pollutants degrade at a higher rate and more completely in aerobic conditions [140–142]. While oxygen concentrations were likely high in the aqueous phase of the sample, as the flasks were placed on a shaker table for the duration of the incubation, oxygen may have been limited at the surface of the oil film stuck to the glass walls. Although *Vibrio* sp. strain J502 is a facultative anaerobe, it will prioritize utilizing oxygen for its metabolic functions when it is available. Thus, the availability of oxygen likely encouraged a higher rate of biodegradation in the aqueous fraction.

3.5.4 Degradation of Polycyclic Aromatic Hydrocarbons (PAHs) by Vibrio sp. strain J502

The concentration of naphthalene, 2-methylnaphthalene and fluorene present in both the CEWAF control, and the CEWAF-BAC treatment decreased throughout the incubation period in the aqueous portion of the incubation. There was a sharp decrease in the concentration of LMW PAHs in both the control and experimental treatment between day 0 and 7, which can be

primarily attributed to abiotic losses via volatilization [143]. Compared to HMW PAHs, LMW PAHs are more volatile and soluble in water, making them more susceptible to volatilization and biodegradation [143]. Between day 7 and day 14, the concentration of LMW PAHs in the aqueous portion of the CEWAF control either remained the same or increased slightly, while the concentration of LMW PAHs in the aqueous portion of the CEWAF-BAC treatment continued to decrease. The continued decrease in the concentration of LMW PAHs after day 7 in the aqueous phase of the CEWAF-BAC treatment, but not in the control, suggests a switch from abiotic loss to biotic loss of these compounds at some time after that timepoint. This implies that biodegradation of the LMW PAHs was mainly occurring in the CEWAF-BAC treatment after the day 7 timepoint. Between day 14 and day 28, there was a much slower decrease in LMW PAH concentration in the aqueous portion of the CEWAF-BAC treatment, indicating that the rate of biodegradation had slowed, potentially due to the depletion of the biodegradable compounds. The genomic analysis of *Vibrio* sp. strain J502 determined that genes related to the degradation of aromatic hydrocarbons such as naphthalene were present, confirming the ability of this bacterium to degrade these substances (Wells *et al*., 2024 *in preparation*).

The LMW PAHs on the wall were apparently less available to the bacteria, likely because the oil adhered to the glass instead of being dispersed (Figure 4). Concentrations of LMW PAHs on the walls decreased similarly throughout the incubation period in both the control and CEWAF-BAC treatment, suggesting abiotic factors such as interaction with air, heat and light played a role and biodegradation was too small to discern. Likely, as time passed, LMW PAHs in the oil film, migrated to its surface, and into the aqueous phase, explaining the decrease over time.

As for HMW PAHs, the initial decrease of pyrene and chrysene/triphenylene must have been mainly abiotic as this occurred in both the control and the treatment. During these first seven days, the loss rate of the HMW PAHs was lower than that of the LMW PAHs, likely because the HMW PAHs are less volatile than the LMW PAHs. The continued decrease of the aqueous concentration of pyrene and chrysene/triphenylene in the CEWAF-BAC treatment between days 7 and 14, compared to no significant change in concentration in the control, suggests that, as with the LMW PAHs, there was a switch from abiotic to biotic loss processes after day 7. By day 14, concentrations of pyrene and chrysene/triphenylene were negligible in the CEWAF-BAC treatment, but still present in the control. These HMW PAH were utilized within less than 14 days in the presence of *Vibrio* sp. strain J502.

3.5.5 Degradation of Aliphatic Compounds by Vibrio sp. strain J502

The lighter aliphatic *n*-C_{10}-C_{12} compounds in the aqueous phase (Figure 6), appeared to decrease more rapidly in the bacteria treatment than in the control, starting before day 7, although the high variability between replicate samples obscures some of these potential differences. However, the consistently lower concentrations of these compounds in the presence of the bacteria and the noticeable difference in concentration between the control and treatment at the end of incubation implies some level of active biodegradation of these substances in the treatment. No evidence of biodegradation of aliphatic *n*-C_{12}-C_{32} compounds was observed in the aqueous phase. A decrease in concentration of all measured aliphatic compounds attached to the flask wall in both the control and the biotic treatment indicates that biodegradation of aliphatic compounds was negligible, although abiotic loss processes continued throughout the experiment. The abiotic decrease in concentration of aliphatic compounds in the flask wall fraction may, as for the PAHs, have resulted from the migration of the lighter compounds to the slick surface,

from where they could escape into the aqueous phase and likely evaporated. It is also possible that they were degraded in bacterial treatment upon re-entering the aqueous fraction. Minimal or no biodegradation of aliphatic compounds is supported by the fact that no genes attributed to the degradation of *n*-alkanes were identified in the genome of *Vibrio* sp. strain J502, but the lack of their identification does not necessarily prove their absence.

3.5.6 Degradation of Aromatic Compounds by Vibrio sp. strain J502

Limited biodegradation of aromatic *n*-$C_{10\text{-}12}$ may have occurred in the aqueous phase possibly starting before day 7 (Figure 7). Concentrations of these compounds were systematically lower in the biotic treatment compared to the control, but the high variability, possibly caused by exchange between flask wall and aqueous fraction, obfuscated a possible trend. In contrast, no indication of biodegradation was present for the larger aromatics (*n*-$C_{>12}$) or of aromatic compounds attached to the flask walls, since no differences were visible between the control and the bacteria treatment.

3.5.7 Partitioning of Oil Between Aqueous and Wall Phase of the Flasks

Most of the oil (> 50% for LMW compounds and up to >95% of the HMW compounds) in all treatments accumulated on the walls of the incubation flask rather than remaining dispersed in the aqueous portion of the sample, reflecting the viscose and dense nature of heavy crude oil. Notably, for each compound or compound class, the fraction associated with the wall was always higher in the biotic treatment compared to the abiotic control.

Vibrio sp. strain J502 has been shown to produce biofilm, therefore, a possible explanation for this trend is that the biofilm supports the attachment of oil to the glass walls. Cells often produce biofilms when they are in stressful conditions, but several studies have also

shown that EPS may play a role in biodegradation of hydrocarbons [123,144], and that bacterial EPS can aid in the formation of clumps and globules that include crude oil [145]. A study published in 2019 by Omarova *et al*. showed that biofilm produced by bacteria may aid in the stabilization of dispersed oil droplets, creating a layer between the oil and surrounding water [35]. The biofilm matrix produced by the bacteria is less polar than water, which attracts oil droplets and promotes the formation of larger clumps of oil that are more likely to stick to the glass surface of the flask. As time passed, agitation of the flasks likely caused the droplets to stick together and form larger sticky clumps which stuck to the walls of the flask and accumulated to form a layer of oil.

Likely the two phases, that is the dispersed oil and the wall-attached oil, did not remain static and separate during the experiment. Pieces of the attached oil-film may have re-entered the aqueous fraction, forming clumps or droplets in the aqueous phase. Lighter compounds trapped in the oil film on flask walls would over time migrate to the film surface and be released into the aqueous phase or directly biodegraded by colonizing microbes. Our discussion largely does not consider such exchange, evaluating each phase separately.

Overall, it appears that the metabolic capacity of *Vibrio* sp. strain J502 targets both LMW and HMW PAHs, and potentially some aliphatic *n*-$C_{10\text{-}12}$ and possibly aromatics *n*-$C_{10\text{-}12}$, but only in the aqueous phase. Bioavailability of the same compounds was low in the film attached to the flask wall. This lack of degradation is thus not the result of a lack in metabolic capacity, but due to structural inhibition, that make the oil on the flask walls less available.

3.6 Conclusion

The bulk oil estimates, the biomarker *n*-C_{17}: phytane ratio, as well as individual compound analysis indicate that after 7 days *Vibrio* sp. strain J502 was actively biodegrading several compounds, especially the LMW PAHs naphthalene, 2-methylnaphthalene, and fluorene in the aqueous phase, but not in the oil adhering to walls of the incubation flasks. In the treatment with bacteria and CEWAF, a greater amount of oil adhered to the flask walls than in the CEWAF control, which was likely due to the formation of larger sticky droplets in the bacterial treatment that came out of the aqueous solution and adhered to the glass surface.

As previously discussed, the evidence of biodegradation does not correlate with the decline in bacterial population indicated by the plate count method results, suggesting that this method of determining bacterial counts did not accurately capture the number of metabolically active bacteria in the samples. The presence of chemical dispersant did not negatively impact the growth or survival of *Vibrio* sp. strain J502.

The trends in oil composition analysis align with the genomic analysis of *Vibrio* sp. strain J502, which revealed that genes related to the degradation of aromatic hydrocarbons such as naphthalene were present (Wells, E. *et al*., 2024, in preparation). However, there were no genes related to the degradation of *n*-aliphatic or *n*-aromatic compounds identified in the genomic data for *Vibrio* sp. strain J502, and the oil composition analysis was inconclusive and did not indicate any clear trends in biodegradation of these compounds either. It is worth noting that there were many genes whose functions remain unknown, therefore it is possible that the bacterium has the capacity to degrade these compounds, perhaps in very small amounts.

4. SUMMARY

In this thesis, the main objectives were to genomically and phenotypically characterize *Vibrio* sp. strain J502, as well as to determine the impact of crude oil exposure on its metabolic and cellular functions. In addition, the objective was to determine the metabolic capability of *Vibrio* sp. strain J502 to degrade the hydrocarbons and other compounds found in crude oil, as well as to determine its ability to survive in the presence of chemically dispersed crude oil.

In Chapter II, we determined that *Vibrio* sp. strain J502 shares many phenotypic and biochemical characteristics with members of the genus *Vibrio*. This, in addition to the phylogenetic analysis allowed us to conclude that this bacterium is a member of the genus *Vibrio*. The genome of *Vibrio* sp. strain J502 is made up of two chromosomes and one small plasmid. Through whole genome alignment and phylogenetic analysis, we determined that *Vibrio* sp. strain J502 clusters most closely with *V. anguillarum* J360, and the percent similarity between the two species is 93.27% (chromosome I) and 98.87% (chromosome II). The percent similarity for chromosome I is significant enough (< 95%) to indicate that *Vibrio* sp. strain J502 is a unique isolate. This information combined with its unique lipidomic and quinone profiles supports our determination that *Vibrio* sp. strain J502 is a novel isolate. The transcriptomic profile of *Vibrio* sp. strain J502 in crude oil exposure conditions indicated that genes related to stress response and degradation of aromatic hydrocarbons were upregulated in the presence of crude oil compared to seawater control conditions, suggesting that the bacterium is capable of utilizing compounds found in crude oil as a source of carbon. Specifically, genes related to the degradation of naphthalene and its variants were identified in the genome of *Vibrio* sp. strain J502 and were found to be upregulated in oil exposure conditions during the transcriptomic experiment. These results suggested that *Vibrio* sp. strain J502 could degrade LMW PAHS such

as naphthalenes, which was further examined during the crude oil composition analysis conducted in chapter III.

In chapter III, we determined that *Vibrio* sp. strain J502 is capable of surviving in the presence of crude oil and chemical dispersant for at least a six-week period. During the incubation period, there was a larger decrease in bulk oil concentration in the presence of bacteria when compared to the control. In addition, the *n*-C_{17}: pristane ratio results indicated that biodegradation of oil was occurring in the presence of the bacteria throughout the experiment. We determined that *Vibrio* sp. strain J502 was capable of degrading LMW PAHs and LMW alkanes, and that its biodegradation activity occurs primarily in well-oxygenated water where the oil is well dispersed into small droplets. These results aligned with the genomic and transcriptomic data collected and presented in chapter II.

4.1 The Metabolism of *Vibrio* sp. strain J502 and Applications for Biotechnology

A complete genomic, phenotypic and phylogenetic characterization of *Vibrio* sp. strain J502 was presented in chapter II. I determined that the bacterium is psychrotrophic and halophilic, and its biochemical profile matches that of the genus *Vibrio*. I also examined the genome of *Vibrio* sp. strain J502 to determine whether there were genes present that encoded for degradation of hydrocarbons. We identified several genes related to the degradation of aromatic hydrocarbons, specifically those involved in the degradation of naphthalene and its variants. These results were supported by the results that we obtained in chapter III, which indicated that the bacterium is capable of metabolizing LMW-PAHs.

While no single species can degrade every compound found in crude oil, a community of diverse bacteria found naturally in the marine ecosystem may work together to biodegrade many of the hydrocarbons and other potentially harmful compounds found in crude oil [146].

Understanding the metabolism and examining the genomes of individual strains contributes to developing general knowledge on the local microbiome and provides a basis to understand how the microbial community might react to an oil spill or sudden exposure to crude oil. I determined that *Vibrio* sp. strain J502 experiences an up-regulation of genes related to stress and degradation of aromatic hydrocarbons in the presence of crude oil compared to the seawater control condition during the transcriptomic experiment in chapter II. Although *Vibrio* sp. strain J502 may be under stress in oil exposure conditions, it is able to survive and adjust its metabolic activity to degrade the LMW PAHs present in the oil. Natural conditions in the marine environment would be impacted by a number of factors that are not possible to replicate in a laboratory setting, meaning that the biodegrading activity of *Vibrio* sp. strain J502 could be more up or down regulated in the natural environment. However, I chose laboratory conditions that were as representative as possible of the natural environment, and therefore the result of my experiment provides a basis of knowledge for understanding how the bacterium may respond in natural conditions and how bioremediation efforts may impact this species. In terms of future work, I would like to conduct the transcriptomic experiment again but with a longer exposure time in the WAF and control conditions. Bacteria often needs time in new exposure conditions for their metabolism to adjust, and increasing the exposure time during the experiment would provide further insight into the metabolic capacity of this bacterium.

While chemical dispersants have been utilized in other countries, such as for the Deep-Water Horizon oil spill in the Gulf of Mexico in 2010 [147], they are not approved for use in Canada. Therefore, it is important to consider other methods of increasing rates of biodegradation of crude oil in the marine environment without the addition of chemical dispersants. I would be interested in repeating the experiment from Chapter 3 using WAF instead

of CEWAF, to determine if similar results would be produced in conditions without the addition of chemical dispersant. Bioremediation of oil by organisms naturally present in the environment has been extensively studied, and mechanisms such as biostimulation and intrinsic bioremediation have been proposed as cleanup methods that are both cost-effective and low risk [148].

The degradation rate of crude oil by bacteria is influenced by the availability of nutrients, particularly nitrogen and phosphorus [146]. Biostimulation involves the addition of these nutrients, and others such as sulfur and potassium to the marine environment where an oil spill has occurred, to stimulate the growth of indigenous hydrocarbon-degrading bacteria and other microorganisms [146]. In the transcriptomic experiment I conducted, I used natural filtered seawater as the control and to create the WAF used in the experimental treatment. Because there were no additional nutrients added to the filtered seawater, the bacteria was only exposed to the nutrients that would be present in its natural environment. In future studies of *Vibrio* sp. strain J502 it would be interesting to conduct similar transcriptomic studies with the addition of varying amounts of other nutrients to determine how they might impact the bacteria's regulation of hydrocarbon-degrading and stress response related genes. Additionally, it would be interesting to repeat the experiment and analyze the transcriptome at different timepoints to determine whether the initial response of the bacteria differs from the long-term response.

Intrinsic bioremediation, also known as natural attenuation, is another biodegradation method that does not involve any form of enhancement to the environment. Instead, this method relies on the passive remediation of polluted sites without human intervention [149]. *Vibrio* sp. strain J502 was isolated from the coastal waters in Logy Bay; therefore, we know that it is present naturally in the environment. In addition, we observed that the bacteria can grow on

traditional microbiological media such as Trypticase Soy Broth (TSB), therefore it is able to utilize multiple sources of carbon including sugars and hydrocarbons. My results suggest that *Vibrio* sp. strain J502 can survive in the marine environment in conditions where there are no hydrocarbons present, as well as in conditions where oil is present due to a spill or natural seepage. Thus, this bacterium is a potential candidate for intrinsic bioremediation, as it is already present in the environment and no human intervention is required for it to become an active hydrocarbon-degrader in the presence of crude oil. Effective intrinsic bioremediation occurs when there is high microbial diversity, and the microbes present have diverse metabolic capabilities and are able to degrade different compounds [149]. *Vibrio* sp. strain J502 contributes to this microbial diversity in the marine ecosystem in Newfoundland and Labrador, and the genomic and transcriptomic data I presented in chapter II will be useful in informing further research on the species and determining its potential role in the microbial community in terms of oil degradation in a natural setting.

4.2 Hydrocarbon Degradation and the Relevance of Oil Research in Newfoundland and Labrador

Research into the interaction between marine microbes and crude oil is particularly relevant in the marine ecosystem around Newfoundland and Labrador due to the ongoing and planned offshore oil exploration, drilling and extraction activities. The region where offshore oil development occurs in Newfoundland (off the Grand Banks) is characterized by severe storm and sea conditions, which challenge all aspects of offshore oil development and increase the potential severity of oil spills associated with platform operations [150]. Even small oil spills originating from these activities could have a severe environmental impact on the marine life in the region. Natural attenuation plays a critical role in the degradation of oil spilled into the marine environment and involves physical, chemical and biological processes such as

evaporation, dispersion, photo-oxidation, emulsification, aggregation and biodegradation by marine microbes [151].

Abiotic degradation of crude oil typically takes place for several hours to several days after the spill has occurred, while the rate of biodegradation by marine microorganisms depends on many factors, including the species present, temperature and the chemical composition of the oil [151,152]. Lighter compounds, such as LMW aliphatic and aromatic hydrocarbons are typically degraded first, while heavier compounds may take much longer to degrade [151,153]. This aligns with the results we obtained in chapter III, where we observed that LMW PAHs were degraded by *Vibrio* sp. strain J502 over a six-week incubation period, while other heavier hydrocarbons showed no signs of degradation during the experiment timeframe. Due to the time constraints of our experiment, we cannot conclusively determine whether *Vibrio* sp. strain J502 has the metabolic capacity to degrade heavier compounds. It would be an interesting expansion on this study to repeat this experiment with a longer incubation period in order to determine whether *Vibrio* sp. strain J502 is able to degrade additional compounds with more time.

In experiment 2 of chapter III, chemical dispersants were used to create CEWAF to incubate the culture of *Vibrio* sp. strain J502. This decision was made for several reasons, including that it increased the dispersion of the oil in the aqueous phase and made extraction of hydrocarbons for measurement more efficient, and it reduced variability between replicates, therefore creating a more consistent dataset. Although chemical dispersants are not currently approved for use in Canada, they have been used extensively in other countries for remediation of oil spills and are continuing to become more widely accepted as an effective oil spill cleanup method. Based on the results of experiment 1, I determined that *Vibrio* sp. strain J502 is able to survive in the presence of a chemical dispersant for at least six weeks. While chemical

dispersants are toxic to some marine bacteria and have been shown to inhibit degradation of hydrocarbons [151], I observed during experiment 1 of chapter III that the chemical dispersant did not have a toxic effect on *Vibrio* sp. strain J502 or appear to inhibit its metabolic activities. I determined that *Vibrio* sp. strain J502 was able to degrade LMW-PAHs in the aqueous phase versus the portion of oil stuck to the wall of the incubation flask, which indicates that *Vibrio* sp. strain J502 has a more active metabolism in the presence of oxygen than in an anoxic environment, despite being a facultative anaerobe.

Understanding the optimal conditions for the metabolic activity of *Vibrio* sp. strain J502 allows us to predict how it may interact in natural conditions if exposed to crude oil. The potential of hydrocarbon degraders within the natural ecosystem needs to be continuously characterized in order to gather knowledge on the potential interactions and impacts of crude oil spills in the area of study.

4.3 Conclusion

In conclusion, the results of this research have identified and characterized a novel marine bacterial isolate, which we have named *Vibrio* sp. strain J502. Our results suggest that this bacterium is capable of survival in the presence of crude oil and chemical dispersant, and that the bacterium is capable of biodegrading compounds found within the crude oil. Given the active oil exploration activity off the coast of Newfoundland and Labrador, knowledge about the indigenous microbial community is critical to understanding the dynamics that would be involved in potential oil spills or leaks. In addition, there are biotechnical applications for species that have the ability to degrade hydrocarbons, such as use for natural attenuation of oil spills and the use of biostimulation and intrinsic biodegradation. Therefore, this research is helpful in

informing oil spill research and potential future research into the biotechnical applications of this species.

5. REFERENCES

1. Morandin, L.A.; O'Hara, P.D. Offshore Oil and Gas, and Operational Sheen Occurrence: Is There Potential Harm to Marine Birds? *Environmental Reviews* 2016, *24*, 285–318.
2. Burke, C.M.; Montevecchi, W.A.; Wiese, F.K. Inadequate Environmental Monitoring around Offshore Oil and Gas Platforms on the Grand Bank of Eastern Canada: Are Risks to Marine Birds Known? *J Environ Manage* **2012**, *104*, 121–126, doi:10.1016/j.jenvman.2012.02.012.
3. Paine, M.D.; DeBlois, E.M.; Kilgour, B.W.; Tracy, E.; Pocklington, P.; Crowley, R.D.; Williams, U.P.; Gregory Janes, G. Effects of the Terra Nova Offshore Oil Development on Benthic Macro-Invertebrates over 10 Years of Development Drilling on the Grand Banks of Newfoundland, Canada. *Deep Sea Research Part II: Topical Studies in Oceanography* **2014**, *110*, 38–64, doi:10.1016/j.dsr2.2014.10.015.
4. McGrath, C.G.G. Preventing a Nationally-Significant Oil Spill on the Grand Banks of Newfoundland. *International Oil Spill Conference Proceedings* **2014**, *2014*, 1226–1238, doi:10.7901/2169-3358-2014.1.1226.
5. Fraser, G.S.; Racine, V. An Evaluation of Oil Spill Responses for Offshore Oil Production Projects in Newfoundland and Labrador, Canada: Implications for Seabird Conservation. *Mar Pollut Bull* **2016**, *107*, 36–45, doi:10.1016/j.marpolbul.2016.04.026.
6. Li, P.; Cai, Q.; Lin, W.; Chen, B.; Zhang, B. Offshore Oil Spill Response Practices and Emerging Challenges. *Mar Pollut Bull* 2016, *110*, 6–27.
7. Xue, J.; Yu, Y.; Bai, Y.; Wang, L.; Wu, Y. Marine Oil-Degrading Microorganisms and Biodegradation Process of Petroleum Hydrocarbon in Marine Environments: A Review. *Curr Microbiol* **2015**, *71*, 220–228, doi:10.1007/s00284-015-0825-7.

8. Daly, K.L.; Passow, U.; Chanton, J.; Hollander, D. Assessing the Impacts of Oil-Associated Marine Snow Formation and Sedimentation during and after the Deepwater Horizon Oil Spill. *Anthropocene* **2016**, *13*, 18–33, doi:10.1016/j.ancene.2016.01.006.

9. Zhang, S.; Wu, W.; Zheng, Q.; Wang, M. Effect of Dispersants on Bio-Degradation of Marine Spilled Oil. *J Coast Res* **2018**, *83*, 364–368, doi:10.2112/SI83-060.1.

10. Barron, M.G.; Vivian, D.N.; Heintz, R.A.; Yim, U.H. Long-Term Ecological Impacts from Oil Spills: Comparison of Exxon Valdez, Hebei Spirit, and Deepwater Horizon. *Environ Sci Technol* **2020**, *54*, 6456–6467, doi:10.1021/acs.est.9b05020.

11. Rohal, M.; Barrera, N.; Escobar-Briones, E.; Brooks, G.; Hollander, D.; Larson, R.; Montagna, P.A.; Pryor, M.; Romero, I.C.; Schwing, P. How Quickly Will the Offshore Ecosystem Recover from the 2010 Deepwater Horizon Oil Spill? Lessons Learned from the 1979 Ixtoc-1 Oil Well Blowout. *Ecol Indic* **2020**, *117*, doi:10.1016/j.ecolind.2020.106593.

12. Dempsey, D.P.; Koen-Alonso, M.; Gentleman, W.C.; Pepin, P. Compilation and Discussion of Driver, Pressure, and State Indicators for the Grand Bank Ecosystem, Northwest Atlantic. *Ecol Indic* **2017**, *75*, 331–339, doi:10.1016/j.ecolind.2016.12.011.

13. Prince, R.C.; Butler, J.D.; Redman, A.D. The Rate of Crude Oil Biodegradation in the Sea. *Environ Sci Technol* **2017**, *51*, 1278–1284, doi:10.1021/acs.est.6b03207.

14. Pagnucco, R.; Phillips, M.L. Comparative Effectiveness of Natural By-Products and Synthetic Sorbents in Oil Spill Booms. *J Environ Manage* **2018**, *225*, 10–16, doi:10.1016/j.jenvman.2018.07.094.

15. Farooq, U.; Taban, I.C.; Daling, P.S. Study of the Oil Interaction towards Oil Spill Recovery Skimmer Material: Effect of the Oil Weathering and Emulsification Properties. *Mar Pollut Bull* **2018**, *135*, 119–128, doi:10.1016/j.marpolbul.2018.06.017.

16. Fingas, M. *In-Situ Burning for Oil Spill Countermeasures*; Taylor & Francis Group, Ed.; 2018;

17. Kleindienst, S.; Seidel, M.; Ziervogel, K.; Grim, S.; Loftis, K.; Harrison, S.; Malkin, S.Y.; Perkins, M.J.; Field, J.; Sogin, M.L.; et al. Chemical Dispersants Can Suppress the Activity of Natural Oil-Degrading Microorganisms. *Proc Natl Acad Sci U S A* **2015**, *112*, 14900–14905, doi:10.1073/pnas.1507380112.

18. Brunswick, P.; MacInnis, C.Y.; Yan, J.; Buday, C.; Fieldhouse, B.; Brown, C.E.; van Aggelen, G.; Shang, D. Enhanced Marine Monitoring and Toxicity Study of Oil Spill Dispersants Including Corexit EC9500A in the Presence of Diluted Bitumen. *J Environ Sci Health A Tox Hazard Subst Environ Eng* **2020**, *55*, 788–799, doi:10.1080/10934529.2020.1744399.

19. Xia, W.; Li, J.; Han, L.; Liu, L.; Yang, X.; Hao, S.; Zhang, M. Influence of Dispersant/Oil Ratio on the Bacterial Community Structure and Petroleum Hydrocarbon Biodegradation in Seawater. *J Coast Res* **2018**, *84*, 77–81, doi:10.2112/SI84-011.1.

20. Sun, X.; Chu, L.; Mercando, E.; Romero, I.; Hollander, D.; Kostka, J.E. Dispersant Enhances Hydrocarbon Degradation and Alters the Structure of Metabolically Active Microbial Communities in Shallow Seawater from the Northeastern Gulf of Mexico. *Front Microbiol* **2019**, *10*, doi:10.3389/fmicb.2019.02387.

21. Rahsepar, S.; Langenhoff, A.A.M.; Smit, M.P.J.; van Eenennaam, J.S.; Murk, A.J.; Rijnaarts, H.H.M. Oil Biodegradation: Interactions of Artificial Marine Snow, Clay

Particles, Oil and Corexit. *Mar Pollut Bull* **2017**, *125*, 186–191, doi:10.1016/j.marpolbul.2017.08.021.

22. Techtmann, S.M.; Zhuang, M.; Campo, P.; Holder, E.; Elk, M.; Hazen, T.C.; Conmy, R.; Santo Domingo, J.W.; Ning-Yi Zhou, E.; Jiao Tong, S. *Corexit 9500 Enhances Oil Biodegradation and Changes Active Bacterial Community Structure of Oil-Enriched Microcosms ENVIRONMENTAL MICROBIOLOGY Crossm Downloaded From*; 2017;
23. Kujawinski, E.B.; Kido Soule, M.C.; Valentine, D.L.; Boysen, A.K.; Longnecker, K.; Redmond, M.C. Fate of Dispersants Associated with the Deepwater Horizon Oil Spill. *Environ Sci Technol* **2011**, *45*, 1298–1306, doi:10.1021/es103838p.
24. Péquin, B.; Cai, Q.; Lee, K.; Greer, C.W. Natural Attenuation of Oil in Marine Environments: A Review. *Mar Pollut Bull* **2022**, *176*, 113464, doi:10.1016/j.marpolbul.2022.113464.
25. Prince et al., 2007(Chapter_11_Biodegradation_of_Oil_Hydrocarbons_and_Its_Implications_for...).
26. Ganesan, M.; Mani, R.; Sai, S.; Kasivelu, G.; Awasthi, M.K.; Rajagopal, R.; Wan Azelee, N.I.; Selvi, P.K.; Chang, S.W.; Ravindran, B. Bioremediation by Oil Degrading Marine Bacteria: An Overview of Supplements and Pathways in Key Processes. *Chemosphere* **2022**, *303*, 134956, doi:10.1016/j.chemosphere.2022.134956.
27. Liu, Y.; Wan, Y.Y.; Wang, C.; Ma, Z.; Liu, X.; Li, S. Biodegradation of N-Alkanes in Crude Oil by Three Identified Bacterial Strains. *Fuel* **2020**, *275*, doi:10.1016/j.fuel.2020.117897.
28. Prince, R.C.; Lessard, R.R.; Clark, J.R. *Bioremediation of Marine Oil Spills*; 2003; Vol. 58;.

29. Carregosa, J.C.; Castiblanco, J.E.B.; Santos, T.M.; Prata, P.S.; Santos, J.M.; Wisniewski, A. Assessment of the Effect of Short-Term Weathering on the Molecular-Level Chemical Composition of Crude Oils in Contact with Aquatic Environments. *Environmental Science and Pollution Research* **2023**, *30*, 95738–95757, doi:10.1007/s11356-023-29148-7.

30. Lemkau, K.L.; McKenna, A.M.; Podgorski, D.C.; Rodgers, R.P.; Reddy, C.M. Molecular Evidence of Heavy-Oil Weathering Following the M/V *Cosco Busan* Spill: Insights from Fourier Transform Ion Cyclotron Resonance Mass Spectrometry. *Environ Sci Technol* **2014**, *48*, 3760–3767, doi:10.1021/es403787u.

31. Yakimov, M.M.; Timmis, K.N.; Golyshin, P.N. Obligate Oil-Degrading Marine Bacteria. *Curr Opin Biotechnol* **2007**, *18*, 257–266, doi:10.1016/j.copbio.2007.04.006.

32. Muriel-Millán, L.F.; Millán-López, S.; Pardo-López, L. Biotechnological Applications of Marine Bacteria in Bioremediation of Environments Polluted with Hydrocarbons and Plastics. *Appl Microbiol Biotechnol* **2021**, *105*, 7171–7185, doi:10.1007/s00253-021-11569-4.

33. Shi, K.; Xue, J.; Xiao, X.; Qiao, Y.; Wu, Y.; Gao, Y. Mechanism of Degrading Petroleum Hydrocarbons by Compound Marine Petroleum-Degrading Bacteria: Surface Adsorption, Cell Uptake, and Biodegradation. *Energy & Fuels* **2019**, *33*, 11373–11379, doi:10.1021/acs.energyfuels.9b02306.

34. Haritash, A.K.; Kaushik, C.P. Biodegradation Aspects of Polycyclic Aromatic Hydrocarbons (PAHs): A Review. *J Hazard Mater* **2009**, *169*, 1–15, doi:10.1016/j.jhazmat.2009.03.137.

35. Omarova, M.; Swientoniewski, L.T.; Mkam Tsengam, I.K.; Blake, D.A.; John, V.; McCormick, A.; Bothun, G.D.; Raghavan, S.R.; Bose, A. Biofilm Formation by

Hydrocarbon-Degrading Marine Bacteria and Its Effects on Oil Dispersion. *ACS Sustain Chem Eng* **2019**, *7*, 14490–14499, doi:10.1021/acssuschemeng.9b01923.

36. Xiao, Y.; Huang, Z.; Yu, K.; Wang, M.; Gao, H.; Bai, X.; Jiang, M.; Wang, D. Distribution and Molecular Characteristics of Vibrio Species Isolated from Aquatic Environments in China, 2020. *Microorganisms* **2022**, *10*, 2007, doi:10.3390/microorganisms10102007.

37. Pruzzo, C.; Huq, A.; Colwell, R.R.; Donelli, G. Pathogenic Vibrio Species in the Marine and Estuarine Environment. In *Oceans and Health: Pathogens in the Marine Environment*; Springer US: Boston, MA; pp. 217–252.

38. Thompson, F.L.; Iida, T.; Swings, J. Biodiversity of Vibrios. *Microbiology and Molecular Biology Reviews* **2004**, *68*, 403–431, doi:10.1128/MMBR.68.3.403-431.2004.

39. Ceccarelli, D.; Amaro, C.; Romalde, J.L.; Suffredini, E.; Vezzulli, L. *Vibrio Species*. In *Food Microbiology*; ASM Press: Washington, DC, USA, 2019; pp. 347–388.

40. Brennan, J.J.; Messerschmidt, J.L.; Williams, L.M.; Matthews, B.J.; Reynoso, M.; Gilmore, T.D. Sea Anemone Model Has a Single Toll-like Receptor That Can Function in Pathogen Detection, NF-KB Signal Transduction, and Development. *Proceedings of the National Academy of Sciences* **2017**, *114*, doi:10.1073/pnas.1711530114.

41. Lukjancenko, O.; Ussery, D.W. Vibrio Chromosome-Specific Families. *Front Microbiol* **2014**, *5*, 73, doi:10.3389/fmicb.2014.00073.

42. Hedlund, B.P.; Staley, J.T. Vibrio Cyclotrophicus Sp. Nov., a Polycyclic Aromatic Hydrocarbon (PAH)-Degrading Marine Bacterium. *Int J Syst Evol Microbiol* **2001**, *51*, 61–66, doi:10.1099/00207713-51-1-61.

43. Dash, H.R.; Mangwani, N.; Chakraborty, J.; Kumari, S.; Das, S. Marine Bacteria: Potential Candidates for Enhanced Bioremediation. *Appl Microbiol Biotechnol* 2013, *97*, 561–571.

44. Godfrin, M.P.; Sihlabela, M.; Bose, A.; Tripathi, A. Behavior of Marine Bacteria in Clean Environment and Oil Spill Conditions. *Langmuir* **2018**, *34*, 9047–9053, doi:10.1021/acs.langmuir.8b01319.

45. Deivakumari, M.; Sanjivkumar, M.; Suganya, A.M.; Prabakaran, J.R.; Palavesam, A.; Immanuel, G. Studies on Reclamation of Crude Oil Polluted Soil by Biosurfactant Producing Pseudomonas Aeruginosa (DKB1). *Biocatal Agric Biotechnol* **2020**, *29*, doi:10.1016/j.bcab.2020.101773.

46. Hackbusch, S.; Noirungsee, N.; Viamonte, J.; Sun, X.; Bubenheim, P.; Kostka, J.E.; Müller, R.; Liese, A. Influence of Pressure and Dispersant on Oil Biodegradation by a Newly Isolated Rhodococcus Strain from Deep-Sea Sediments of the Gulf of Mexico. *Mar Pollut Bull* **2020**, *150*, doi:10.1016/j.marpolbul.2019.110683.

47. Das, D.; Mawlong, G.T.; Sarki, Y.N.; Singh, A.K.; Chikkaputtaiah, C.; Boruah, H.P.D. Transcriptome Analysis of Crude Oil Degrading Pseudomonas Aeruginosa Strains for Identification of Potential Genes Involved in Crude Oil Degradation. *Gene* **2020**, *755*, doi:10.1016/j.gene.2020.144909.

48. Liu, Y.; Hu, H.; Zanaroli, G.; Xu, P.; Tang, H. A Pseudomonas Sp. Strain Uniquely Degrades PAHs and Heterocyclic Derivatives via Lateral Dioxygenation Pathways. *J Hazard Mater* **2021**, *403*, doi:10.1016/j.jhazmat.2020.123956.

49. Imron, M.F.; Kurniawan, S.B.; Titah, H.S. Potential of Bacteria Isolated from Diesel-Contaminated Seawater in Diesel Biodegradation. *Environ Technol Innov* **2019**, *14*, 100368, doi:10.1016/j.eti.2019.100368.

50. Wang, J.; Sandoval, K.; Ding, Y.; Stoeckel, D.; Minard-Smith, A.; Andersen, G.; Dubinsky, E.A.; Atlas, R.; Gardinali, P. Biodegradation of Dispersed Macondo Crude Oil by Indigenous Gulf of Mexico Microbial Communities. *Science of the Total Environment* **2016**, *557–558*, 453–468, doi:10.1016/j.scitotenv.2016.03.015.

51. Sambrook, J.; Russell, D. *Molecular Cloning: A Laboratory Manual*; Cold Spring Harbor: Cold Spring Habor Laboratory, 2001;

52. Umasuthan, N.; Valderrama, K.; Vasquez, I.; Segovia, C.; Hossain, A.; Cao, T.; Gnanagobal, H.; Monk, J.; Boyce, D.; Santander, J. A Novel Marine Pathogen Isolated from Wild Cunners (Tautogolabrus Adspersus): Comparative Genomics and Transcriptome Profiling of Pseudomonas Sp. Strain J380. *Microorganisms* **2021**, *9*, 812, doi:10.3390/microorganisms9040812.

53. Leboffe, M.J.; P.B.E. *Microbiology Laboratory Theory and Application*; 3rd ed.; Morton Publishing Company: Colorado, 2010;

54. P, R.; Rani J, S.; DR, G. Assessment of Antibiotic Sensitivity and Pathogenecity of Vibriospp. and Aeromonasspp. from Aquaculture Environment. *MOJ Ecology & Environmental Sciences* **2018**, *3*, doi:10.15406/mojes.2018.03.00077.

55. Myhr, E.; Larsen, J.L.; Lillehaug, A.; Gudding, R.; Heum, M.; H&#xfffd;stein, T. Characterization of Vibrio Anguillarum and Closely Related Species Isolated from Farmed Fish in Norway. *Appl Environ Microbiol* **1991**, *57*, 2750–2757, doi:10.1128/aem.57.9.2750-2757.1991.

56. P, R.; Rani J, S.; DR, G. Assessment of Antibiotic Sensitivity and Pathogenecity of Vibriospp. and Aeromonasspp. from Aquaculture Environment. *MOJ Ecology & Environmental Sciences* **2018**, *3*, doi:10.15406/mojes.2018.03.00077.

57. Tamura, K.; Stecher, G.; Kumar, S. MEGA11: Molecular Evolutionary Genetics Analysis Version 11. *Mol Biol Evol* **2021**, *38*, 3022–3027, doi:10.1093/molbev/msab120.

58. Bertelli, C.; Laird, M.R.; Williams, K.P.; Lau, B.Y.; Hoad, G.; Winsor, G.L.; Brinkman, F.S. IslandViewer 4: Expanded Prediction of Genomic Islands for Larger-Scale Datasets. *Nucleic Acids Res* **2017**, *45*, W30–W35, doi:10.1093/nar/gkx343.

59. Kado, C.I.; Liu, S.T. Rapid Procedure for Detection and Isolation of Large and Small Plasmids. *J Bacteriol* **1981**, *145*, 1365–1373, doi:10.1128/jb.145.3.1365-1373.1981.

60. Sasser, M.C. Identification of Bacteria by Gas Chromatography of Cellular Fatty Acids. *Technical Note #101.* 2001.

61. Vieira, S.; Huber, K.J.; Neumann-Schaal, M.; Geppert, A.; Luckner, M.; Wanner, G.; Overmann, J. Usitatibacter Rugosus Gen. Nov., Sp. Nov. and Usitatibacter Palustris Sp. Nov., Novel Members of Usitatibacteraceae Fam. Nov. within the Order Nitrosomonadales Isolated from Soil. *Int J Syst Evol Microbiol* **2021**, *71*, doi:10.1099/ijsem.0.004631.

62. Moss, C.W.; Lambert-Fair, M.A. Location of Double Bonds in Monounsaturated Fatty Acids of Campylobacter Cryaerophila with Dimethyl Disulfide Derivatives and Combined Gas Chromatography-Mass Spectrometry. *J Clin Microbiol* **1989**, *27*, 1467–1470, doi:10.1128/jcm.27.7.1467-1470.1989.

63. Harvey, D.J. Picolinyl Esters as Derivatives for the Structural Determination of Long Chain Branched and Unsaturated Fatty Acids. *Biol Mass Spectrom* **1982**, *9*, 33–38, doi:10.1002/bms.1200090107.

64. SPITZER, V. Structure Analysis of Fatty Acids by Gas Chromatography ? Low Resolution Electron Impact Mass Spectrometry of Their 4,4-Dimethyloxazoline Derivatives ? A Review. *Prog Lipid Res* **1996**, *35*, 387–408, doi:10.1016/S0163-7827(96)00011-2.

65. Yu, Q.T.; Liu, B.N.; Zhang, J.Y.; Huang, Z.H. Location of Methyl Branchings in Fatty Acids: Fatty Acids in Uropygial Secretion of Shanghai Duck by GC-MS of 4,4-dimethyloxazoline Derivatives. *Lipids* **1988**, *23*, 804–810, doi:10.1007/BF02536225.

66. Schumann, P.; Kalensee, F.; Cao, J.; Criscuolo, A.; Clermont, D.; Köhler, J.M.; Meier-Kolthoff, J.P.; Neumann-Schaal, M.; Tindall, B.J.; Pukall, R. Reclassification of Haloactinobacterium Glacieicola as Occultella Glacieicola Gen. Nov., Comb. Nov., of Haloactinobacterium Album as Ruania Alba Comb. Nov, with an Emended Description of the Genus Ruania, Recognition That the Genus Names Haloactinobacterium and Ruania Are Heterotypic Synonyms and Description of Occultella Aeris Sp. Nov., a Halotolerant Isolate from Surface Soil Sampled at an Ancient Copper Smelter. *Int J Syst Evol Microbiol* **2021**, *71*, doi:10.1099/ijsem.0.004769.

67. S. Andrews FastQC: A Quality Control Tool for High Throughput Sequence Data. .

68. Teng, M.; Love, M.I.; Davis, C.A.; Djebali, S.; Dobin, A.; Graveley, B.R.; Li, S.; Mason, C.E.; Olson, S.; Pervouchine, D.; et al. A Benchmark for RNA-Seq Quantification Pipelines. *Genome Biol* **2016**, *17*, 74, doi:10.1186/s13059-016-0940-1.

69. Li, B.; Ruotti, V.; Stewart, R.M.; Thomson, J.A.; Dewey, C.N. RNA-Seq Gene Expression Estimation with Read Mapping Uncertainty. *Bioinformatics* **2010**, *26*, 493–500, doi:10.1093/bioinformatics/btp692.

70. Pereira, M.B.; Wallroth, M.; Jonsson, V.; Kristiansson, E. Comparison of Normalization Methods for the Analysis of Metagenomic Gene Abundance Data. *BMC Genomics* **2018**, *19*, 274, doi:10.1186/s12864-018-4637-6.

71. Vasquez, I.; Cao, T.; Chakraborty, S.; Gnanagobal, H.; O'Brien, N.; Monk, J.; Boyce, D.; Westcott, J.D.; Santander, J. Comparative Genomics Analysis of Vibrio Anguillarum Isolated from Lumpfish (Cyclopterus Lumpus) in Newfoundland Reveal Novel Chromosomal Organizations. *Microorganisms* **2020**, *8*, 1–25, doi:10.3390/microorganisms8111666.

72. Machimbirike, V.I.; Vasquez, I.; Cao, T.; Chukwu-Osazuwa, J.; Onireti, O.; Segovia, C.; Khunrae, P.; Rattanarojpong, T.; Booman, M.; Jones, S.; et al. Comparative Genomic Analysis of Virulent Vibrio (Listonella) Anguillarum Serotypes Revealed Genetic Diversity and Genomic Signatures in the O-Antigen Biosynthesis Gene Cluster. *Microorganisms* **2023**, *11*, 792, doi:10.3390/microorganisms11030792.

73. Aussel, L.; Pierrel, F.; Loiseau, L.; Lombard, M.; Fontecave, M.; Barras, F. Biosynthesis and Physiology of Coenzyme Q in Bacteria. *Biochimica et Biophysica Acta (BBA) - Bioenergetics* **2014**, *1837*, 1004–1011, doi:10.1016/j.bbabio.2014.01.015.

74. Reimer, L.C.; Sardà Carbasse, J.; Koblitz, J.; Ebeling, C.; Podstawka, A.; Overmann, J. Bac *Dive* in 2022: The Knowledge Base for Standardized Bacterial and Archaeal Data. *Nucleic Acids Res* **2022**, *50*, D741–D746, doi:10.1093/nar/gkab961.

75. Germain, E.; Castro-Roa, D.; Zenkin, N.; Gerdes, K. Molecular Mechanism of Bacterial Persistence by HipA. *Mol Cell* **2013**, *52*, 248–254, doi:10.1016/j.molcel.2013.08.045.

76. Harvey, K.L.; Jarocki, V.M.; Charles, I.G.; Djordjevic, S.P. The Diverse Functional Roles of Elongation Factor Tu (EF-Tu) in Microbial Pathogenesis. *Front Microbiol* **2019**, *10*, doi:10.3389/fmicb.2019.02351.

77. Thompson, F.L.; Iida, T.; Swings, J. Biodiversity of Vibrios. *Microbiology and Molecular Biology Reviews* **2004**, *68*, 403–431, doi:10.1128/MMBR.68.3.403-431.2004.

78. Hedlund, B.P.; Staley, J.T. Vibrio Cyclotrophicus Sp. Nov., a Polycyclic Aromatic Hydrocarbon (PAH)-Degrading Marine Bacterium. *Int J Syst Evol Microbiol* **2001**, *51*, 61–66, doi:10.1099/00207713-51-1-61.

79. Han, F.; Walker, R.D.; Janes, M.E.; Prinyawiwatkul, W.; Ge, B. Antimicrobial Susceptibilities of *Vibrio Parahaemolyticus* and *Vibrio Vulnificus* Isolates from Louisiana Gulf and Retail Raw Oysters. *Appl Environ Microbiol* **2007**, *73*, 7096–7098, doi:10.1128/AEM.01116-07.

80. Ceccarelli, D.; Alam, M.; Huq, A.; Colwell, R.R. Reduced Susceptibility to Extended-Spectrum β-Lactams in Vibrio Cholerae Isolated in Bangladesh. *Front Public Health* **2016**, *4*, doi:10.3389/fpubh.2016.00231.

81. O'Hara, C.M.; Sowers, E.G.; Bopp, C.A.; Duda, S.B.; Strockbine, N.A. Accuracy of Six Commercially Available Systems for Identification of Members of the Family *Vibrionaceae*. *J Clin Microbiol* **2003**, *41*, 5654–5659, doi:10.1128/JCM.41.12.5654-5659.2003.

82. Gomez-Gil, B.; Thompson, F.L.; Thompson, C.C.; Swings, J. Vibrio Rotiferianus Sp. Nov., Isolated from Cultures of the Rotifer Brachionus Plicatilis. *Int J Syst Evol Microbiol* **2003**, *53*, 239–243, doi:10.1099/ijs.0.02430-0.

83. Holm, K.O.; Bækkedal, C.; Söderberg, J.J.; Haugen, P. Complete Genome Sequences of Seven Vibrio Anguillarum Strains as Derived from PacBio Sequencing. *Genome Biol Evol* **2018**, *10*, 1127–1131, doi:10.1093/gbe/evy074.

84. Ciufo, S.; Kannan, S.; Sharma, S.; Badretdin, A.; Clark, K.; Turner, S.; Brover, S.; Schoch, C.L.; Kimchi, A.; DiCuccio, M. Using Average Nucleotide Identity to Improve Taxonomic Assignments in Prokaryotic Genomes at the NCBI. *Int J Syst Evol Microbiol* **2018**, *68*, 2386–2392, doi:10.1099/ijsem.0.002809.

85. Lin, H.; Yu, M.; Wang, X.; Zhang, X.-H. Comparative Genomic Analysis Reveals the Evolution and Environmental Adaptation Strategies of Vibrios. *BMC Genomics* **2018**, *19*, 135, doi:10.1186/s12864-018-4531-2.

86. Jain, C.; Rodriguez-R, L.M.; Phillippy, A.M.; Konstantinidis, K.T.; Aluru, S. High Throughput ANI Analysis of 90K Prokaryotic Genomes Reveals Clear Species Boundaries. *Nat Commun* **2018**, *9*, 5114, doi:10.1038/s41467-018-07641-9.

87. Okada, K.; Iida, T.; Kita-Tsukamoto, K.; Honda, T. Vibrios Commonly Possess Two Chromosomes. *J Bacteriol* **2005**, *187*, 752–757, doi:10.1128/JB.187.2.752-757.2005.

88. Kirkup, B.C.; Chang, L.; Chang, S.; Gevers, D.; Polz, M.F. Vibrio Chromosomes Share Common History. *BMC Microbiol* **2010**, *10*, 137, doi:10.1186/1471-2180-10-137.

89. Hiraishi, A.; Ueda, Y.; Ishihara, J. Quinone Profiling of Bacterial Communities in Natural and Synthetic Sewage Activated Sludge for Enhanced Phosphate Removal. *Appl Environ Microbiol* **1998**, *64*, 992–998, doi:10.1128/AEM.64.3.992-998.1998.

90. Collins, M.D.; Jones, D. Distribution of Isoprenoid Quinone Structural Types in Bacteria and Their Taxonomic Implication. *Microbiol Rev* **1981**, *45*, 316–354, doi:10.1128/mr.45.2.316-354.1981.

91. Guo, Z.; Li, W.; Wang, Y.; Hou, Q.; Zhao, H.; Sun, Z.; Zhang, Z. Vibrio Zhugei Sp. Nov., a Moderately Halophilic Bacterium Isolated from Pickling Sauce. *Int J Syst Evol Microbiol* **2019**, *69*, 1313–1319, doi:10.1099/ijsem.0.003308.

92. Zhang, X.-H.; Austin, B. Haemolysins in Vibrio Species. *J Appl Microbiol* **2005**, *98*, 1011–1019, doi:10.1111/j.1365-2672.2005.02583.x.

93. Peng, Y.; Wang, X.; Shou, J.; Zong, B.; Zhang, Y.; Tan, J.; Chen, J.; Hu, L.; Zhu, Y.; Chen, H.; et al. Roles of Hcp Family Proteins in the Pathogenesis of the Porcine Extraintestinal Pathogenic Escherichia Coli Type VI Secretion System. *Sci Rep* **2016**, *6*, 26816, doi:10.1038/srep26816.

94. Fridman, C.M.; Keppel, K.; Gerlic, M.; Bosis, E.; Salomon, D. A Comparative Genomics Methodology Reveals a Widespread Family of Membrane-Disrupting T6SS Effectors. *Nat Commun* **2020**, *11*, 1085, doi:10.1038/s41467-020-14951-4.

95. Wallden, K.; Rivera-Calzada, A.; Waksman, G. Microreview: Type IV Secretion Systems: Versatility and Diversity in Function. *Cell Microbiol* **2010**, *12*, 1203–1212, doi:10.1111/j.1462-5822.2010.01499.x.

96. Farmer, J.J.; Michael Janda, J.; Brenner, F.W.; Cameron, D.N.; Birkhead, K.M. *Vibrio*. In *Bergey's Manual of Systematics of Archaea and Bacteria*; Wiley, 2015; pp. 1–79.

97. Germain, E.; Castro-Roa, D.; Zenkin, N.; Gerdes, K. Molecular Mechanism of Bacterial Persistence by HipA. *Mol Cell* **2013**, *52*, 248–254, doi:10.1016/j.molcel.2013.08.045.

98. Yoshida, H.; Nakayama, H.; Maki, Y.; Ueta, M.; Wada, C.; Wada, A. Functional Sites of Ribosome Modulation Factor (RMF) Involved in the Formation of 100S Ribosome. *Front Mol Biosci* **2021**, *8*, doi:10.3389/fmolb.2021.661691.

99. Pasqua, M.; Bonaccorsi di Patti, M.C.; Fanelli, G.; Utsumi, R.; Eguchi, Y.; Trirocco, R.; Prosseda, G.; Grossi, M.; Colonna, B. Host - Bacterial Pathogen Communication: The Wily Role of the Multidrug Efflux Pumps of the MFS Family. *Front Mol Biosci* **2021**, *8*, doi:10.3389/fmolb.2021.723274.

100. Pasqua; Grossi; Zennaro; Fanelli; Micheli; Barras; Colonna; Prosseda The Varied Role of Efflux Pumps of the MFS Family in the Interplay of Bacteria with Animal and Plant Cells. *Microorganisms* **2019**, *7*, 285, doi:10.3390/microorganisms7090285.

101. Kvint, K.; Nachin, L.; Diez, A.; Nyström, T. The Bacterial Universal Stress Protein: Function and Regulation. *Curr Opin Microbiol* **2003**, *6*, 140–145, doi:10.1016/S1369-5274(03)00025-0.

102. Mitchell, A.M.; Silhavy, T.J. Envelope Stress Responses: Balancing Damage Repair and Toxicity. *Nat Rev Microbiol* **2019**, *17*, 417–428, doi:10.1038/s41579-019-0199-0.

103. Gasperotti, A.; Göing, S.; Fajardo-Ruiz, E.; Forné, I.; Jung, K. Function and Regulation of the Pyruvate Transporter CstA in Escherichia Coli. *Int J Mol Sci* **2020**, *21*, 9068, doi:10.3390/ijms21239068.

104. Timmermans, J.; Van Melderen, L. Conditional Essentiality of the *CsrA* Gene in *Escherichia Coli*. *J Bacteriol* **2009**, *191*, 1722–1724, doi:10.1128/JB.01573-08.

105. Karas, V.O.; Westerlaken, I.; Meyer, A.S. The DNA-Binding Protein from Starved Cells (Dps) Utilizes Dual Functions To Defend Cells against Multiple Stresses. *J Bacteriol* **2015**, *197*, 3206–3215, doi:10.1128/JB.00475-15.

106. Pagni, S.V.M. The Elusive Roles of Bacterial Glutathione S- Transferases: New Lessons from Genomes. *Appl Microbiol Biotechnol* **2002**, *58*, 138–146, doi:10.1007/s00253-001-0836-0.

107. Shehu, D.; Abdullahi, N.; Alias, Z. Cytosolic Glutathione S-Transferase in Bacteria: A Review. *Pol J Environ Stud* **2018**, *28*, 515–528, doi:10.15244/pjoes/85200.

108. Mohapatra, B.; Phale, P.S. Microbial Degradation of Naphthalene and Substituted Naphthalenes: Metabolic Diversity and Genomic Insight for Bioremediation. *Front Bioeng Biotechnol* 2021, *9*.

109. Zhou, N.Y.; Fuenmayor, S.L.; Williams, P.A. Nag Genes of Ralstonia (Formerly Pseudomonas) Sp. Strain U2 Encoding Enzymes for Gentisate Catabolism. *J Bacteriol* **2001**, *183*, 700–708, doi:10.1128/JB.183.2.700-708.2001.

110. Natalia, I.; de Oliveir, V.M. Microbial Hydrocarbon Degradation: Efforts to Understand Biodegradation in Petroleum Reservoirs. In *Biodegradation - Engineering and Technology*; InTech, 2013.

111. Potts, A.H.; Vakulskas, C.A.; Pannuri, A.; Yakhnin, H.; Babitzke, P.; Romeo, T. Global Role of the Bacterial Post-Transcriptional Regulator CsrA Revealed by Integrated Transcriptomics. *Nat Commun* **2017**, *8*, 1596, doi:10.1038/s41467-017-01613-1.

112. Zhang, S.-P.; Wang, Q.; Quan, S.-W.; Yu, X.-Q.; Wang, Y.; Guo, D.-D.; Peng, L.; Feng, H.-Y.; He, Y.-X. Type II Toxin–Antitoxin System in Bacteria: Activation, Function, and Mode of Action. *Biophys Rep* **2020**, *6*, 68–79, doi:10.1007/s41048-020-00109-8.

113. Wheeler, J.R.; Lyon, D.; Di Paolo, C.; Grosso, A.; Crane, M. Challenges in the Regulatory Use of Water-Accommodated Fractions for Assessing Complex Substances. *Environ Sci Eur* **2020**, *32*, 153, doi:10.1186/s12302-020-00432-4.

114. Bilbao, D.; De Miguel-Jiménez, L.; Igartua, A.; Olivares, M.; Izagirre, U.; Prieto, A.; Etxebarria, N. Chemical Characterization of Oil and Water Accommodated Fraction (WAF) at Different Temperatures. *Results in Engineering* **2022**, *14*, 100433, doi:10.1016/j.rineng.2022.100433.

115. Di Gregorio, F.; Parrillo, F.; Salzano, E.; Cammarota, F.; Arena, U. Removal of Naphthalene by Activated Carbons from Hot Gas. *Chemical Engineering Journal* **2016**, *291*, 244–253, doi:10.1016/j.cej.2016.01.081.

116. Gigliotti, C.L.; Brunciak, P.A.; Dachs, J.; Glenn, T.R.; Nelson, E.D.; Totten, L.A.; Eisenreich, S.J. Air—Water Exchange of Polycyclic Aromatic Hydrocarbons in the New York—New Jersey, USA, Harbor Estuary. *Environ Toxicol Chem* **2002**, *21*, 235–244, doi:10.1002/etc.5620210203.

117. Zhao, Q.; Weise, L.; Li, P.; Yang, K.; Zhang, Y.; Dong, D.; Li, P.; Li, X. Ageing Behavior of Phenanthrene and Pyrene in Soils: A Study Using Sodium Dodecylbenzenesulfonate Extraction. *J Hazard Mater* **2010**, *183*, 881–887, doi:10.1016/j.jhazmat.2010.07.111.

118. Godfrin, M.P.; Sihlabela, M.; Bose, A.; Tripathi, A. Behavior of Marine Bacteria in Clean Environment and Oil Spill Conditions. *Langmuir* **2018**, *34*, 9047–9053, doi:10.1021/acs.langmuir.8b01319.

119. Overton, E.B.; Adhikari, P.L.; Radović, J.R.; Passow, U. Fates of Petroleum during the Deepwater Horizon Oil Spill: A Chemistry Perspective. *Front Mar Sci* **2022**, *9*, doi:10.3389/fmars.2022.928576.

120. Moore, J.W.; Ramamoorthy, S. Aliphatic Hydrocarbons. In; 1984; pp. 16–42.

121. Nzila, A. Current Status of the Degradation of Aliphatic and Aromatic Petroleum Hydrocarbons by Thermophilic Microbes and Future Perspectives. *Int J Environ Res Public Health* **2018**, *15*, 2782, doi:10.3390/ijerph15122782.

122. Patel, A.B.; Shaikh, S.; Jain, K.R.; Desai, C.; Madamwar, D. Polycyclic Aromatic Hydrocarbons: Sources, Toxicity, and Remediation Approaches. *Front Microbiol* **2020**, *11*, doi:10.3389/fmicb.2020.562813.

123. Premnath, N.; Mohanrasu, K.; Guru Raj Rao, R.; Dinesh, G.H.; Prakash, G.S.; Ananthi, V.; Ponnuchamy, K.; Muthusamy, G.; Arun, A. A Crucial Review on Polycyclic Aromatic Hydrocarbons - Environmental Occurrence and Strategies for Microbial Degradation. *Chemosphere* **2021**, *280*, 130608, doi:10.1016/j.chemosphere.2021.130608.

124. KESTER, D.R.; DUEDALL, I.W.; CONNORS, D.N.; PYTKOWICZ, R.M. PREPARATION OF ARTIFICIAL SEAWATER. *Limnol Oceanogr* **1967**, *12*, 176–179, doi:10.4319/lo.1967.12.1.0176.

125. Guillard, R.R.L. Culture of Phytoplankton for Feeding Marine Invertebrates. In *Culture of Marine Invertebrate Animals*; Springer US: Boston, MA, 1975; pp. 29–60.

126. de Jourdan, B.P.; Boloori, T.; Burridge, L.E. Newly Hatched Stage I American Lobster (Homarus Americanus) Survival Following Exposure to Physically and Chemically Dispersed Crude Oil. *Arch Environ Contam Toxicol* **2022**, *82*, 307–316, doi:10.1007/s00244-022-00912-z.

127. Ou, F.; McGoverin, C.; White, J.; Swift, S.; Vanholsbeeck, F. Bead-Based Flow-Cytometric Cell Counting of Live and Dead Bacteria. In; 2019; pp. 123–134.

128. Tarnowski, B.I.; Spinale, F.G.; Nicholson, J.H. DAPI as a Useful Stain for Nuclear Quantitation. *Biotechnic & Histochemistry* **1991**, *66*, 296–302, doi:10.3109/10520299109109990.

129. Koch, A.L. Growth Measurement. In *Methods for General and Molecular Microbiology*; ASM Press: Washington, DC, USA, 2014; pp. 172–199.

130. Chandrasekar, S.; Sorial, G.A.; Weaver, J.W. Dispersant Effectiveness on Three Oils Under Various Simulated Environmental Conditions. *Environ Eng Sci* **2005**, *22*, 324–336, doi:10.1089/ees.2005.22.324.

131. Kleindienst, S.; Paul, J.H.; Joye, S.B. Using Dispersants after Oil Spills: Impacts on the Composition and Activity of Microbial Communities. *Nat Rev Microbiol* **2015**, *13*, 388–396, doi:10.1038/nrmicro3452.

132. Bodor, A.; Bounedjoum, N.; Vincze, G.E.; Erdeiné Kis, Á.; Laczi, K.; Bende, G.; Szilágyi, Á.; Kovács, T.; Perei, K.; Rákhely, G. Challenges of Unculturable Bacteria: Environmental Perspectives. *Rev Environ Sci Biotechnol* **2020**, *19*, 1–22, doi:10.1007/s11157-020-09522-4.

133. Li, X.; Liao, G.; Ju, Z.; Wang, C.; Li, N.; Xiong, D.; Zhang, Y. Antioxidant Response and Oxidative Stress in the Respiratory Tree of Sea Cucumber (Apostichopus Japonicus) Following Exposure to Crude Oil and Chemical Dispersant. *J Mar Sci Eng* **2020**, *8*, 547, doi:10.3390/jmse8080547.

134. Sathishkumar, M.; Binupriya, A.R.; Baik, S.-H.; Yun, S.-E. Biodegradation of Crude Oil by Individual Bacterial Strains and a Mixed Bacterial Consortium Isolated from Hydrocarbon Contaminated Areas. *Clean (Weinh)* **2008**, *36*, 92–96, doi:10.1002/clen.200700042.

135. Wang, A.; Li, Y.; Yang, X.; Bao, M.; Cheng, H. The Enhanced Stability and Biodegradation of Dispersed Crude Oil Droplets by Xanthan Gum as an Additive of Chemical Dispersant. *Mar Pollut Bull* **2017**, *118*, 275–280, doi:10.1016/j.marpolbul.2017.03.001.

136. Bao, M.; Wang, L.; Sun, P.; Cao, L.; Zou, J.; Li, Y. Biodegradation of Crude Oil Using an Efficient Microbial Consortium in a Simulated Marine Environment. *Mar Pollut Bull* **2012**, *64*, 1177–1185, doi:10.1016/j.marpolbul.2012.03.020.

137. Morales-McDevitt, M.E.; Shi, D.; Knap, A.H.; Quigg, A.; Sweet, S.T.; Sericano, J.L.; Wade, T.L. Mesocosm Experiments to Better Understand Hydrocarbon Half-Lives for Oil and Oil Dispersant Mixtures. *PLoS One* **2020**, *15*, e0228554, doi:10.1371/journal.pone.0228554.

138. Wang, C.; Chen, B.; Zhang, B.; He, S.; Zhao, M. Fingerprint and Weathering Characteristics of Crude Oils after Dalian Oil Spill, China. *Mar Pollut Bull* **2013**, *71*, 64–68, doi:10.1016/j.marpolbul.2013.03.034.

139. Rahsepar, S.; Smit, M.P.J.; Murk, A.J.; Rijnaarts, H.H.M.; Langenhoff, A.A.M. Chemical Dispersants: Oil Biodegradation Friend or Foe? *Mar Pollut Bull* **2016**, *108*, 113–119, doi:10.1016/j.marpolbul.2016.04.044.

140. Olajire AA, E.J. Aerobic Degradation of Petroleum Components by Microbial Consortia. *J Pet Environ Biotechnol* **2014**, *05*, doi:10.4172/2157-7463.1000195.

141. Grishchenkov, V.G.; Townsend, R.T.; McDonald, T.J.; Autenrieth, R.L.; Bonner, J.S.; Boronin, A.M. Degradation of Petroleum Hydrocarbons by Facultative Anaerobic Bacteria under Aerobic and Anaerobic Conditions. *Process Biochemistry* **2000**, *35*, 889–896, doi:10.1016/S0032-9592(99)00145-4.

142. McNally, D.L.; Mihelcic, J.R.; Lueking, D.R. Biodegradation of Three- and Four-Ring Polycyclic Aromatic Hydrocarbons under Aerobic and Denitrifying Conditions. *Environ Sci Technol* **1998**, *32*, 2633–2639, doi:10.1021/es980006c.

143. Ghosal, D.; Ghosh, S.; Dutta, T.K.; Ahn, Y. Current State of Knowledge in Microbial Degradation of Polycyclic Aromatic Hydrocarbons (PAHs): A Review. *Front Microbiol* **2016**, *7*, doi:10.3389/fmicb.2016.01369.

144. Mangwani, N.; Shukla, S.K.; Kumari, S.; Das, S.; Rao, T.S. Effect of Biofilm Parameters and Extracellular Polymeric Substance Composition on Polycyclic Aromatic Hydrocarbon Degradation. *RSC Adv* **2016**, *6*, 57540–57551, doi:10.1039/C6RA12824F.

145. Dong, R.; Wan, Z.; Wang, X.; Bai, Y.; Bao, M.; Li, H. The Role of Bacteria in the Formation and Migration of Oil–Particle Aggregates (OPAs) after Marine Oil Spills and the Associated Mechanism. *Environ Sci Technol* **2023**, *57*, 7018–7028, doi:10.1021/acs.est.3c00647.

146. Dell' Anno, F.; Rastelli, E.; Sansone, C.; Brunet, C.; Ianora, A.; Dell' Anno, A. Bacteria, Fungi and Microalgae for the Bioremediation of Marine Sediments Contaminated by Petroleum Hydrocarbons in the Omics Era. *Microorganisms* **2021**, *9*, doi:10.3390/microorganisms9081695.

147. Mascarelli, A. Deepwater Horizon Dispersants Lingered in the Deep. *Nature* **2011**, doi:10.1038/news.2011.54.

148. Ganesan, M.; Mani, R.; Sai, S.; Kasivelu, G.; Awasthi, M.K.; Rajagopal, R.; Wan Azelee, N.I.; Selvi, P.K.; Chang, S.W.; Ravindran, B. Bioremediation by Oil Degrading Marine Bacteria: An Overview of Supplements and Pathways in Key Processes. *Chemosphere* **2022**, *303*, 134956, doi:10.1016/j.chemosphere.2022.134956.

149. Azubuike, C.C.; Chikere, C.B.; Okpokwasili, G.C. Bioremediation Techniques-Classification Based on Site of Application: Principles, Advantages, Limitations and Prospects. *World J Microbiol Biotechnol* **2016**, *32*, 180, doi:10.1007/s11274-016-2137-x.

150. Kaiser, M.J. A Review of Exploration, Development, and Production Cost Offshore Newfoundland. *Natural Resources Research* **2021**, *30*, 1253–1290, doi:10.1007/s11053-020-09784-3.

151. Péquin, B.; Cai, Q.; Lee, K.; Greer, C.W. Natural Attenuation of Oil in Marine Environments: A Review. *Mar Pollut Bull* **2022**, *176*, 113464, doi:10.1016/j.marpolbul.2022.113464.

152. Passow, U. Formation of Rapidly-Sinking, Oil-Associated Marine Snow. *Deep Sea Research Part II: Topical Studies in Oceanography* **2016**, *129*, 232–240, doi:10.1016/j.dsr2.2014.10.001.

153. Head, I.M.; Jones, D.M.; Röling, W.F.M. Marine Microorganisms Make a Meal of Oil. *Nat Rev Microbiol* **2006**, *4*, 173–182, doi:10.1038/nrmicro1348.

6. SUPPLEMENTARY TABLES AND FIGURES

A)

B)

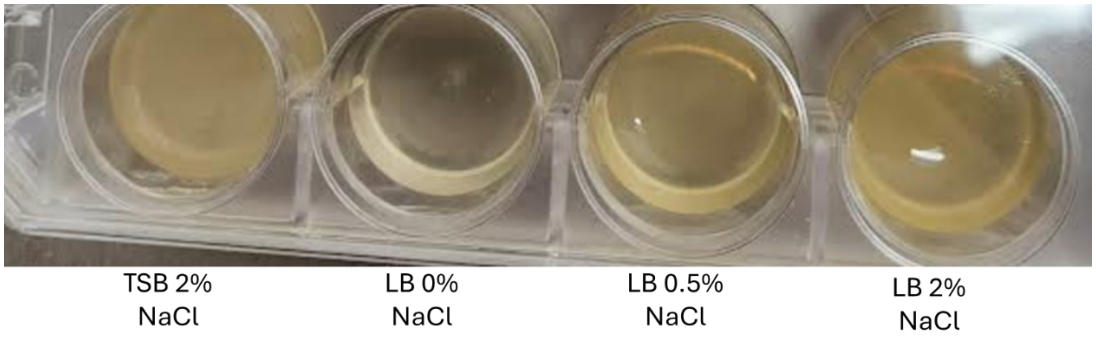

Figure S1. A) *Vibrio sp. strain J502* grown in different types of media. B) *Vibrio sp. strain J502* grown on TSA 2% NaCl agar plate.

A) 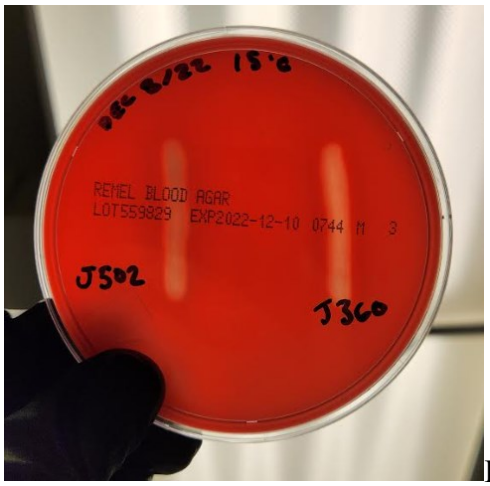

B) 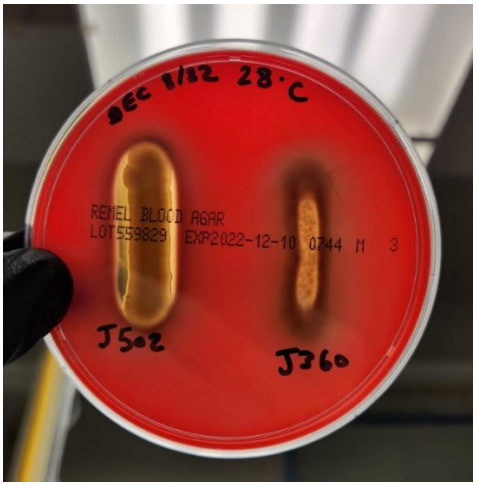

Figure S2. B-Hemolysin production on sheep's blood agar of *Vibrio sp. strain J502* (J502) and *V. anguillarum* (J360) at A) 15°C and B) 28°C.

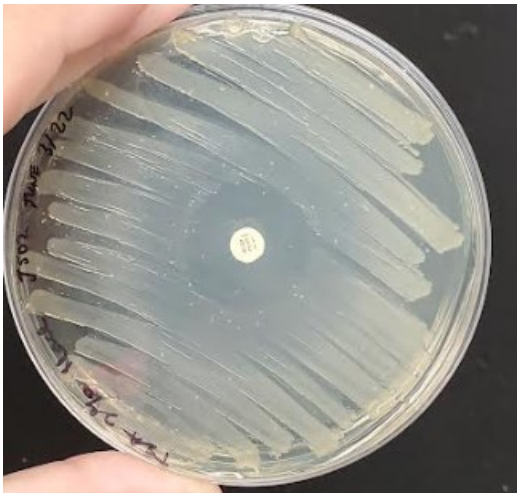

Figure S3. Antibiotic resistance test using O-129 and *Vibrio sp. strain J502*.

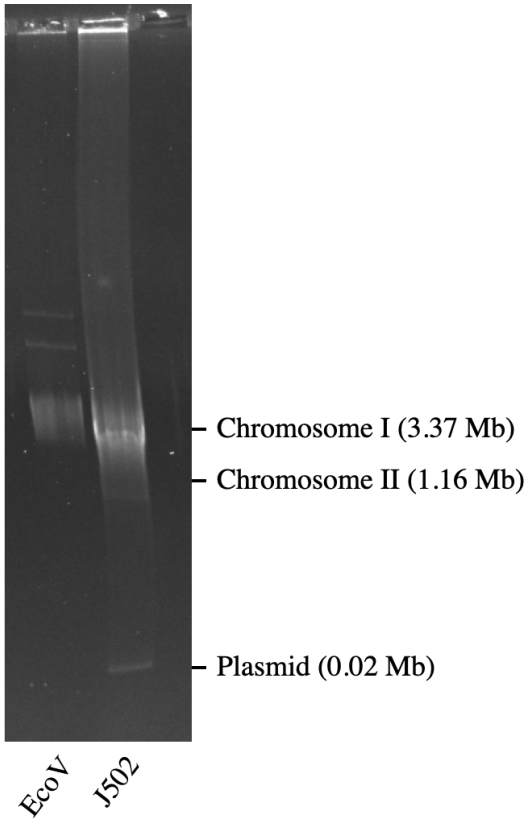

Figure S4. Kado and Liu plasmid profile of EcoV (control) and *Vibrio* sp. J02.

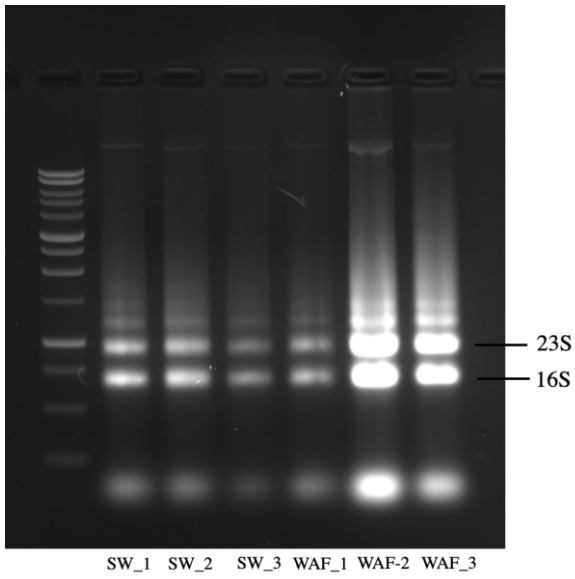

Figure S5. RNA evaluated by agarose gel electrophoresis.

Table S1. Experiment 1 bacterial counts via the plate counting method.

Time (days)	Replicate	# colonies	Dilution	CFU/ml	Average CFU/ml	Standard Deviation
0	INITIAL1	75	-4	7500000	7366667	1703917
	INITIAL2	56	-4	5600000		
	INITIAL3	90	-4	9000000		
1	SW1	118	-4	11800000	12100000	264575
	SW2	123	-4	12300000		
	SW3	122	-4	12200000		
	CEWAF1	96	-4	9600000	7500000	2389561
	CEWAF2	49	-4	4900000		
	CEWAF3	80	-4	8000000		
	COREXIT1	77	-4	7700000	6266667	1320353
	COREXIT2	60	-4	6000000		
	COREXIT3	51	-4	5100000		
2	SW1	71	-4	7100000	7866667	709460
	SW2	80	-4	8000000		
	SW3	85	-4	8500000		
	CEWAF1	32	-3	320000	248000	151433
	CEWAF2	74	-2	74000		
	CEWAF3	35	-3	350000		
	COREXIT1	70	-3	700000	480000	190526
	COREXIT2	37	-3	370000		
	COREXIT3	37	-3	370000		
3	SW1	32	-4	3200000	2676667	740023
	SW2	30	-4	3000000		
	SW3	183	-3	1830000		
	CEWAF1	23	-2	23000	11333	11504
	CEWAF2	11	-2	11000		
	CEWAF3	0		0		
	COREXIT1	31	-3	310000	225333	146647
	COREXIT2	31	-3	310000		
	COREXIT3	56	-2	56000		
4	SW1	88	-3	880000	1053333	165630
	SW2	121	-3	1210000		
	SW3	107	-3	1070000		

Table S1. Continued.

	CEWAF1	0		0	0	0
	CEWAF2	0		0		
	CEWAF3	0		0		
	COREXIT1	89	-3	890000	583333	400666
	COREXIT2	73	-3	730000		
	COREXIT3	130	-2	130000		
6	SW1	183	-1	18300	22233	3612
	SW2	254	-1	25400		
	SW3	230	-1	23000		
	CEWAF1	0		0	0	0
	CEWAF2	0		0		
	CEWAF3	0		0		
	COREXIT1	32	-1	3200	32267	46586
	COREXIT2	76	-1	7600		
	COREXIT3	86	-2	86000		

A)

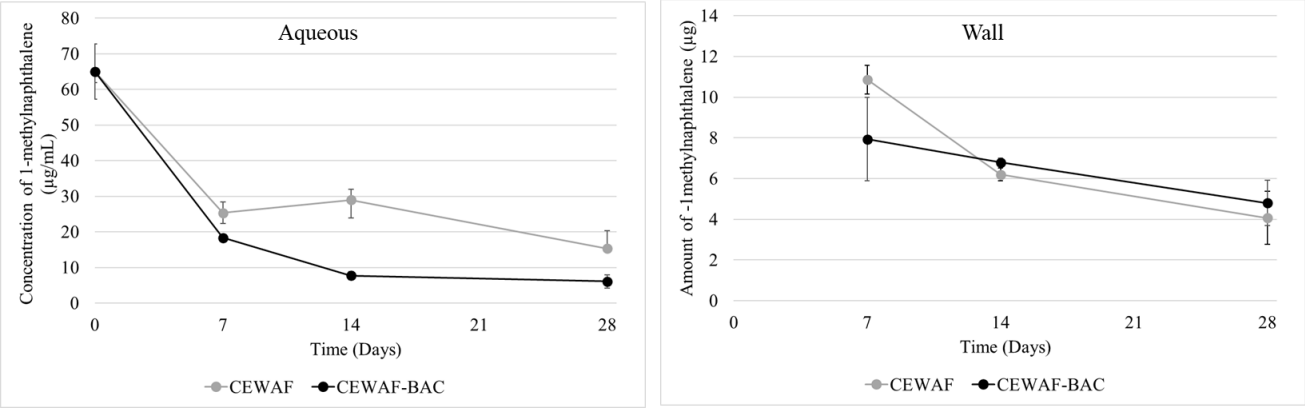

B)

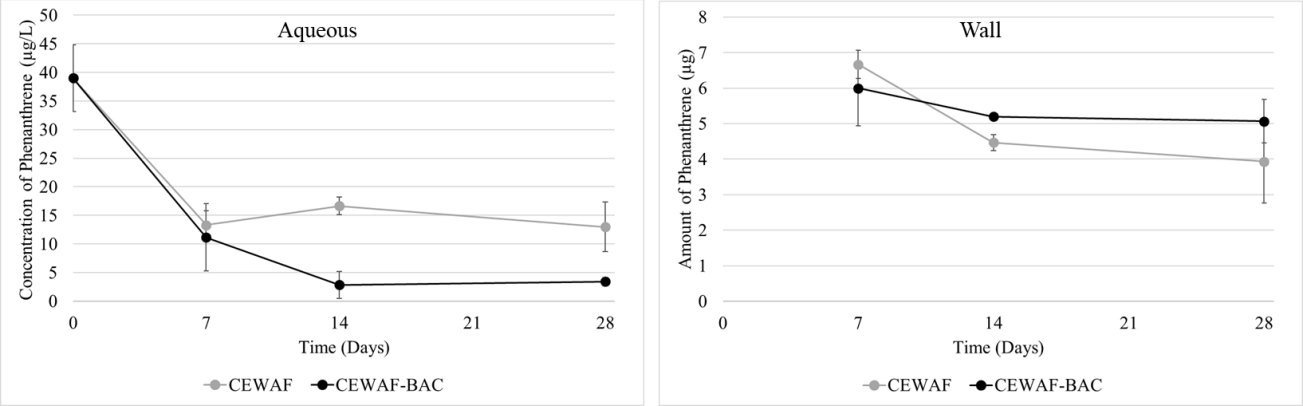

Figure S6. Change in concentrations of PAHs; A) 1-methylnaphthalene B) phenanthrene, from the aqueous (left) and wall (right) fractions, respectively, over time.

A)

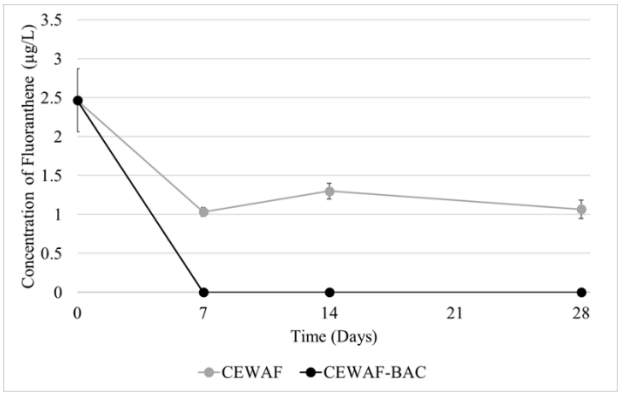
Concentration of Fluoranthene (µg/L)
3.5
3
2.5
2
1.5
1
0.5
0
0
7
14
21
28
Time (Days)
CEWAF
CEWAF-BAC

B)

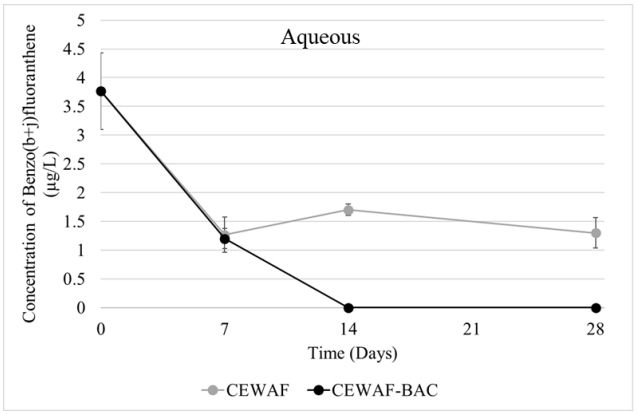
Aqueous
Concentration of Benzo(b+j)fluoranthene (µg/L)
5
4.5
4
3.5
3
2.5
2
1.5
1
0.5
0
0
7
14
21
28
Time (Days)
CEWAF
CEWAF-BAC

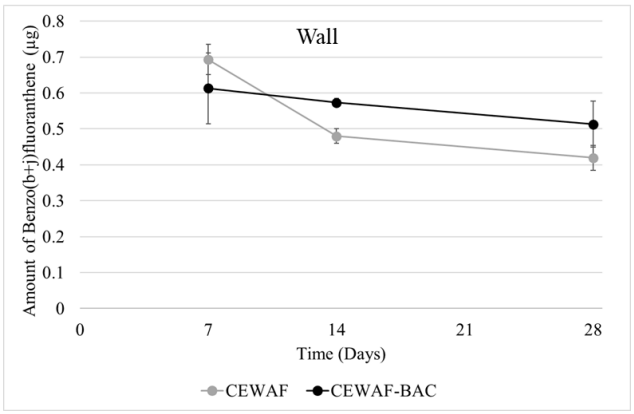
Wall
Amount of Benzo(b+j)fluoranthene (µg)
0.8
0.7
0.6
0.5
0.4
0.3
0.2
0.1
0
0
7
14
21
28
Time (Days)
CEWAF
CEWAF-BAC

C)

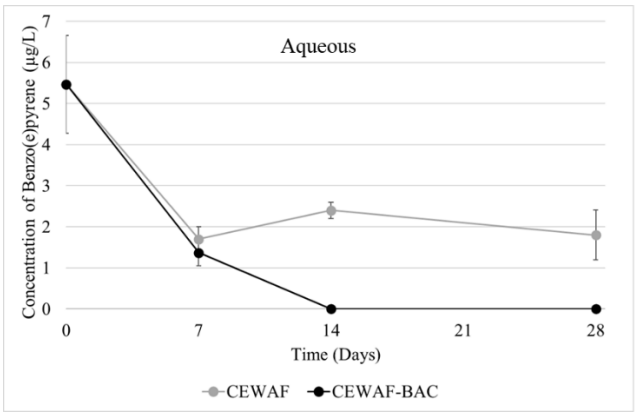
Aqueous
Concentration of Benzo(e)pyrene (µg/L)
7
6
5
4
3
2
1
0
0
7
14
21
28
Time (Days)
CEWAF
CEWAF-BAC

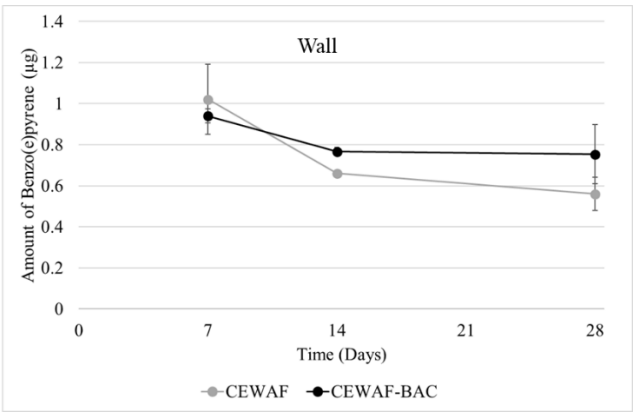
Wall
Amount of Benzo(e)pyrene (µg)
1.4
1.2
1
0.8
0.6
0.4
0.2
0
0
7
14
21
28
Time (Days)
CEWAF
CEWAF-BAC

D)

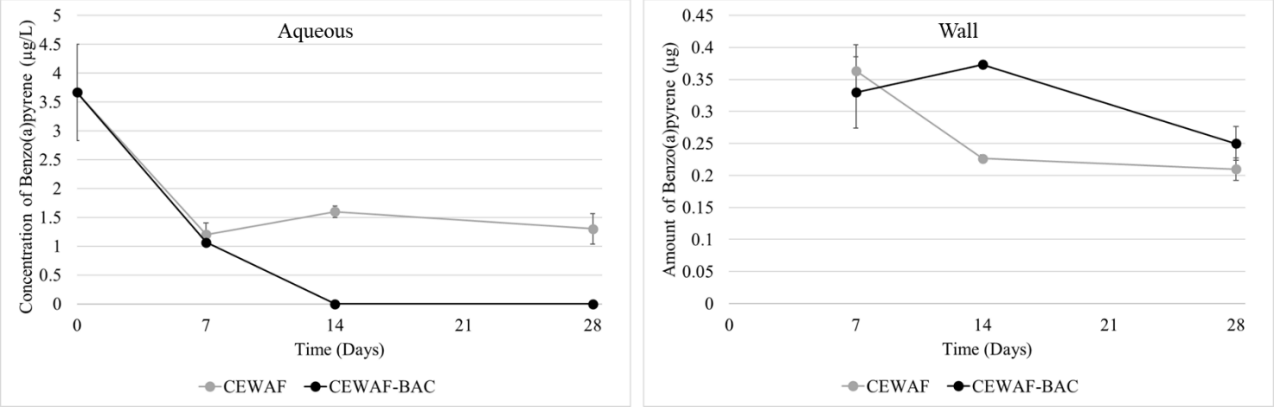

E)

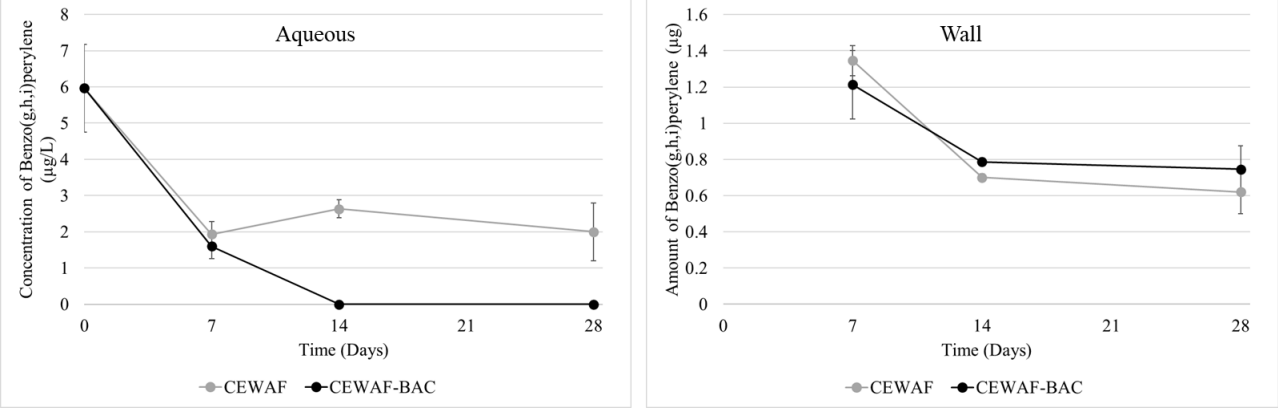

Figure S7. Change in concentrations of PAHs; A) fluoranthene, B) Benzo(b+j)fluoranthene, C) Benzo(e)pyrene, D) Benzo(a)pyrene, E) Benzo(g,h,i)perylene, from the aqueous (left) and wall (right) fractions, respectively, over time.

A)

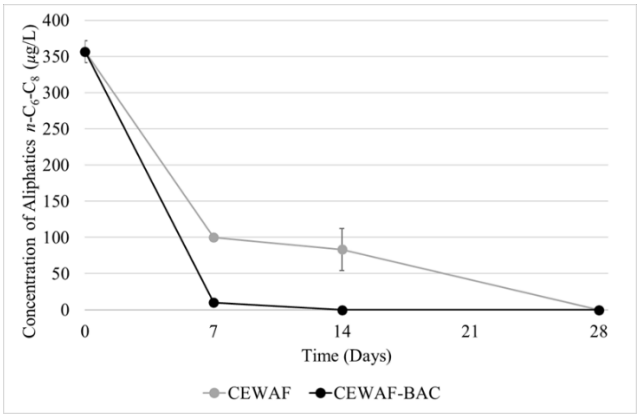

B)

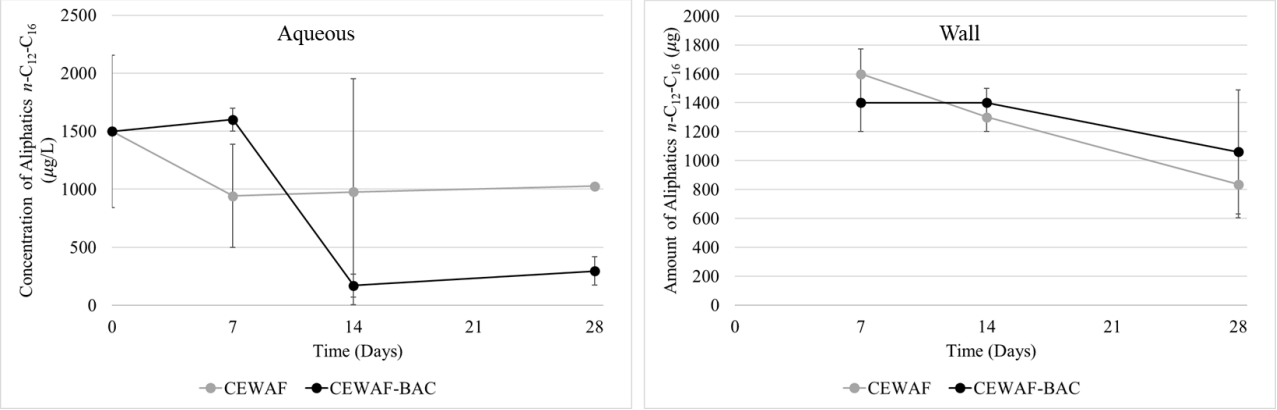

C)

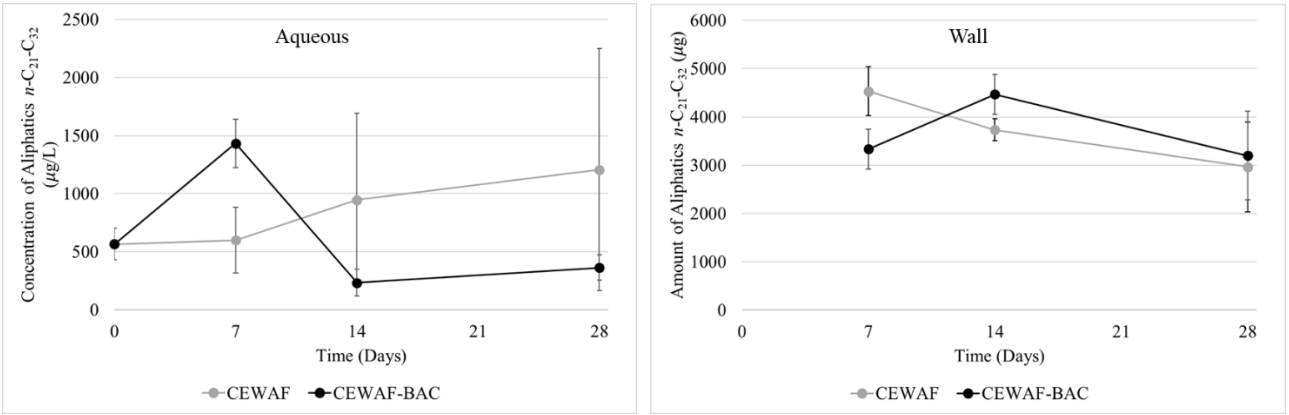

Figure S8. Change in concentrations of fractionated aliphatic compounds; A) *n*-C_6-C_8, B) *n*-C_{12}-C_{16}, C) *n*-C_{21}-C_{32} from the aqueous (left) and wall (right) fractions, respectively, over time.

A)

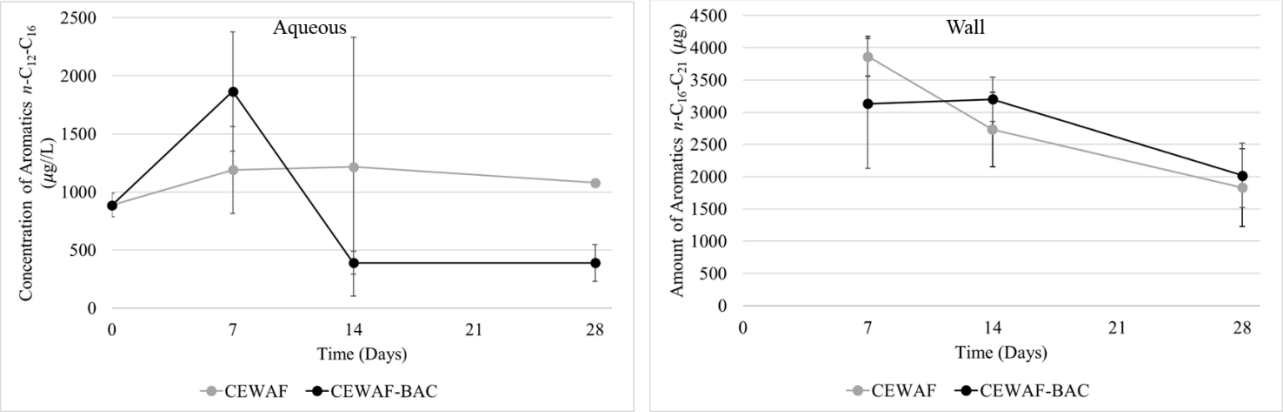

B)

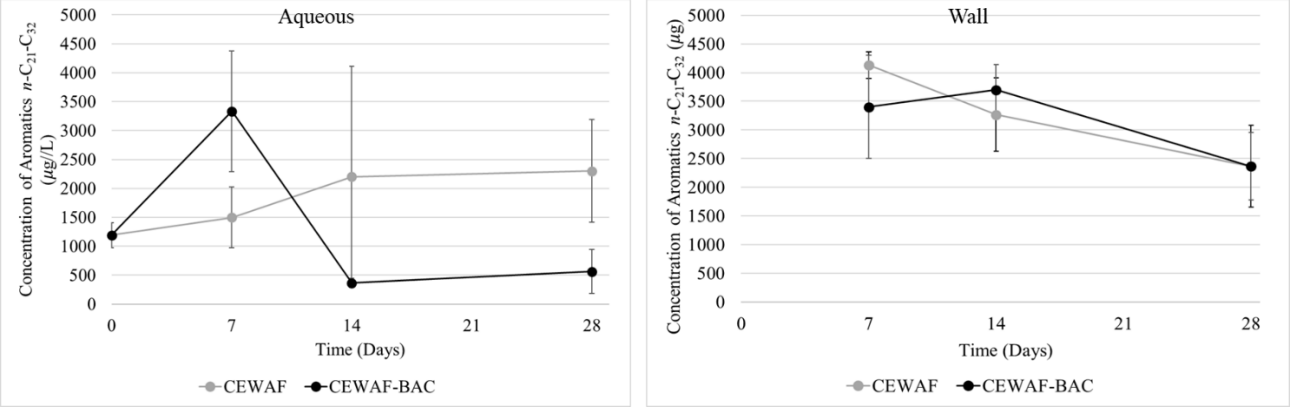

Figure S9. Change in concentrations of fractionated aromatic compounds; A) *n*-C_{12}-C_{16}, B) *n*-C_{21}-C_{32} from the aqueous (left) and wall (right) fractions, respectively, over time.